Investigations of Irgm1 during experimental infections with *Mycobacterium avium paratuberculosis*

Louis Kreitmann
Laboratory of Dr. Marcel Behr

Department of Experimental Medicine
McGill University
Montreal, Quebec, Canada
December 2013

A thesis submitted to McGill University in partial fulfilment
of the requirements of the degree of Master of Science

This work is dedicated to my mice.

Table of Contents

Abstract

Introduction: *Mycobacterium avium paratuberculosis* (MAP) is the causative agent of a chronic granulomatous enteritis of ruminants called Johne's disease (JD). Crohn's disease (CD) is an inflammatory bowel disease of unknown etiology affecting humans. Due to histological similarities between the two conditions, it has been suggested that MAP could be responsible for a subset of cases of CD. *Irgm1* (murine ortholog of *IRGM*, a CD susceptibility gene) has been linked to host defence against mycobacteria.

Methods: In the first part of this work, we have attempted to study the immune response of the *Irgm1*-/- mouse to systemic infection with MAP. In the second part, we have attempted to use the *Irgm1*-/- mouse as a host susceptible to lead to significant pathology after intra-intestinal infection with MAP (a murine model of JD) and documented its response to therapeutics used in the care of patients with CD.

Results: First, we have shown that mice deleted for *Irgm1* have a major susceptibility to systemic MAP infection, with accelerated rate of death and uncontrolled bacterial replication. To explain this, we have identified a defect of *Irgm1*-/- macrophages in controlling the intracellular growth of MAP. We have also identified severe haematological abnormalities leading to their death. Second, we have devised a protocol for the surgical inoculation of ~ 10^9 MAP colony forming units (CFUs) in the jejunum of *Irgm1*-/- mice. After 1 and 2 months of infection, we have observed significant intestinal histopathological lesions resembling those seen in Johne's disease, including focal and transmural lympho-histiocytic infiltrates and mesenteric lymphadenopathy. Mice infected according to this protocol were submitted to: 1) a systemic treatment with methylprednisolone, which did not lead to increased mortality; and 2) a treatment with an anti-tumor necrosis factor-alpha (TNF-α) antibody, which did not lead to uncontrolled MAP replication in the host.

Conclusion: *Irgm1*-/- mice are markedly susceptible to systemic MAP infection. When inoculated with ~ 10^9 MAP CFUs in the lumen of the jejunum, they develop stable histological lesions resembling those of JD. Interestingly, treatments used in the cure of patients with CD did not have a deleterious effect.

Résumé

Titre du mémoire : Etude du rôle d'Irgm1 au cours d'infections expérimentales par *Mycobacterium avium paratuberculosis*

Introduction : *Mycobacterium avium paratuberculosis* (MAP) est responsable d'une entérite chronique granulomateuse chez les ruminants, la maladie de Johne (ou paratuberculose). La maladie de Crohn est une maladie inflammatoire chronique du tube digestif d'étiologie indéterminée qui affecte les humains. Du fait de similarités histologiques entre les deux conditions, il a été suggéré que MAP pouvait être responsable de certains cas de maladie de Crohn. *Irgm1* (orthologue murin de *IRGM*, un gène de susceptibilité à la maladie de Crohn), a été impliqué dans la réponse immunitaire contre les mycobactéries.

Méthodes : Dans la première partie de ce travail, nous avons étudié la réponse immunitaire de la souris *Irgm1*-/- au cours d'une infection systémique par MAP. Dans la second partie, nous avons cherché à utiliser la souris *Irgm1*-/- pour induire des lésions histologiques après infection intra-intestinale par MAP (réalisant un modèle murin de maladie de Johne), et avons documenté la réponse de ce modèle à des traitements utilisés chez les patients atteints de maladie de Crohn.

Résultats : Nous avons montré que la souris *Irgm1*-/- présente une susceptibilité majeure à une infection systémique par MAP, avec mortalité accélérée et réplication bactérienne incontrôlée. Nous avons identifié un défaut des macrophages *Irgm1*-/- à contrôler la croissance intra-cellulaire de MAP. Nous avons aussi identifié des anomalies hématologiques expliquant leur mortalité accélérée. Dans un second temps, nous avons conçu un protocole consistant en l'injection par voie chirurgicale de ~ 10^9 unités formant colonies (UFC) de MAP au sein de la lumière du jéjunum de souris *Irgm1*-/-. Nous avons observé qu'à 1 et 2 mois post-infection, nous avions induit des lésions histologiques ressemblant à celles rencontrées dans la maladie de Johne, notamment des infiltrats lympho-histiocytiques focaux et transmuraux et une lymphadénopathie mésenterique. Des souries infectées selon ce protocole ont été soumises à: 1) un traitement systémique par

methylprednilosone, qui n'a pas entrainé une augmentation de la mortalité; et 2) un traitement par anticorps anti-tumor necrosis factor-alpha (TNF-α), qui n'a pas provoqué une réplication bactérienne incontrôlée.

Conclusion : Les souris *Irgm1*-/- sont susceptibles à une infection systémique par MAP. Après inoculation par voie chirurgicale de ~ 10^9 UFC de MAP, elles développent des lésions histologiques stables analogues à celles de la maladie de Johne. Des traitements utilisés pour traiter la maladie de Crohn n'ont pas entrainé d'effet délétère. Des travaux supplémentaires sont nécessaires pour évaluer l'utilité de ce modèle dans les recherches sur la maladie de Johne et sur la maladie de Crohn.

Acknowledgements

I would like to thank warmly:

- Dr. Behr and all the members of the Behr lab: Fiona McIntosh, Lynn Dery Capes, Joyce Wang, Dr. Nicolas Radomski, Dr. Louise Lefrançois, Robyn Lee, Cathevine Yang, Andrei Dan. Special thanks to Fiona and Nicolas for their help on some experiments.
- Past members of the Behr lab: Dr. Solmaz Golchin, Jean-Daniel Lalande, Alex Dufort, Angela Moore, Jemery Dabor. Special thanks to Jean-Daniel and Jeremy for their help on some experiments.
- Dr. Maziar Divangahi and the members of his lab: Dr. Fanny Tzelepis, Dr. Joanna Jaworska, Josh Gillard, Kimya Hassaniardakani, François Coulombe. Special thanks to Fanny and Kimya for their advice and help.
- Dr. Michael Reed, Dr. Pilar Domenech and the members of the Reed lab: Anya Rog, Mahé Racaud, Nishath Syed, Danielle Curtis.
- Dr. Erwin Schurr and the members of his lab: Dr. Tania Di Pietrantonio, Dr. Aurélie Cobat, Jason Yu, Dr. Jeremy Manry, Dr. Vinicius Fava, Dr. Marianna Orlova, Aimée Bouka.
- Dr Donald Vinh and Christina Gavino.
- Dr. Jim Gourdon for his invaluable help on the surgeries.
- Dr. Marylene Paquet, Ms. Jo-Ann Bader and all the members of the Histology Facility of the Rosalind and Morris Goodman Cancer Research Centre of McGill University.
- Guylaine Gadoury for her invaluable help on the mice, Daniel Houle, and all the members of the animal facility of the Montreal General Hospital.
- Dr. Lucie Coté for her help on diagnostic necropsies.
- Dr. Danielle Malo, Dr. Philippe Gros and Dr. Jacques Lapointe for their advice and help on being part of my thesis committees.
- All the people working at the Research Institute of the McGill University Health Center that helped me during the last two years.
- Dr. Fadi Fakhouri, Dr. Raymond Azar, Dr. Martin Albert for their support.
- The department of Experimental Medicine at McGill University.

List of figures

List of tables

List of abbreviations

ADC	Albumin dextrose complex
AIDS	Acquired immunodeficiency syndrome
AIEC	Adherent and invasive *Escherichia coli*
APC	Antigen presenting cell
ATCC	American Type Cell Culture
ATG16L1	Autophagy related 16-like 1
BCG	Bacille de Calmette et Guérin
BSC	Biosafety cabinet
CARD	Caspase recruitment domain
CD	Crohn's disease
CD	Cluster of differenciation
CFU	Colony forming unit
DC	Dendritic cell
DNA	Deoxyribonucleic acid
ELISA	Enzyme-linked immunosorbent assay
ERV9	Endogenous retrovirus 9
FACS	Fluorescence-activated cell sorting
GALT	Gut-associate lymphoid tissue
GFP	Green fluorescent protein
GI	Gastrointestinal
GWAS	Genome-wide association study
FACC	Facility Animal Care Committees
FBS	Fetal bovine serum
GTP	Guanosine triphosphate
GTPase	Guanosine triphosphatase
HSC	Hematopoietic stem cell
HSCT	Hematopoietic stem cell transplantation
H&E	Hematoxylin and eosin
IBD	Inflammatory bowel disease
IDO	Indoleamine 2,3-dioxygenase
IFN-γ	Interferon gamma
IL	Interleukin
iNOS2	Inducible nitric oxide synthetase type-2
IP	Intraperitoneal
IJ	Intrajejunal
IRG	Immunity-related GTPases
IRGM	Immunity-related GTPase family M protein
Irgm1	Immunity-related GTPase family M member 1
IS	Insertion sequence
JD	Johne's disease
LF82	*Escherichia coli* LF82

LPS	Lipopolysaccharide
LRR	Leucine Rich Repeats
LSP	Large sequence polymorphim
MAA	*Mycobacteria avium* ssp. *avium*
MAC	*Mycobacteria avium* Complex
MAH	*Mycobacteria avium* ssp. *hominissuis*
ManLAM	Mannosylated lipoarabinomanna
MAP	*Mycobacterium avium* ssp. *paratuberculosis*
MAP	Mitogen-activated protein
M-cell	Microfold cell
MDP	Muramyl dipeptide
MHC	Major histocompatibility complex
MLN	Mesenteric lymph nodes
MOI	Multiplicity of infection
mRNA	Mesenger ribonucleic acid
MSMD	Mendelian susceptibility to mycobacterial disease
MTC	*Mycobacterium tuberculosis* Complex
M. tb	*Mycobacterium tuberculosis*
NF-κB	Nuclear factor-kappa B
NK cells	Natural killer cells
NLR	NOD-like receptor
Nod2	Nucleotide-binding oligomerization domain 2
NOD2	Nucleotide-binding oligomerization domain 2
NRAMP1	Natural resistance associated macrophage protein 1
OADC	Oleic acid albumin dextrose complex
OD	Optical density
ORF	Open reading frame
P91-PHOX	P91-phagocyte oxydase
PAMPs	Pathogen-associated molecular patterns
PBS	Phosphate-buffered saline
PCR	Polymerase chain reaction
PRR	Pathogen recognition receptor
rcf	Relative centrifugal force
siRNA	Small interfering ribonucleic acid
TB	Tuberculosis
TGF-β	Transforming growth factor beta
Th1	T helper cells subtype 1
Th2	T helper cells subtype 2
TLR	Toll-like receptor
TNF-α	Tumor necrosis factor-alpha
STAT	Signal Transducers and Activators of Transcription
UC	Ulcerative colitis
ZN	Ziehl Neelsen

1) Introduction and review of the literature

The genus *Mycobacterium* comprises more than 100 species of aerobic micro-organisms related to the genera *Corynebacterium*, *Nocardia*, *Rhodococcus*, and *Streptomyces*[1]. Mycobacteria are characterized by a high G+C genomic content (~ 61-71%) and a cell wall enriched with certain specific long-chain lipids (such as mycolic acids). This thick, hydrophobic, "waxy" cell wall makes them acid-fast positive and weakly gram-positive.

The genus comprises a majority of fast-growing members: these are saprophytic organisms, widespread in water and soils. The slow-growing members are characterized by generation times of 12 to 36 hours, and some species in this group have evolved into highly successful pathogens, causing acute and chronic diseases across a variety of hosts (figure 1.1, from reference 2). Amongst these species are the *M. tuberculosis* Complex (MTC), that causes tuberculosis (TB) in humans (*M. tuberculosis*, *M. africanum*) and in other mammals (*M. bovis*, *M. microti*); *M. leprae*, that causes leprosy in humans; *M. marinum*, responsible for fish infections; and finally the *M. avium* Complex (MAC), on which we will now focus[1,2].

1.1) *Mycobacterium avium* ssp. *paratuberculosis*

The *Mycobacterium avium* Complex (MAC) refers to a group of slow-growing mycobacteria, prevalent in environmental, as well as in veterinary and human clinical settings, that display significant phenotypic and genomic heterogeneity[3–5].

Historically, the classification of MAC organisms was based solely on phenotypic features, such as growth characteristics, morphology, and ability to cause disease in naturally- or experimentally-infected animals. Soon after the identification of *M. tuberculosis* as the causative agent of human TB by Robert Koch (1882), it was recognized that a similar disease occurring in wild and domesticated fowl (avian TB) was also caused

by a mycobacterium. However, this "avian tubercle bacillus" possessed phenotypic characteristics that made it clearly different from the mammalian isolates *M. tuberculosis* and *M. bovis*; thus it was named *Mycobacterium avium*. The same microorganism was later found to cause disease in a wide variety of hosts, predominantly swine, but also cattle, sheep, deer, etc., while humans were seemingly resistant to infection. Despite this, several reports were published in the following decades on human infections caused by "anonymous" or "atypical" acid-fast organisms resembling *M. avium* (see chapter 7 in reference 6).

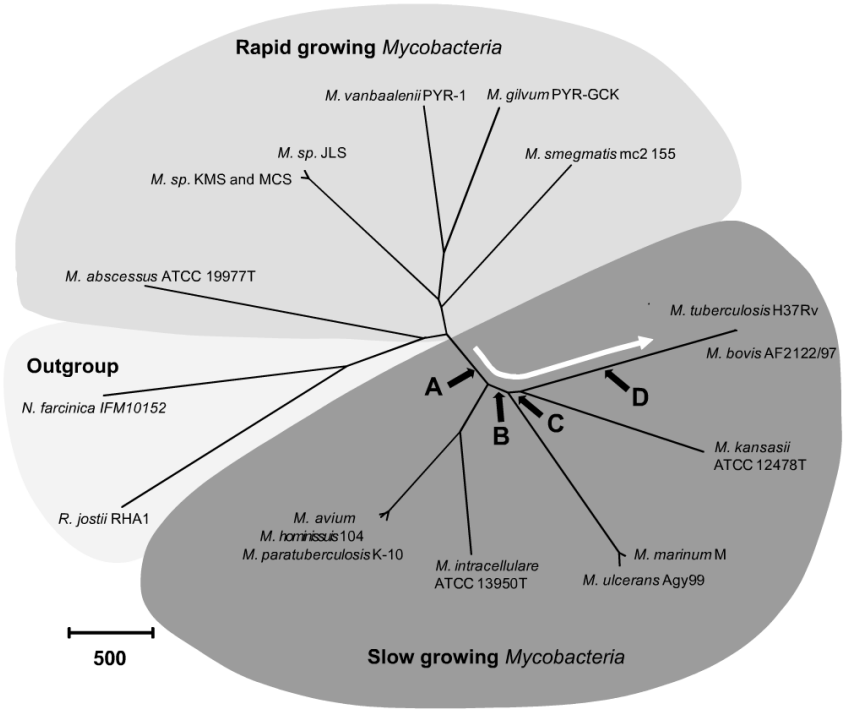

Figure 1.1: Phylogeny of Mycobacterium genus and schematic representation of acquisition of foreign genes at different strata of evolution.
The different mycobacterial lineages, based on slow-growing versus rapid-growing organisms, are indicated. The arrows indicate schematically the positions of the different list of horizontal gene transfer during the step-wise evolution of slow-growing mycobacteria. The scale represents the number of amino acid differences. From reference 2.

Collaborative effort attempting at collecting, analyzing and classifying these various strains of "non-tuberculous mycobacteria" in a coherent and unifying manner kept on going throughout the 20th century; it eventually led to the demonstration that some members of the MAC could behave as actual human pathogens. It is out of the scope of this introduction to review in detail these various classifications, and there is a vast body of literature that summarizes the long and tedious path that led to a clearer understanding of the MAC phylogeny[3–5]. Beyond their historic interest, these papers tell a “scientific story” that exemplifies well the notion that taxonomic classifications are inherently limited by the characteristics of the tools they are based on. Furthermore, it illustrates two notions that apply to the whole mycobacterial genus and attest to the complexity of its biology: 1) that hundreds of members of a set of genetically related microorganisms are endowed with such a wide range of phenotypic characteristics and virulence capabilities; and 2) that the same isolate can be either harmless or pathogenic in different individuals within one given species, which is a strong indicator of the importance of host factors in the susceptibility to mycobacterial diseases.

In 1990, Thorel et al. proposed a classification of the MAC based on both phenotypic and genetic features, which comprised 4 main sub-species: *M. avium* ssp. *avium*, *M. avium* ssp. *silvaticum*, *M. avium* ssp. *intracellulare*, and *M. avium* ssp. *hominissuis*[7]. Since then, the advent of molecular methods has allowed to identify variable genetic elements (including insertion sequences (IS) and large sequence polymorphims (LSPs)) specific to each sub-species, which was the basis for the more recent taxonomic classification illustrated by the phylogenetic tree presented in figure 1.2 (copied from reference 5). *Mycobacterium avium* ssp. *avium* (ATCC 25291) designates the causative agent of avian TB, but also includes agents of disseminated disease in patients with AIDS, cervical lymphadenitis in children, and chronic lung infection in adolescents with cystic fibrosis and in older adults[3]. *M. avium* ssp. *silvaticum* (ATCC 48898) applies to the previously named "wood pigeon bacillus", an acid-fast organism causing TB-like lesions in this bird species. *M. avium* ssp. *intracellulare* (ATCC 13950) was isolated in 1949 from a young girl deceased from a disseminated infection, and later found to be identical to the "Battey bacillus", responsible for chronic pulmonary infections in humans[3]. *M. avium* ssp.

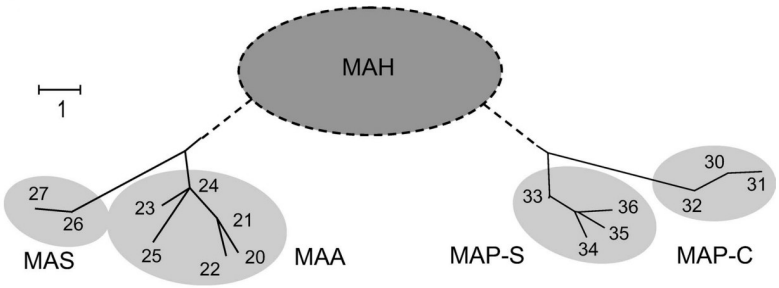

Figure 1.2: Expanded sub-tree of the *M. avium* ssp. *paratuberculosis* branch and expanded sub-tree of the *M. avium* ssp. *avium* and ssp. *silvaticum* branch.
Scale bar, 1 nucleotide difference. From reference 5.

hominissuis (MAH) refers a group of microorganisms with considerable genetic heterogeneity that are mostly prevalent in the environment but can also be responsible for opportunistic infections in humans and in swine, as the reference strain (MAH strain 104) was isolated from an AIDS patient in the early 1990s[3].

Finally, *Mycobacterium avium* ssp. *paratuberculosis* is the agent of paratuberculosis, a chronic intestinal infection of ruminants (also called Johne's disease when it affects cattle)[6,8,9]. Its phylogenetic evolution has been studied in detail by members of Dr. Behr's lab by using multilocus sequence analysis of 10 conserved genes in 56 strains of *M. avium*, and subsequently polymerase chain reaction (PCR)-based amplification of LSPs in 23 strains[4,5]. They have showed that MAP has evolved from a putative *M. avium* ssp. *hominissius* ancestor in 2 phases of genomic reshaping (represented in figures 1.2 and 1.3): first by the acquisition of 6 LSPs (comprising ~ 125 kb of new genetic material with 82 putative open reading frames (ORFs)), followed by a second phase of reductive genomics. MAP strains can be divided in 2 major groups (or strain types) based on their growth characteristics, host preference, and pathogenicity (see reference 5 and chapter 12 in reference 6). Historically, these strain types were initially named according to the species from which they had been first isolated, and were designated as type S (sheep) and C (cattle). Since it later appeared that MAP could be isolated from a wide range of mammalian hosts, and that the species of origin was not necessarily indicative of the strain type, the nomenclature was changed to type I (S type) and type II (C type). Recently,

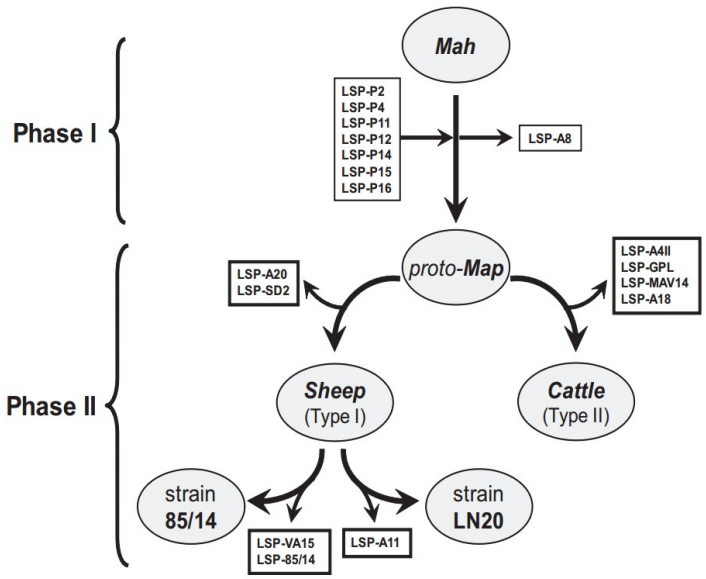

Figure 1.3: Biphasic evolution of modern *M. avium* spp. *paratuberculosis* strains
Phase I: emergence of the original pathogenic clone of *M. avium* ssp. *paratuberculosis* (proto-MAP) from a strain of *M. avium* spp. *hominissuis* via acquisition of novel DNA and polymorphisms shared by all modern strains. Phase II: subsequent differentiation of two major M. avium ssp. *paratuberculosis* lineages (sheep and cattle) and individual strains via genomic deletion events. From reference 4.

whole-genome comparison studies (conducted in part in the Behr lab) provided molecular data supporting this classification by defining regions of the genome specific to each one of these 2 strains[5].

1.2) Johne's disease

MAP has been proven, through the fulfilment of Koch's postulates, to be the causative agent of a chronic gastrointestinal infection of ruminants named paratuberculosis, or Johne's disease[8,9].

1.2.1) Historical background

The first reports of a "wasting" or "consumptive" disease in cattle date from the early 19th

century. In 1894, Drs. Johne and Frothingham, two veterinarian pathologists, proceeded to the pathological examination of the intestines of a cow that had died of such disease. They noted a thickened intestinal mucosa, enlarged lymph nodes, and under the microscope they reported the infiltration of the gut wall by leukocytes, epithelioid and occasional giant cells. Using an acid-fast stain, they observed abundant red-staining bacteria throughout the inflamed tissues; on the basis of distinct phenotypic characteristics (inability to reproduce the disease after inoculation to guinea pigs), they concluded that this microorganism was not a member of the MTC. The two pathologists proposed to name the disease "pseudotuberculosis enteritis" (partly in recognition of its pathological similarity to intestinal TB), and its yet uncultivable agent was coined *Mycobacterium enteriditis chronicae pseudotuberculosae bovis*. Several reports of the same disease were published in the following years, and its name was changed to Johne's disease in 1906 (see chapter 1 in reference 6).

In 1912, British scientist Frederick William Twort observed very small colonies on tissue cultures from diseased animals confined to the area immediately surrounding colonies of a contaminating organism called *Mycobacterium phlei*. Suspecting that the *M. phlei* bacteria were contributing an essential nutrient to the growth of the smaller colonies, he discovered that a culture medium containing heat-killed *M. phlei* could support the growth of this novel organism[10]. The ability to grow MAP in pure culture would then lead to the fulfilment of Koch's postulates, when in 1914 Twort was able to successfully reproduce Jonhe's disease in experimentally infected cattle[11]. It was not until much later that the specific growth factor provided by *M. phlei* was discovered to be mycobactin, a type of iron-binding compound (siderophore) normally produced by mycobacteria (and absent from MAP type II strains due to a defective biosynthesis pathway).

1.2.2) Epidemiology

MAP mainly infects ruminants (mainly cattle, sheep and goats) but has a wide host range (with infections reported in many species, including badger, bison, camelids, deer, elk, fox, non-human primates, rabbits, dogs and swine). Research efforts to describe the epidemiology of MAP infection stem mostly from its economic impact on the farming

industry, and has thus mainly concentrated on dairy and beef cattle. There have been few surveys in non-bovine animals, which makes it difficult to interpret with confidence the observed differences in infection rates between species: these could be due to a true host preference, or could reflect a difference in infection opportunity (influenced by human agricultural practices for instance), or even be due to a biased estimation towards those species that are most economically important to humans (see chapters 2 and 3 in reference 6).

Even in domesticated cattle, the actual prevalence of MAP infection is difficult to estimate. The main reason for this is that there exists to this date no reliable, validated, commonly accepted set of diagnostic tools to: 1) detect (let alone quantify) with sufficient sensitivity and specificity, in a timely manner and at reasonable cost, the presence of the bacterium in a living animal; and 2) differentiate between asymptomatic MAP infection and MAP-driven disease, nor between different stages of the disease itself (see chapters 22 to 24 in reference 6).

However, it is clear that MAP infection is world wide, affecting now most countries with a significant dairy industry, having spread on all 5 continents since its first reports in Europe in the early 1900s. The herd-level prevalence of MAP infection was calculated at approximately 10% during the 1990s, and current estimates have between 30% and 50% of dairy cattle herds in Europe and North America infected[12,13]. In the United States, losses to the cattle industry have been estimated at $1.5 billion per year[14].

1.2.3) Clinical evolution

MAP is transmitted primarily through the faecal-oral route, either by direct ingestion of MAP-contaminated feces or indirectly via manure-contaminated colostrum, milk, water or feed[8,9]. However, transmission of MAP from infected cows has also been documented to take place *in utero*, and through MAP-contaminated milk.

MAP infection is most often acquired by calves during neonatal age. Both observational and experimental studies have documented a clearly age-dependent infectious susceptibility profile, at least in cattle, with minimal infectious doses ranging from 10^3 to 10^6 CFUs in calves; in any case, with concentrations of MAP in feces of diseased

animals estimated at 10^6-10^8 CFUs per gram of feces, only a few milligrams of manure ingested by a young calf can lead to a productive infection (see chapter 14 in reference 6). Older heifers and steers can also become infected, as age-dependent resistance can be overcome with an increased infectious pressure (higher doses and/or repeated exposure).

The incubation period (time between ingestion of the bacteria leading to establishment of a productive infection and occurrence of clinical signs) is prolonged: it has been estimated to be ~ 5 years in cattle, ranging from 2 to 10 years, and is probably slightly shorter in goats and Cervidae.

The natural history of MAP infection has been divided into four stages, depending on the severity of clinical signs and the potential of fecal shedding of MAP in the environment. Stage I corresponds to the initial infection of a calf and is asymptomatic: MAP is ingested, transported passively along the lumen of the intestinal tract, translocates across the jejunal and ileal mucosa where it replicates transiently, spreads to the draining mesenteric lymph nodes and establishes a chronic yet silent infection. At this stage, there is only minimal and transient fecal shedding of MAP, if any. Stage II refers to adult animals that are still asymptomatic, have a slightly higher MAP tissue burden, and become active fecal shedders (thus serving as sources of contamination for other animals). Clinical signs appear at stage III: diseased animals display gradual weight loss despite conserved appetite, and eventually emaciation; milk production dampens (which often leads to the culling of the animal). MAP population in the intestinal mucosal cells is high; the normal absorptive capacity of the bowel is abrogated, leading to a protein-losing enteropathy responsible for chronic diarrhoea (with high shedding of MAP). Progression to stage IV takes a few weeks to months: animals become cachectic, and usually have permanent and profuse diarrhoea: most animals are culled at this stage, or death occurs as a result of dehydration (reviewed in chapter 14 from reference 6).

Interestingly, not all infected animal progress to disease (which is another reason why a clear understanding of the epidemiology of MAP infection has not been achieved yet): stating that diseased animals only reflect the "tip of the iceberg", investigators have estimated that for every cow in stage IV, it is likely that 15 to 25 others are infected at stage I. However to this date, the factors that mediate the progression from initial infection

to clinical disease are still far from totally uncovered.

Finally, it is worth noting that there exists some variations in the symptomatology across species: most notably goat and sheep at late stages of the disease seldom display diarrhoea.

1.2.4) Histopathology

Paratuberculosis in ruminants is a characterized by a chronic enteritis and a mesenteric lymphadenopathy predominant in the distal ileum[8,9]. On gross examination, the gut wall appears thickened, oedematous, the mucosa thrown into transverse ridges; the mesenteric lymph nodes are enlarged, there may be cording of the subserosal lymphatic channels which become palpable.

On histology, the gut mucosa is infiltrated with foci of epithelioid macrophages, lymphocytes and plasma cells (see figure 1.4, from reference 8). Granulomas are characteristic: they result from the fusion of activated macrophages in giant multinucleated cells surrounded by a crown of activated lymphocytes; they are found both in the gut wall

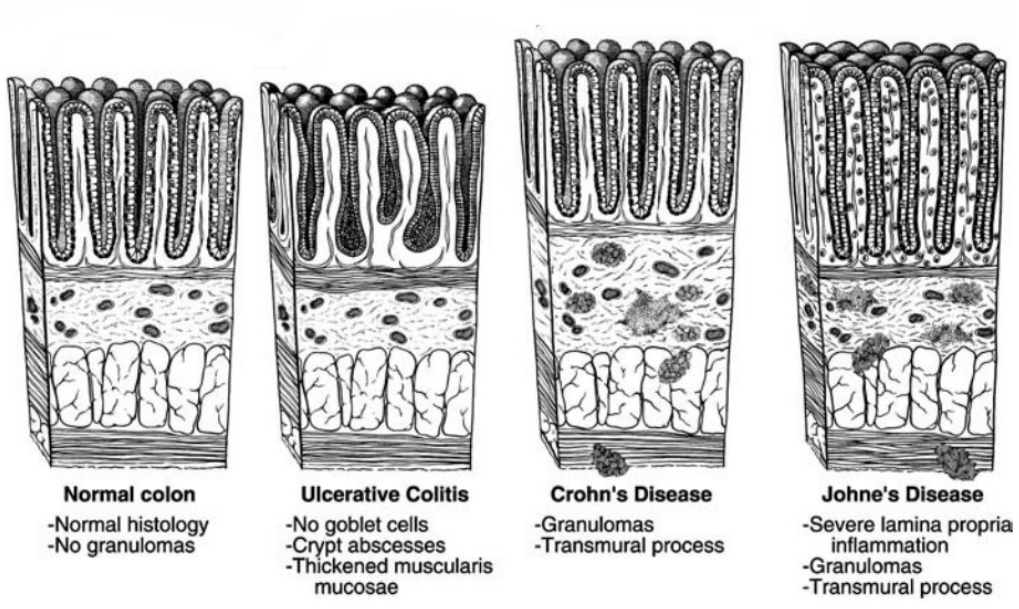

Figure 1.4: Schematic intestinal histology of humans and animals with normal and inflammatory conditions.
From reference 8.

and in the adjacent lymphatic system. Lesions are patchy (segmental) and present in all layers of the gut wall (transmural pathology)[8]. Necrosis is uncommon in cattle but sheep, goats and deer sometimes develop foci of caseation with subsequent calcification of granulomas.

Foci of acid-fast cocco-bacilli corresponding to MAP are usually visible after Ziehl-Neelssen (ZN) staining, most abundant in areas of active inflammation (especially granulomas), both in the intestine wall and in the adjacent mesenteric lymphatics and lymph nodes. In sheep and goat, some animals present a reduced bacterial burden, which has led to the description of two forms of the disease, in reference to leprosy[15]: multi-bacillary (> 10 acid-fast bacteria per macrophage) and pauci-bacillary (< 10 acid-fast bacteria per macrophage) (see chapter 15 in reference 6).

Extra-intestinal involvement is not common and usually limited to acid-fast-loaded granulomas in the liver (mostly seen in cattle).

1.2.5) Pathogenesis

a- Mammalian immunity to mycobacteria

Macrophages are specialized phagocytic cells that, as part of the innate arm of the mammalian immune system, constitute the first line of defence against pathogenic mycobacteria. They can sense and interact with pathogens through the expression of pattern-recognition receptors (PRRs) (such as Toll-like receptors (TLRs) and Nod-like receptors (NLRs)) that recognize highly conserved molecular motifs expressed by microorganisms named pathogen-associated molecular patterns (PAMPs). Pathogens are engulfed and trapped in phagosomes, and subsequently delivered to lysosomal compartments displaying an acidic content and a high concentration of hydrolytic enzymes, reactive oxygen species (such as $O_2^{\bullet -}$, H_2O_2, and $OH^{\bullet}$) and reactive nitrogen species (such as NO), which culminates in their elimination[16,17].

Dendritic cells (DCs), on the other hand, have reduced bactericidal capabilities, but are the only antigen-presenting cells (APCs) that can activate naive T lymphocytes. They capture microorganisms by phagocytosis and present their fragmented antigens at the cell surface, bound to major histocompatibility complex (MHC) molecules. They interact with

antigen-specific T cells in secondary lymphoid organs and activate them (in part through the expression of co-stimulatory molecules) to migrate back to the site of infection, where they can then mediate their functions (cytotoxicity for CD8+ T cells, orchestration of the adaptive response for CD4+ T cells). DCs are also capable to drive the orientation of the CD4+ T cell response either towards a T helper 1 (Th1) (as is the case during mycobacterial infections), Th2 or Th17 cytokine profile[16,17].

The cooperation between macrophages and CD4+ T cells is at the core of the adaptive immune response to mycobacteria[17]. Macrophages infected with mycobacteria produce pro-inflammatory cytokines such as interleukine-1 beta (IL-1β), IL-12, IL-18 and tumor necrosis factor-alpha (TNF-α), which activate CD4+ T cells. In return, activated CD4+ T cells secrete interferon-gamma (IFN-γ), a pro-inflammatory cytokine that has a pivotal role in immunity to mycobacteria, as evidenced by the high susceptibility of humans who have naturally occurring mutations in their IFN-γ receptor genes, as well as mice that lack expression of IFN-γ or its receptor due to targeted mutations (reviewed in references [17–19]). By regulating the expression of more than 1,200 genes in target cells, INF-γ mediates most cellular processes that constitute the macrophage bactericidal program[20,21]. This auto-reinforced interplay between macrophages and CD4+ T cells culminates in the formation of granulomas, specialized structures designed to contain the replication of the bacteria[22,23] (as exemplified in figure 1.5, from reference 17).

b- MAP infection

MAP infection process starts after the ingestion of the bacteria and their translocation across the intestinal epithelium. The gut-associated lymphoid tissue (GALT) in ruminants is organized in aggregates named Peyer's patches, above which are found a distinct type of enterocytes named microfold cells (M-cells); these cells are devoid of phagocytic capacities and physiologically deliver bacterial antigens to underlying APCs by transcytosis[24]. MAP preferentially interacts with M-cells through fibronectin attachment proteins, but can also cross the intestinal epithelial barrier by translocating across classical intestinal epithelial cells (IECs)[25]. It could also be taken up by intestinal dendritic cells protruding dendrites into the intestinal lumen to sample its content, after interaction between its cell wall glycolipid mannosylated lipoarabinomannan (ManLAM) and the

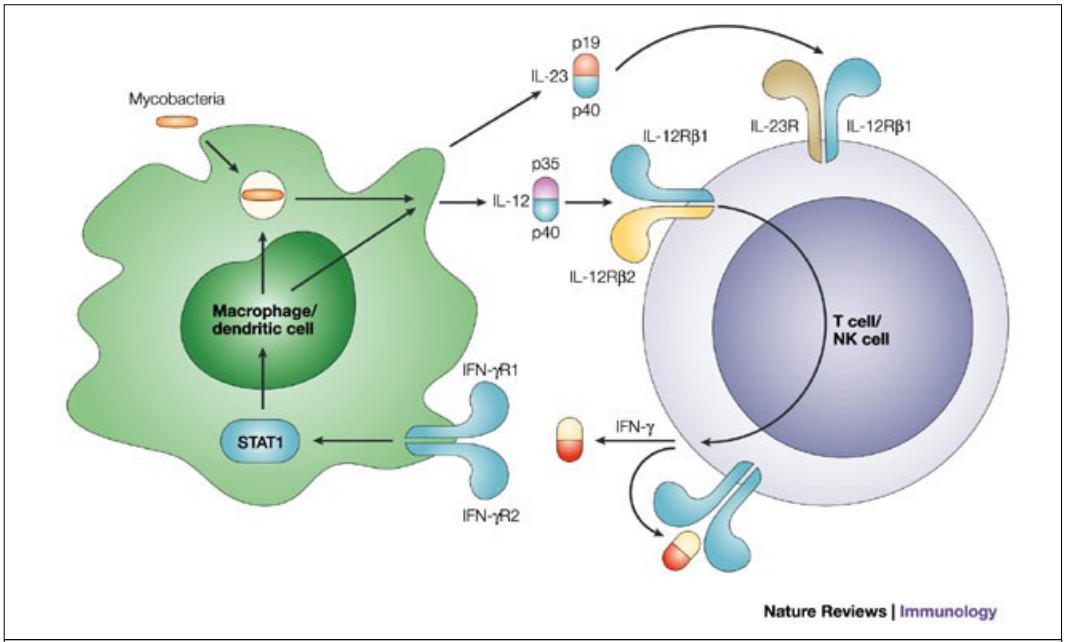

Figure 1.5: The IL-12/IL-23/IFN-γ loop and cooperation between antigen-presenting cells (macrophages and dendritic cells) and lymphocytes (natural killer and T cells).
After infection with mycobacteria, primary host response cells, such as macrophages, release a range of cytokines, including interleukin-12 (IL-12) and IL-23, which stimulate T and natural killer (NK) cells to secrete interferon-gamma (IFN-γ). IFN-γ activates macrophages to kill intracellular pathogens. Mutant molecules in patients with the syndrome of Mendelian susceptibility to mycobacterial disease (MSMD) are indicated in blue. From reference 17.

dendritic cell receptor DC-SIGN (reviewed in chapter 11 from reference 6; see also figure 1.6).

After invasion, MAP is at the baso-lateral side of the epithelium, into the sub-epithelial dome of the Peyer's patch; its next encounter is a macrophage, or a dendritic cell. MAP, like most pathogenic mycobacteria, is endowed with the striking ability to survive for prolonged periods of time within activated macrophages[26], a feature that could have been evolutionary selected from growth in protozoa[27]. This is due to a combination of molecular tools that inhibit the successive fusion events that constitute the phagosomal maturation process[28]. There is evidence, for instance, that phagosomes containing live MAP organisms acidify less (pH ~ 6.0-6.3) than phagosomes containing heat-killed MAP or avirulent mycobacteria (which attain pH ~ 5.0-5.5); similarly, MAP can survive for up to 15 days during *in vitro* culture in the J774 macrophage-like cell line, when the environmental

M. smegmatis is completely cleared after 48 hours[29]. MAP has also evolved strategies to avoid the activation of T lymphocytes by actively down-regulating the expression of MHC class I and II molecules in macrophages and in DCs, thus impairing the presentation of antigens at their surface[30,31]. Due to its ability to dampen innate and adaptive immune mechanisms, MAP is able to survive its primary encounter with the host, following which it is transported within APCs to the draining mesenteric lymph nodes. There, it enters a phase of chronic yet silent infection (with only minimal pathology at the site of entry)[9,32].

There is still activation of a lymphocyte-mediated response towards MAP at the early stage of the infection; initially CD4+ T cell activation is skewed towards a Th1 response, with lymphocytes secreting high amounts of IFN-γ, IL-2 and TNF-α, which allows for the initial control of the bacterial replication[8,9,32]. There ensues a state of equilibrium where bacterial survival and killing by macrophages are in balance: this corresponds to the sub-clinical phase of JD, with limited pathology and low bacterial burden (see chapter 21 from reference 6).

The transition of paratuberculosis from a subclinical to a clinical state is associated

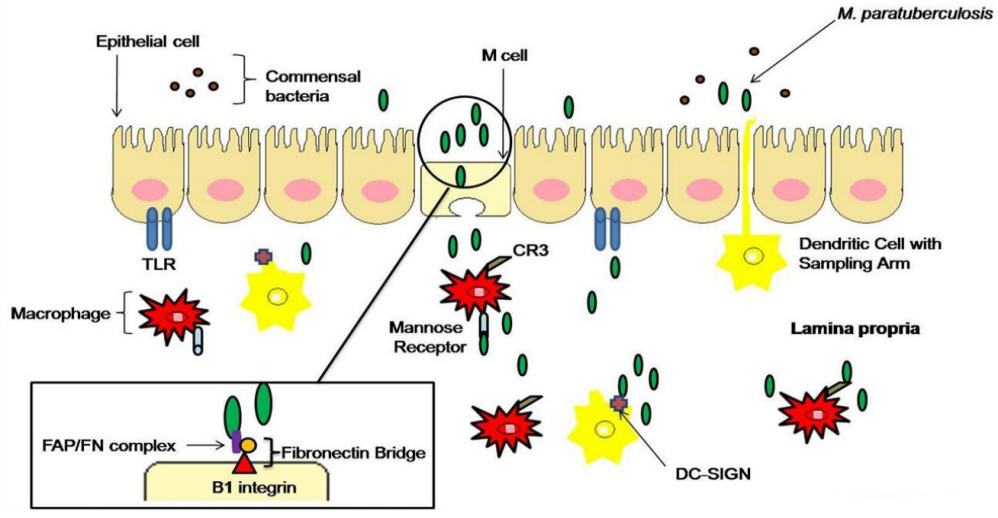

Figure 1.6: MAP infection pathogenesis.
MAP preferentially crosses the intestinal epithelial barrier through M-cells above Peyer's patches. Transcytosis of MAP across M-cells is dependent upon generation of fibronectin bridges. Alternatively, MAP may directly invade epithelial intestinal cells. From chapter 11 of reference 6.

with a switch from a Th1- to a Th2-oriented cytokine response[9]. The production of Th2 regulatory cytokines (IL-4, IL-5, IL-10) supports a humoral immune response characterized by the expansion of B lymphocytes and secretion of immunoglobulins (which have little role in controlling an intracellular pathogen like MAP), and the down-regulation of Th1-mediated immunity (as for instance IL-4 and IL-10 have been shown to suppress the production of IFN-γ by CD4+ T cells)[16]. The activation CD4+CD25+ regulatory T cells may also have a role in the progression of the disease through the synthesis of anti-inflammatory cytokines (IL-10, transforming growth factor beta (TGF-β))[32]. MAP replication inside of macrophages becomes uncontrolled, with higher bacterial burden in both the intestine wall and its draining lymph nodes. There ensues a continuous recruitment of immune competent cells and the progression of immune-mediated lesions (histiocytic infiltrates, granulomas) that constitute the histological hallmark of JD.

1.2.6) Animal models of MAP infection

It is beyond the scope of this introduction to dwell on the many animal models developped in MAP research, and the interested reader is invited to refer to two recent review papers that summarize over 50 years of research in experimental MAP infections, both in large ruminants and in smaller animal models[33,34]. Notably, Hines and colleagues have attempted to establish international standard guidelines by defining the parameters essential to the development of long-term and short-term models in each species tested so far, hoping it "would gain acceptance worldwide"[33].

Conceptually, bovine models of paratuberculosis are ideal because cattle is the natural host of MAP; they are generally used for studies of host-pathogen interactions and immune responses, vaccination studies, testing of novel diagnostic assays and therapeutics, as well as long-term pathogenesis studies (see chapter 19 from reference 6). However, bovine models present major limitations that explain why they only account for a minor part of the MAP literature, including the requirement for specialized large animal facilities, the high cost and duration of studies (infected calves need to be contained for a minimum of 2-3 years before disease onset), the absence of adequate laboratory reagents, etc.

Therefore, more approachable small animal models have been developed, including guinea pigs, rabbits, chickens, hamsters... and of course mice, which represent the forefront animal model in paratuberculosis, essentially because they prove easy alternatives to the hurdles encountered when working with cows and goats (see chapter 20 in reference 6). Given the vast repertoire (and relative affordability) of immunological reagents and genetically distinct breeds, mice serve as a model for testing the virulence of MAP mutants, conducting early candidate vaccine studies, and most importantly dissecting host-pathogen interactions.

Nevertheless, the use of mice to reproduce paratuberculosis in the laboratory is hindered by a series of factors. First, there exists a significant variability in the susceptibility to MAP of the most conventionally used strains of laboratory immunocompetent mice, with susceptible breeds (such as BALC/c[35] and C57Bl/6[36,37]), and resistant ones (such as C3H[37]) in which there is only transient pathology and rapid bacterial elimination. To add further complexity, the outcome of the infection (in terms of bacterial colonization and pathological findings) in one given strain of mice still varies with the infective dose, and with the route of administration[33,34]. Second, MAP-infected mice do not accurately recapitulate the clinical disease that is paratuberculosis (see chapter 20 from reference 6): they do not display its characteristic clinical symptoms (notably the diarrhoea); they most commonly do not shed bacteria in their feces (which is considered a key event leading to the transmission of MAP); and finally the vast majority of immunocompetent strains do not get infected if challenged orally[36] (which is why the current recommended route of infection is intra-peritoneal[33]). Finally, mice fail to reproduce the key histopathological features of JD: they present granulomatous pathology after intra-peritoneal infection, but it is usually limited to the liver and the mesenteric lymph nodes[38]. Intestinal pathology, especially of the severity of that seen in affected cattle and sheep, has never been reported after an intra-peritoneal infection of immunocompetent mice[39], and there exists only one report on such lesions after gavage infections: to achieve this, investigators had to use germ-free *nu-/-* athymic mice, born and raised in sterile isolators, infected with 10^{10} CFUs of MAP by gavage, and respect an incubation period of 6 months for the first intestinal lesions to appear[40,41].

Therefore, as stated in reference 34, even if "in experimental animal research there is always a trade-off between what can be achieved with the resources available and what is ideal, [in paratuberculosis] there is room for improvement in the way models have been designed and carried out to date."

1.3) Crohn's disease

Inflammatory bowel disease (IBD) is a general term that describes a group of chronic intestinal inflammatory disorders of unknown or still unproven etiology in humans. It can be divided in two major groups, ulcerative colitis (UC) and Crohn's disease (CD)[42–44].

1.3.1) Historical background

Crohn's disease was first described in 1904 by Polish surgeon Antoni Leśniowski. It was later named for American gastroenterologist Burrill Bernard Crohn, who in 1932, in collaboration with fellow physicians Leon Ginzburg and Gordon D. Oppenheimer, published a thorough description of this then-unknown intestinal disorder they called "regional ileitis".

1.3.2) Epidemiology

IBD affects millions of people worldwide; its prevalence in North America is approximately 200 per 100,000, is unevenly distributed (higher in urban than in rural areas and in some populations, such as the Ashkenazi Jews), yet is overall on the rise. IBD may affect male and female equally, with a peak age at onset between 15 and 25 years of age[44].

1.3.3) Clinical evolution

CD shows a wide variability in severity and both spatial and temporal evolution across patients, but typically evolves in any given individual in a relapsing and remitting pattern. As there is to date no cure for CD, patients alternate between periods of stability and flare-ups, the latter potentially leading to sequelae that are responsible for a progressive

worsening of the symptomatology.

The main symptoms encountered by patients with CD are abdominal pain and intermittent diarrhoea (which can be accompanied by rectal bleeding, fecal urgency, tenesmus, especially in case of colic involvement)[45]. Other manifestations include aphtous ulcers, fistulas, phlegmons and abscesses, anal fissures. Systemic symptoms can be observed: there can be low-grade fever (mostly during severe relapses), fatigue, malnutrition, as well as certain specific extra-intestinal manifestations, such as central or peripheral arthritis, uveitis, iritis, and episcleritis, primary sclerosing cholangitis, etc.

1.3.4) Histopathology

Whereas UC is characterized by diffuse and superficial mucosal inflammation affecting only anus, rectum and colon, CD can affect any segment of the gastrointestinal tract, from mouth to anus[46]. One salient feature of CD is its segmental pathology, with spared areas of normal mucosa surrounded by inflammed tissue, a characteristic that gives the disease a macroscopic patchy or “cobblestone” appearance (see figure 1.4, from reference 8).

On gross examination, the gut appears thickened and oedematous, hyperemic; there are aphtoid lesions on the mucosal side, that become confluent and form ulcers, and inflammed lymphatics on the serosal side. Characteristic lesions appear at latter stages of the disease: fistulas (abnormal communication between the inflamed intestinal tissue and adjacent organs) and fibrotic strictures (that can result in gut stenosis and obstruction). Finally, patients with CD have an increased risk of developing small bowel and colorectal cancers (relative risk ~ 30 and ~ 2, respectively)[47].

Characteristic histological features of CD is that inflammation in the gut is focal (foci of immune cells on a background of normal mucosa) and transmural (affecting all layers of the gut). Mucosal abnormalities include: aphtoid ulcers and fissures at the surface of the epithelium, neutrophil abscesses at the base of the crypts, oedema in the mucosa and in the sub-mucosa. Foci of inflammatory cells are composed of macrophages and lymphocytes; immunohistochemical analyzes show an enrichment in CD4+ T cells, CD8+ T cells and plasma cells[48]. Granulomas, usually considered a hallmark of CD, are seen in ~ 50% of patients. Histological abnormalities can be seen in the enteric nervous system

(hypertrophy and hyperplasia of nerve fibres and alterations of neuronal cell bodies), the vascular system (infiltration of blood vessels and obliterative lesions), and the lymphatics (oedema, cellular infiltrates and granuloma in the lymphatics nodes and channels). Fibrotic lesions affect both the gut itself and the adjacent mesentery. Metaplastic lesions in the epithelium of the colon or small intestine can be seen at later stages.

1.3.5) Pathogenesis

Attempting to write a coherent and concise summary of the recent literature on the pathogenesis of Crohn's disease is a daunting task: it is overwhelmingly abundant, and filled with contradictory messages. We conducted a search in Pubmed to retrieve review articles published on the pathogenesis CD and IBD in a set of 17 top-ranked biomedical journals during the last 10 years (the details of the search methodology are presented in table 1.1). We retrieved a total of 21 articles, and despite the breadth of the topics covered, we found that one sentence was mentioned 16 times with little variation across papers: "The widely accepted hypothesis for disease pathogenesis is that CD is caused by an overly aggressive immune response to bacterial antigens in genetically predisposed individuals"[8,42–44,49–65].

Thus, we will try to summarize in the next paragraphs what has been written on the role of these three factors in the development of CD: immune response, environmental factors (including microbial antigens) and genetic predisposition.

a- Immunopathology

That CD is in essence an immune-mediated disease has long been suggested, most simply due to its characteristic tissue lesions (infiltrates of immune cells)[48], but also by the fact that patients often respond to immunosuppressive therapies[66] or by the reports that CD could be cured in patients receiving allogeneic hematopoietic stem cell transplantation (HSCT)[67]. 3 models have been proposed: 1) autoimmunity; 2) immune dysregulation; and 3) immune deficiency[68].

First, there is (to our knowledge) no formal proof that CD is autoimmune, simply because there has never been proven that one auto-reactive B or T lymphocyte clone could recapitulate the disease upon experimental transfer to a laboratory animal[67–69].

As for the immune dysregulation hypothesis, there is an abundance of research that aimed at documenting the many immunological abnormalities observed in CD (reviewed in 69). It has for instance been reported that isolated CD mucosal T cells showed enhanced proliferation and increased production of pro-inflammatory cytokines when exposed to bacterial antigens[70]; that B cells extracted from intestines of patients with CD had major alterations of immunogloblulin synthesis[71]; that there is increased production in the intestinal mucosa of CD patients of the Th17 cytokine IL-17[61,64,72] and the Th1 cytokines INF-γ and TNF-α[73]; that leukocyte adherence and recruitment are increased in the microvessels of CD-affected intestine[74], etc. However this literature is rendered extremely complex to interpret (let alone summarize) by the fact that it combines studies on human with CD, and studies on murine models of colitis (most often triggered by a chemical insult to the gut) that lack the characteristic clinical and histopathological features of CD. Furthermore, methodological limitations of such studies make it rarely possible to document a clear causal role of such abnormalities: a detailed examination of the way the immune system is dysfunctional in CD does not inform necessarily, in itself, on the factors that trigger such dysfunctions[67–69].

Finally, the immune deficiency model[75,76] was suggested long ago by work from Segal et al.[77], who demonstrated an impaired influx of granulocytes into the skin of CD patients upon bacterial exposure, a finding that was confirmed and extended to the gut in 2006[78,79]. A defective systemic immunity to bacteria in a disease characterized by overaggressive inflammation in the gut is paradoxical[67,80], but as is explained below, major genetic epidemiology studies carried out in the 2000s have also provided independent evidence in support of this hypothesis.

In conclusion, if much work has been done to document the many defects of the immune system of patients with CD (characterized either by an overreactive or impaired immunity), research efforts have not provided so far a clear view of whether and how these abnormalities lead to (or result from) the gut inflammation that is characteristic of CD.

Search #1	"Annu Rev Chem Biomol Eng"[Journal] OR "Annu Rev Biophys"[Journal] OR "Annu Rev Pathol"[Journal] OR "Annu Rev Genomics Hum Genet"[Journal] OR "Annu Rev Biomed Eng"[Journal] OR "Annu Rev Cell Dev Biol"[Journal] OR "Annu Rev Biophys Biomol Struct"[Journal] OR "Annu Rev Biophys Biophys Chem"[Journal] OR "Annu Rev Cell Biol"[Journal] OR "Annu Rev Immunol"[Journal] OR "Annu Rev Pharmacol Toxicol"[Journal] OR "Annu Rev Nutr"[Journal] OR "Annu Rev Public Health"[Journal] OR "Annu Rev Biophys Bioeng"[Journal] OR "Annu Rev Genet"[Journal] OR "Annu Rev Pharmacol"[Journal] OR "Annu Rev Med"[Journal] OR "Annu Rev Microbiol"[Journal] OR "Annu Rev Physiol"[Journal] OR "Annu Rev Biochem"[Journal]
Search #2	"Nature"[Journal] OR Nat Rev Gastroenterol Hepatol"[Journal] OR "Nat Rev Microbiol"[Journal] OR "Nat Rev Immunol"[Journal] OR "Nat Rev Genet"[Journal] OR "Nat Rev Mol Cell Biol"[Journal]
Search #3	"N Engl J Med"[Journal] OR "JAMA Intern Med"[Journal] OR "J Am Med Assoc"[Journal] OR "JAMA"[Journal] OR "Lancet Infect Dis"[Journal] OR "Lancet"[Journal] OR "Br Med J"[Journal] OR "Gut"[Journal]
Search #4	Crohn's disease[title/abstract] OR inflammatory bowel disease[title/abstract]
Final search	(Search #1 OR Search #2 OR Search #3) AND Search #4
Filters	Reviews Articles in English Date < 10 years Abstract available

Table 1.1: Details of search methodology in Pubmed for literature review on Crohn's disease pathogenesis.
The combination of search queries 1 to 4 allows to retrieve review articles published in a set of high-impact journals on CD and IBD pathogenesis.

b- Environmental factors

If CD is a genetic disorder, the role of environmental factors in its pathogenesis has long been recognized, for instance quite simply because the rate of concordance between monozygotic twins is not 100% (see below "c- Genetic predisposition" for details on these studies). Epidemiological association between higher prevalence of CD and environmental factors as diverse as breastfeeding, childhood infections, smoking[81], oral contraceptives, diet, hygiene, occupation, education, climate, pollution (...) have been reported[44]. The veracity of such associations, let alone the biological meaning of a potential causal link between these factors and CD, has still to be clearly demonstrated[82].

The role of potential bacterial triggers has however been investigated in more

detail[51,52,57]. The potential role of bacteria in CD pathogenesis is first suggested by the observation that in most experimental models, gut inflammation does not develop spontaneously in animals raised in germ-free conditions[52]; and second, in humans affected with CD, antibiotic treatment has been reported to have benefits during flare-ups[66]. A traditional approach to identify microbial agents linked to IBD has been the demonstration of antibodies against known microorganisms, but essentially all patients with IBD have elevated titres of antibodies against bacteria, viruses, and fungi, making the mere presence of serum or intestinal antibodies of limited value. The same applied when cell-mediated immunity against microbes was assessed. This reactivity to enteric bacterial antigens likely represents a secondary sensitization to cross-reacting antigens or a nonspecific enhancement of immune reactivity[69].

The recent advent of culture-independent techniques, such as metagenomics and the large-scale analyzes of the 16S ribosomal RNA genes, has allowed an in-depth analysis of the composition of the intestinal microbiota in patients with Crohn's disease and healthy controls[50]. They have led to the finding that in patients with Crohn's disease, the abundance of members of the Firmicutes (Gram-positive bacteria, including *Clostridium* and *Bacillus* species) is decreased, whereas members of the Proteobacteria (Gram-negative rods, including *Escherichia* ssp.) are increased in comparison to healthy controls, a imbalance that has been termed "dysbiosis"[50,51]. However much variability exists across studies, and most importantly no experimental data has been produced so far that would implicate this dysbiosis as a causal factor in CD.

MAP has been suggested as a potential triggering agent in CD for now exactly a century[8,68,83,84]. The first reason for this is the quite obvious clinical and histopathological similarities between JD and CD, and the fact that MAP has been documented to induce chronic ileal granulomatous lesions in a wide host range, including non-human primates. Another strong argument for a role of MAP in CD is that several CD-predisposing loci have also been shown to modulate the host response to mycobacteria: 1) in genetic epidemiology studies, *NOD2* variants have been associated with not only CD, but also tuberculosis[85,86] and leprosy[87,88], and similarly, *IRGM* variants have been linked with CD and also with tuberculosis in certain populations[89,90]; 2) in experimental studies carried out by

independent groups (including in the lab of Dr. Behr), the role of these two genes in the immune response to different mycobacterial species has been confirmed (both in human and murine settings)[91–95]. In an attempt to fulfil Koch's postulates, numerous studies have attempted to isolate MAP in tissues from CD patients. In 1984, Dr. Rod Chiodini was able to cultivate MAP from such a sample[96], and the bacterium was later found to cause granulomatous lesions in the terminal ileum of baby goats fed with it[97]. However since then, similar attempts have been inconsistent. The search for MAP in CD patients is hindered mostly by the absence of validated diagnostic tests, making it hazardous to interpret with confidence the findings of research labs reporting on the isolation of MAP (or its antigens, or specific DNA fragments) in humans. A recent meta-analysis found that compared with individuals free of IBD, the pooled odds ratio for recovering MAP in tissue samples was 7.01 ($CI_{95\%}$ = 3.95-12.4) in studies using PCR-based assays, and 1.72 ($CI_{95\%}$ = 1.02-2.90) in studies using ELISA in serum[98,99]. However, because of the case-control design of the 28 studies included, it remains impossible to draw any conclusion of causality from this meta-analysis. And this is probably the major conceptual obstacle on the path to investigating the potential role of MAP in CD: because CD is by definition a human disease, attempting to fulfil Koch's postulates with MAP is unethical and will thus always remain impossible to carry out (see figure 1.7)[84].

Finally, it is worth mentioning the recent characterization of a group of *Escherichia coli* strains, named adherent and invasive *E. coli* (AIEC), that have been proposed to constitute a distinct pathovar associated with some cases of CD[51]. The first strain of this group (*E. coli* LF82) was isolated from a patient with CD in Lille (France) in 1998 on the basis of strictly phenotypic characteristics: 1) its ability to adhere and colonize a set of epithelial intestinal cell lines *in vitro*; and 2) its ability to survive in macrophages[100]. Since then, much work has been done to isolate new strains belonging to this pathovar[101,102], perform a complete genome sequencing of several of them[103,104], characterize their different virulence factors[105,106], etc. What this body of work suggests is that, if AIEC are to be implicated in some cases of CD, it is not as the result of their sole pathogenic properties, but in the context of a dysfunctional host-pathogen interaction: first AIEC are enriched in biopsies of CD patients, but they also colonize the gut of healthy individuals (one study for instance

showed a rate of recovery of 22% in CD patients, versus 6.2% in non-IBD controls[101]); and second it was also shown that AIEC pathogenicity was enhanced by host factors, such as the host adhesion receptor carcinoembryonic antigen-related cell adhesion molecule 6 (CEACAM6), expressed in the human gut[107]. As is the case for MAP, AIEC researchers are confronted with the impossibility of formally fulfilling Koch's postulates, and despite intensive research efforts, AIEC have not yet gained wide acceptance as a causal factor in CD pathogenesis.

c- Genetic predisposition

Familial aggregation in CD has long been known, most notably as a result of large studies conducted on twins more than 70 years ago, showing higher rates of concordance in monozygotic than in dizygotic pairs (~ 35% vs. 3% respectively, see reference 108). Interestingly, concordance between monozygotic twins applies to a range of phenotypic traits (location and temporal evolution of the disease), both at diagnosis and longitudinally[44]. Further indication of a genetic predisposition in CD comes from the higher relative risk of developing the disease in first-degree relatives of affected individuals[63], and

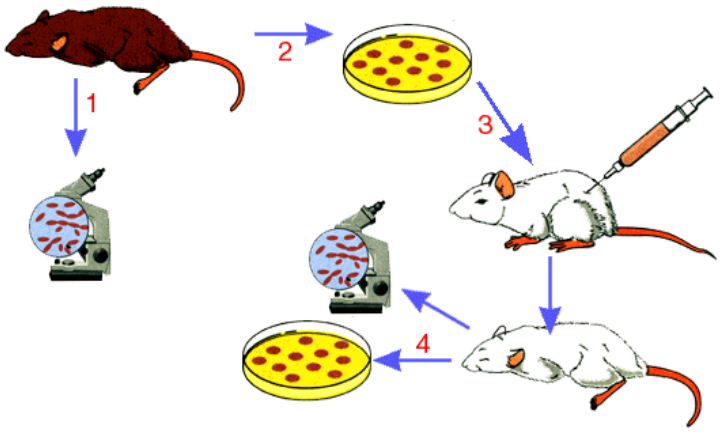

Figure 1.7: Schematic representation of Koch's postulates
The demonstration of an infectious cause for a disease traditionally necessitates the fulfilment of Koch's postulates. Due to the definition of Crohn's disease (CD) as a human disease, attempting to fulfil Koch's postulates with MAP (or other microorganisms) is unethical, which prompts researchers to explore the link between MAP and CD through alternative experimental strategies.

from the observation of CD-like lesions in certain genetically-determined primary immunodeficiencies (PID) (such as chronic granulomatous disease (CGD) for instance)[80].

In 2001, 2 independent family-based linkage studies identified *NOD2* as the first susceptibility locus for CD[109,110]. Since then, more than 10 genome-wide association studies (GWAS) and subsequent meta-analyzes have been conducted: IBD have clearly proven to be the most tractable of complex disorders for discovering susceptibility genes[63]. These genetic epidemiology studies have the inherent strength to be essentially "hypothesis-free": statistical analysis precedes biological plausibility[59]. GWAs point to susceptibility loci and shed light on pathways involved in disease pathogenesis, which in turn urges researchers to explore experimentally the biological significance of such genetic variation (that is, understanding how one mutation in one gene leads to a phenotype as complex and heterogeneous as CD). In such, GWAS have had a major impact of CD research and have led in some instances to real changes of paradigm.

To exemplify this, we will briefly review the contribution that had the discovery of CD-associated variants in three genes, namely *NOD2*, *ATG16L1* and *IRGM*, in our current understanding of CD pathogenesis. NOD2 is a pattern-recognition receptor that functions as an intracellular sensor for bacterial peptidoglycan[111]. Through its C-terminal leucine-rich repeat (LRR) domain, NOD2 recognizes a minimal bioactive component of peptidoglycan, muramyl dipeptide (MDP), which results in the activation of nuclear factor-κB (NF-κB) and mitogen-activated protein (MAP) kinase signalling pathways. The three main CD-associated *NOD2* variants (accounting for > 80% of the identified germline variants) are situated in or close to the LRR-domain, and all three led to a loss-of-function phenotype in studies using either cellular transfectants or primary human cells containing mutant NOD2. It is interesting to note here the impact of such findings: because of their unbiased nature, genetic association studies hinted towards a defective innate immune response towards bacteria, while CD was seemingly characterized by a dysregulated and destructive immune response; despite the apparent paradox, this discovery paved the way for intensive research efforts aiming at elucidating the role of innate immunity in CD pathogenesis. In a similar manner, the identification of *ATG16L1* and *IRGM*, encoding for two autophagy effectors, as susceptibility loci specific to CD, originated a vast body of work

on the molecular mechanisms leading from defective autophagy to intestinal inflammation[60]. Noteworthy, key functional links have been recently elicited between NOD2 and autophagy, as it was shown: 1) that NOD2 initiates autophagy by recruiting ATG16L1 to the cell membrane at the site of bacterial entry[112]; and 2) that dendritic cells from CD patients with *NOD2* or *ATG16L1* mutations are defective in autophagy, bacterial handling and antigen presentation[113].

Since the publication of the first report on the association between *NOD2* variants and CD, intense collaborative research work has been carried out to uncover new CD-associated genes: the most recent meta-analysis of GWAs in IBD was conducted on more than 75,000 patients and controls and identified163 loci associated with IBD (110 common to both UC and CD, 30 CD-specific and 23 UC-specific)[114]. These loci encode genes involved in a number of homeostatic mechanisms, amongst which: innate pattern recognition receptors (*NOD2, TLR4, CARD9*); the differentiation of Th17-lymphocytes (*IL-23R, JAK2, STAT3, CCR6, ICOSLG*); autophagy (*ATG16L1, IRGM, LRRK2*); maintenance of epithelial barrier integrity (*IBD5, DLG5, PTGER4, ITLN1, DMBT1,* and *XBP1*); the orchestration of the secondary immune response (*HLA*-region, *TNFSF15/TL1A, IRF5, PTPN2, PTPN22, NKX2-3, IL-12B, IL-18RAP, MST1*)[63].

Nevertheless, despite the considerable amount of data they have yielded to, genetic epidemiology studies have major limitations. First, in spite of their high sample sizes and statistical power, GWAs have only uncovered a minor part of the global genetic architecture of CD: even under the unproven assumptions that the > 160 susceptibility loci identified to date are individually causal and collectively additive, the relative risk conferred by each of them is extremely small (with odds-ration rarely > 3[114]), and their overall contribution calculated to account for less than 30% of total CD heritability[67]. Several explanations for this “missing heritability” exist, such as the yet unquantified impact of gene-gene interactions, epigenetic modifications, or gene-environment interactions. The second conceptual hurdle stems from the genetic overlap of IBD with other disorders[59]. The fact that the genetic predisposition to both CD and UC — despite their distinct phenotypic features — is underpinned by common gene variants can appear to be biologically plausible. That IBD also shares susceptibility loci with diseases as diverse as

alopecia areatia (*PRDX5, IL-2RA*), ankylosing spondylitis (*IL-23R, PSMG1* and *ERAP1/2*), psoriasis (*IL-23R, IL-12B* and *CDKAL1*), rheumatoid arthritis (*PTPN22, CCR6, FCGR2A, REL, PRDM1, IL-2/IL-21, TNFRSF14, IL2-RA* and *IRF5*) or even type 1 diabetes mellitus (*PTPN2, PTPN22, ORMDL3, IL-18RAP, IL-27, IL-10, IL-2/IL-21, IL-2RA, BACH2* and *TYK2*) is much less straightforward to understand. This has led Dr. Jean-Laurent Casanova to coin the term "missing intelligibility" to refer to the impossibility to use the vast amount of genetic data to conceive a unified and plausible immunological scenario for the pathogenesis of CD[67]. Finally, the most puzzling about the results of the GWAS is that, despite massive research efforts aiming at understanding how one gene variant translates into a defective function that could explain CD pathogenesis, the myriad of different experimental findings produced for each locus is most often too complex, partial and contradictory to offer one plausible unified biological explanation. The case of *NOD2* is exemplary, as it has been found in different experimental settings (in human cells or in animal models, using different cell types and different genetic constructs) that the role of *NOD2* polymorphisms in conferring an increased risk of CD could be explained by the following[111,115]: 1) a decreased synthesis of pro-inflammatory cytokines by macrophages upon interaction with MDP, leading to defective control of commensal or pathogenic bacteria[116,117]; 2) a dysregulated TLR-mediated pro-inflammatory response (in a model where wild-type NOD2 was found to be a negative regulator of TLR signalling, in opposition to the majority of the NOD2 literature)[118]; 3) an impaired secretion of the anti-inflammatory cytokine IL-10 (which was found in human PBMC, but not in murine bone marrow-derived macrophages)[119]; 4) an impaired production of α-defensins by Paneth cells, leading to overgrowth of certain species of the gut microbiota[120]; 5) an impaired induction of autophagy in dendritic cells, leading to impaired antigen processing and presentation[113]; 6) an abnormal development of a Th1 cytokine response to bacterial antigens (in a model where NOD2 signalling physiologically leads to polarization of the adaptive immune response towards a Th2 response)[121]; and finally 7) a defective induction of autophagy in macrophages[112].

d- Conclusion

What is striking when one contemplates this abundance of data produced on CD pathogeneis, is that in 2013 it still deserves to be coined a "complex disease": the nature of its genetic predisposition is complex (as opposed to a Mendellian type of heritability), its phenotypic characteristics are heterogeneous, and moreover the interplay of factors potentially at play in its development makes it still challenging for the scientific community to conceive one unifying and coherent physiopathological scenario.

Out of 21 high-impact review papers published since 2003, 16 indicated that "the widely accepted hypothesis for disease pathogenesis is that CD is caused by an overly aggressive immune response to bacterial antigens in genetically predisposed individuals". However, strikingly, this statement was accompanied by a reference in only 5 papers out of 16, and in all 5 cases the citation referred to another review, not to an original study. This exemplifies the fact that despite an abundance of experimental data, there are still numerous missing pieces in the puzzle of CD pathogenesis. As stated by Dr. Casanova: “To date, CD is widely accepted as a genetically determined immunological disease that manifests principally in the gut and is triggered by bowel contents, but this is as far as scientific consensus and certainty go”[67].

1.4) IRGM and Irgm1

1.4.1) Immunity-related GTPases

IFN-γ is a pro-inflammatory cytokine that is central in host resistance to intracellular pathogens, including mycobacteria[17]. It mediates its effect by inducing the transcription of more than 1,200 genes in target cells. The resulting proteins display anti-microbial properties and act together as part of a potent host defence program, thus conferring cell-autonomous immunity. Amongst these are iNOS2, NRAMP1, gp91-phox and IDO, the activity of which has been previously linked to resistance to mycobacteria[20,21]. More recently, researchers have uncovered the prominent role in early pathogen resistance of a

family of ~ 47kDa immunity-related GTPases (IRGs) induced by INF-γ[21,122–125]. Targeted deletions of 5 IRG genes in mice (*Irgm1, Irgm3, Irgd, Irga6* and *Irgd*) have caused susceptibility phenotypes to *Toxoplasma gondii*[126], and *Irgm1* (previously called *LRG-47*) has additionally been implicated in resistance to a remarkable range of pathogens, including *Trypanosoma cruzi*, *Leishmania major*, *Salmonella typhimurium, Chlamydia trachomatis*, *Chlamydia psittaci, Mycobacterium tuberculosis, M. avium*, *Mycobacterium bovis* BCG, and *Listeria monocytogenes*[122,21].

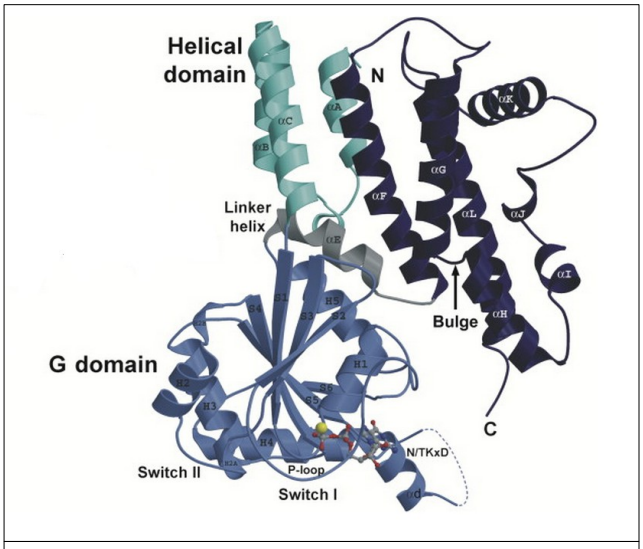

Figure 1.8: Crystal structure of Irga6.
Bidomain architecture consisting of a globular G domain and a helical domain combining N- and C-terminal elements. From reference 128.

There are 23 IRG genes in the mouse genome (21 functional genes and 2 pseudo-genes), organized in chromosomal clusters[127]. Crystal structures for several IFN-inducible GTPases reveal a bidomain architecture consisting of a globular G domain and a helical domain combining N- and C-terminal elements (see figure 1.8, copied from reference 128), which led to their classification as part of the dynamin-like family of proteins[21]. Studies of sequence homology between IRGs have shown that they fall into 5 groups named Irga, Irgb, Irgc, Irgd and Irgm. The first 4 groups (Irga, Irgb, Irgc, Irgd) possess the canonical and highly conserved GxxxxGKS/T P-loop sequence in the first nucleotide-binding motif (G1) and form the "GKS" subfamily, while 3 Irgm proteins (Irgm1, Irgm2 and Irgm3) contain the altered GxxxxGMS motif and together form the GMS sub-family (see figure 1.9, taken from reference 123).

Basal expression of the p47 GTPases is uniformly low in tissues and cultured cells. Once activated by IFN-γ, however, their expression is clearly up-regulated, even at minimal

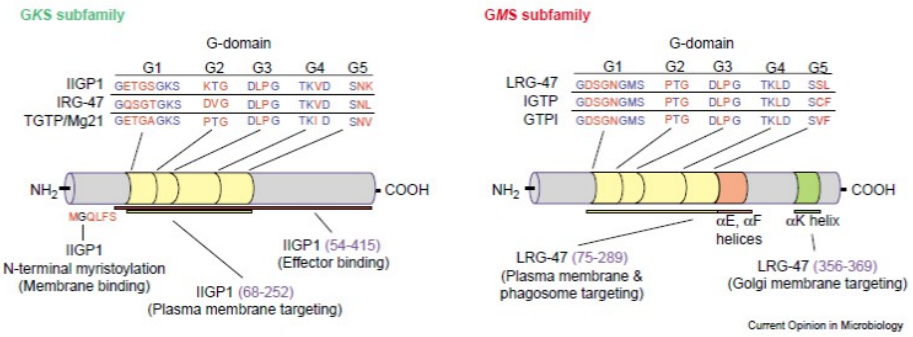

Figure 1.9: Mouse IRGs structure-function relationships.
Studies of sequence homology between IRGs have shown that they fall into 5 groups named Irga, Irgb, Irgc, Irgd and Irgm. The first 4 groups (Irga, Irgb, Irgc, Irgd) possess the canonical and highly conserved GxxxxGKS/T P-loop sequence in the first nucleotide-binding motif (G1) and form the "GKS" subfamily, while 3 Irgm proteins (Irgm1, Irgm2 and Irgm3) contain the altered GxxxxGMS motif and together form the GMS sub-family. From reference 123.

cytokine concentrations. Gene induction by these agonists is rapid, with mRNA transcripts detectable 1-4 h after cellular activation[123]. The specificity of the IFN-γ-driven response is corroborated using other cytokines — IL-1α, IL-1β, IL-2, IL-4, IL-6, TNF-α and granulocyte-macrophage-colony stimulating factor (GM-CSF) — all of which fail to activate IRG gene expression *in vitro*[127].

IRGs display unique structural and biochemical features (state of polymerization, rate of GTP hydrolysis, intracellular localization, etc.) that distinguish them from most other known GTPases[21]. Moreover, these characteristics vary widely between members of the family: for instance some of them are mostly membrane-bound (GMS sub-group), some remain mainly cytosolic (Irgd), and some are equally distributed between the cytosol and membrane fractions (Irga6, Irgb6). However, the current understanding is that IRGs act together to target compartmentalized pathogens (bacterial phagosomes, chlamydial inclusion bodies, and protozoan parasitophorous vacuoles) and orchestrate the recruitment of other proteins responsible for the localized delivery of antimicrobial effectors, culminating in the elimination of the pathogen.

1.4.2) Irgm1 mediates resistance to mycobacteria

As previously stated, Irgm1 has been shown to confer resistance to a wide range of pathogens, but quite surprisingly, the exact mechanisms underpinning its functions seem to differ for each of the microbial species studied so far (and as is the case for Mycobacteria, even sometimes within one genus)[129].

The function of Irgm1 in the context of experimental murine infections with the MTC has been studied in great detail by Dr. John MacMicking[93,94]. In a seminal paper published in 2003[93], he showed that: 1) *Irgm1*-/- mice display a striking susceptibility to infection with *M. tuberculosis* (both systemic and via aerosol), with accelerated mortality due to uncontrolled bacterial replication; 2) *Irgm1*-/- bone marrow-derived macrophages present a reduced ability to eliminate engulfed mycobacteria upon stimulation with IFN-γ (see figure 1.10); and 3) this phenotype is secondary to an impaired maturation of the *M. tb*-containing

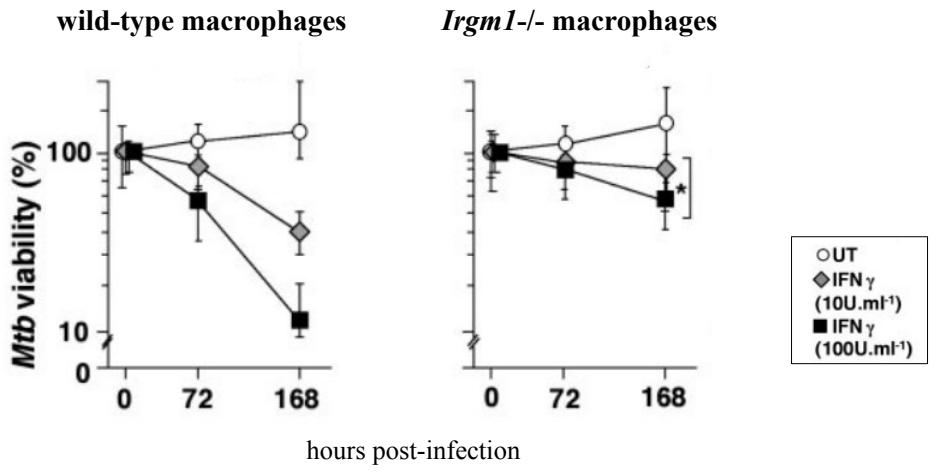

Figure 1.10: *In vitro* infection of bone marrow-derived macrophages from *Irgm1*-/- and wild-type mice with *Mycobacterium tuberculosis*
Bone-marrow derived macrophages were harvested from *Irgm1*-/- and wild-type mice and infected *in vitro* with *M. tuberculosis* (MOI 10:1). Cells were left untreated or stimulated with increasing concentration of murine recombinant INF-γ. At different time points, macrophages were lysed to recover intra-cellular bacteria and the resulting lysates were diluted and plated for subsequent CFU enumeration. Viability is given as a percentage of the starting (4 hours post-infection) CFU uptake.
* indicates statistical significance between IFN-γ-stimulated *Irgm1*-/- and wild-type macrophages with $p < 0.01$.
This experiment carried out by Dr. MacMicking in reference 94 shows an impaired ability of IFN-γ-stimulated *Irgm1*-/- macrophages to kill *M. tb*.

phagosomes. His group then published a second article[94] where the authors combined meticulous biochemical analyzes and astonishing microscopy work to further investigate how Irgm1 mediates these effects. They demonstrated that: 1) Irgm1 targets the mycobacterial phagosome through lipid-mediated interactions with phosphatidylinositol-3,4-bisphosphate ($PtdIns_{(3,4)}P_2$) and $PtdIns_{(3,4,5)}P_3$ through its C-terminal αK helix; and 2) this interaction further facilitates the engagement of Irgm1 with its fusogenic effectors, including Snapin, a protein known to take part in mycobacterial resistance through binding with t-SNARE complexes, which promotes the fusion of phagosomes with lysosomal compartments. This model is represented in figure 1.11, copied from reference 20.

A second group studied the function of Irgm1 in the context of a mycobacterial infection with a virulent member of the MAC. Using the same *Irgm1*-/- mouse as Dr. MacMicking, Dr. Karl Feng showed in reference 130 that, as is the case with *M. tb*, *Irgm1*-/- mice infected systemically with a virulent strain of *M. avium (M. avium* strain SmT 2151, on which details can be found in reference 131) show a markedly decreased survival associated with an increased bacterial burden when compared to wild-type controls. However in this experimental setting, there was no difference in mycobacterial survival inside of *Irgm1*-/- and wild-type bone marrow derived-macrophages infected *in vitro* with live *M. avium*, indicating that the Irgm1 deficiency in macrophages could not explain the uncontrolled bacterial replication (but it is important to note that the paper only reports the bacterial counts at day 3, a time-point at which there is no difference either in Dr. MacMicking's experiments). Furthermore, Dr. Feng showed that *Irgm1*-/- mice infected *in vivo* with *M. avium* presented decreased blood and splenic CD4+ and CD8+ T cells counts, which was apparent after 2 weeks of infection. Later on, he published a second study[132] demonstrating: 1) an *in vitro* expansion defect of *Irgm1*-/- CD4+ T cells; 2) a paradoxical role for IFN-γ in inducing the death of *Irgm1*-/- CD4+ T cells upon infection with *M. avium*; and 3) the role of Irgm1 in preventing this IFN-γ-induced death of CD4+ T cells.

The apparent contradiction in the work produced by these two groups is interesting because these studies pertain to the role of the two major cell types involved in host defence against mycobacteria, that is, the macrophage and the CD4+ T cell, but attribute clearly opposing roles to the two of them in experimental settings where the major

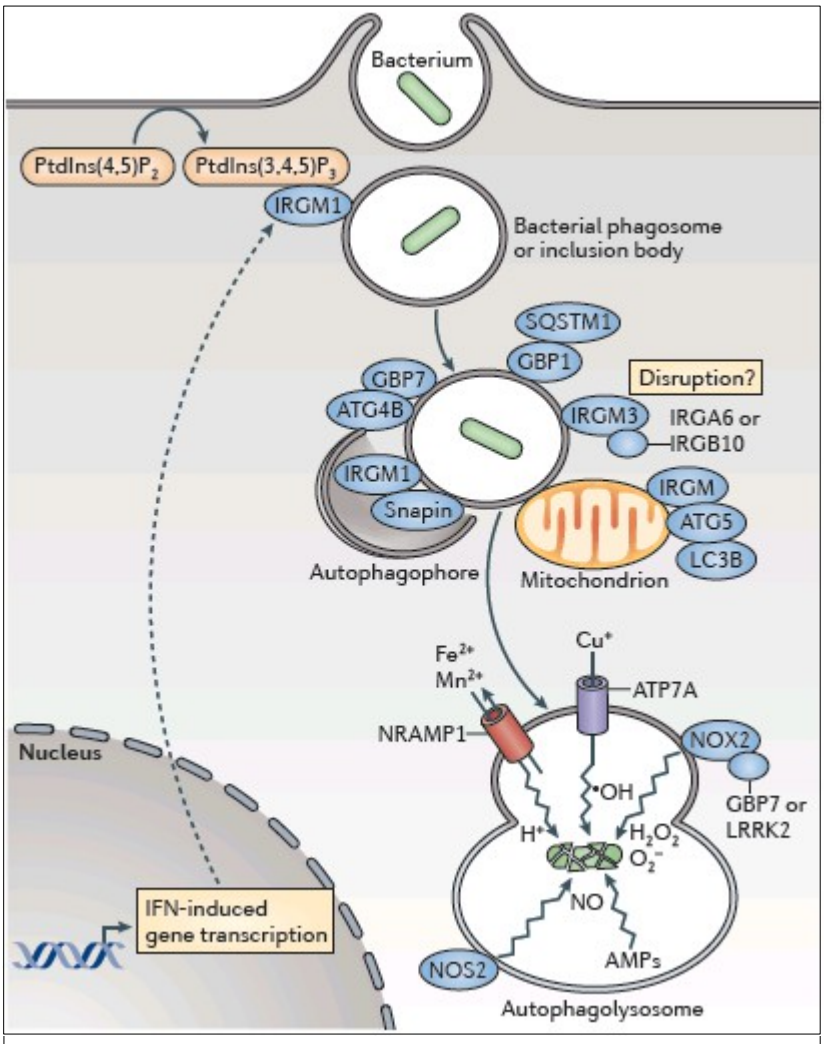

Figure 1.11: Proposed role of Immunity-related GTPases in cell-autonomous immunity to intracellular bacteria.
Immunity-related GTPases (IRGs) and other GTPases translocate to bacteria-containing phagosomes, where different membrane regulatory complexes (including Irgm1–snapin) are assembled. These complexes initiate autophagic capture and SNARE-mediated fusion of the bacterial compartments with lysosomes. These GTPases can also deliver antimicrobial peptides to the autophagolysosome and, in the case of human IRGM, may instigate mitochondrial fission before autophagy. Other IFN-inducible components, such as natural resistance-associated macrophage protein 1 (NRAMP1), nitric oxide synthase 2 (NOS2) and NOX2, work in concert to ensure bacterial killing. From reference 20.

difference seems to reside in the mycobacterial species (because the same mouse and (roughly) the same protocols are used).

1.4.3) Irgm1 has a broad and complex range of functions in immunity and hematopoiesis

To further add to the complexity, various groups have documented additional functions of murine Irgm1, first in the context of experimental infections with a wide range of pathogens, but also in non-immune homeostatic mechanisms.

First, it has been suggested that Irgm1 could promote eradication of intracellular organisms through the induction of autophagy. Autophagy is an ubiquitous and highly conserved eukaryotic process through which cells engulf parts of their cytoplasm into double-membrane-bound structures called autophagosomes, which are then merged with the lysosomal compartiment. It is thought to mediate a broad range of functions such as removal of disused organelles and toxic macromolecular aggregates, cell survival upon starvation or growth factor withdrawal, induction of cell death programs, and regulation of innate and adaptive immunity and inflammation[133,134]. It has been reported that in macrophages, expression of Irgm1 induces autophagosomes formation, whereas siRNA-mediated knockdown reduces it, and that induction of autophagy in *Mtb*-infected cells (either by means of IFN-γ stimulation or after transduction of active Irgm1) leads to effective intracellular control of the microbe's replication[135,95].

Second, authors that have studied Irgm1 during infection with *Toxoplasma gondii* have observed that in this setting, Irgm1 remained associated to the Golgi apparatus and failed to migrate to the *Toxoplasma*-containing vacuole after phagocytotis[136–139]. They proposed an alternative scenario to explain the role of Irgm1 in host defence, in which the three GMS proteins (Irgm1, Irgm2 and Irgm3) act as regulators of the GTPase cycle of the GKS proteins, preventing deleterious premature activation of GKS proteins by the binding of GTP[129,139,140].

Third and finally, as mentioned briefly above, *Irgm1-/-* mice rapidly display a striking lymphomyeloid deficiency after infection with several pathogens such as *Trypanosoma*, *Mycobacteria* and *Salmonella,* whereas their blood and bone-marrow only present minor abnormalities under basal conditions[140]. These findings are consistent in different models studied by different research groups, with induction of peripheral pancytopenia affecting

red cells, lymphocytes and platelets. Furthermore, it has been demonstrated that *Irgm1*-deficient mice show a delayed hematopoietic recovery after exposure to sub-lethal irradiation or cytotoxic treatment, and that their hematopoietic stem cells (HSC) present severe functional defects in competitive and non-competitive bone-marrow transplantation assays[141,142]. These functional defects are mediated by IFN-γ signaling because in double KO animals lacking both Irgm1 and IFN-γ (or Irgm1 and signal transducer and activator of transcription 1 (STAT1)), HSCs perform similarly to wild-type HSCs in reconstituting the bone marrow of lethally-irradiated animals. Thus, it appears that Irgm1 acts as a powerful negative regulator of IFN-γ-dependent stimulation in bone marrow myeloid progenitors, with an essential role in preserving their number and function.

1.4.4) Human IRGM, mycobacteria and Crohn's disease

Despite their impact on mouse resistance to infection, the phylogeny of IRGs genes is extremely puzzling): dogs have 8 potentially functional IRG genes (with both GMS and GKS sub-families represented and inducible by IFN-γ), fish present large variation in the number of IRGs (with GMS subfamily *Irgm* genes absent from all fish genomes examined so far), and finally IRGs are absent from the genomes of domestic cat, birds, horse, bat and pig[143,144]. In primates, it was shown that: 1) prosimians have 3 copies of the *Irgm* genes (just as rodents, but with only Irgm1 conserving structural properties compatible with a functional protein) whereas most of the IRG gene cluster was deleted early in primate evolution; 2) Old and New World monkeys have a single-copy *IRGM* gene that became pseudogenized as a result of an Alu retrotransposition event that disrupted the ORF, and 3) the ORF was reestablished as a part of a polymorphic stop codon in the common ancestor of humans and great apes, an event that coincided with the insertion of an endogenous retrovirus (ERV9) which now serves as the functional promoter driving human gene expression[143] (see figure 1.12, taken from reference 21).

The human *IRGM* gene codes for an amino- and carboxyl-terminally truncated G-domain homologous to the *Irgm* genes of mice, and is transcribed in 5 splicing mRNA isoforms. Contrary to what is seen in mice, IRGM transcripts are induced neither by IFN-γ, nor by infection. At the protein level, the shortest isoform of IRGM is shorter than a

canonical G-domain, being truncated in the middle of β-strand 6 just before the G5 sequence motif, and the longer isoforms are terminated by short sequence extensions that are unrelated to known GTPase domains[127].

Despite these striking differences between murine and human orthologs of this gene, it is very interesting to note that IRGM has been found to mediate resistance to mycobacteria in a manner similar to that of Irgm1[135,95]. Specifically, it was shown that: 1) IRGM acts as a necessary effector of the autophagic pathway in human macrophages cell lines; 2) IRGM-dependent processes are required for autophagy-induced BCG-containing phagosome maturation in human cells; and 3) these IRGM-dependent events culminate in mycobacterial killing (again in human macrophages cell lines)[95]. In a subsequent report, the same group documented the that certain isoforms of the protein were targeted to the mitochondria, where by regulating the mitochondrial membrane polarization state, they could mediate both autophagy-dependent and autophagy-independent cell death in a manner that affected cell-autonomous immunity to mycobacteria[145].

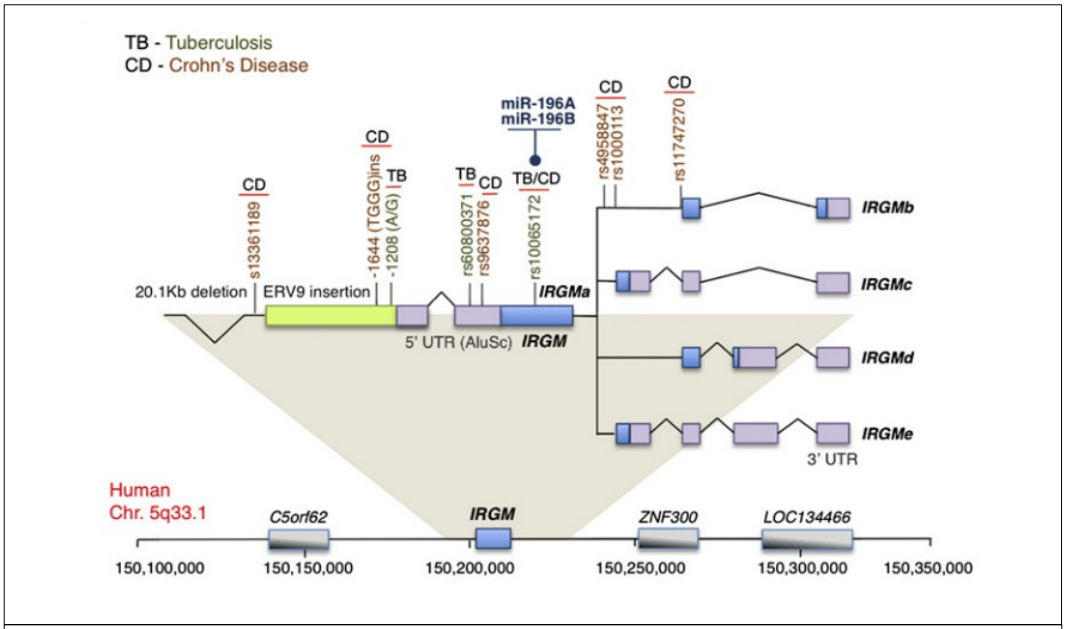

Figure 1.12: *IRGM* locus on human chromosome 5q33.1
The *IRGM* locus yields five splice mRNA isoforms (IRGMa–IRGMe) predicted to encode four different IRGM proteins (IRGMa, IRGMb, IRGMc/e, and IRGMd). Upstream ERV9 retroelement insertion plus Alu repeats are shown. Polymorphisms associated with Crohn's disease and tuberculosis are depicted. From reference 21.

These studies on the role of IRGM in experimental mycobacterial infections all come from one group and thus need to be replicated independently, but they provide a particularly interesting fundamental basis that could explain the findings of several genetic epidemiology studies reporting an association of the IRGM locus with the most prevalent human mycobacterial disease, tuberculosis.

As previoulsy stated, genetic epidemiological studies have repeatedly identified the *IRGM* locus in humans as being specifically associated with Crohn's disease[146,147], which is of particular interest when one considers the potential involvement of MAP in CD pathogenesis. Indeed, IRGM variants predispose to CD and IRGM mediates resistance to mycobacteria, and in a similar manner defective autophagy has been linked to CD and IRGM-mediated autophagy leads to mycobacterial killing; as a result of this, one can logically conceive that MAP could exploit a mutated IRGM to establish a chronic infection mimicking CD in humans.

However, how *IRGM* polymorphisms impact on the development of inflammation in the gut is still far from being perfectly understood, as 1) sequence variation is not thought to account for the increased risk of developing CD due to IRGM polymorphisms, and a recent study identified as potentially implicated a 20-kb deletion polymorphism upstream of IRGM and in perfect linkage disequilibrium with the most strongly CD-associated SNP[148]; and 2) in apparent contraction with these findings, another study showed that a common exonic synonymous SNP was responsible for IRGM expression to be differentially regulated by the means of small-interfering RNA[149].

2) Rationale and objectives

It has been hypothesized that chronic MAP infections in humans could account for a subset of cases of Crohn's disease[68,83], most importantly because: 1) MAP induces a disease with similar clinical and histopathological features in a wide range of mammals[8]; and 2) there is significant overlap between susceptibility loci associated with CD and pathways involved in host defence against mycobacterial infections[114]. On the opposite, one of the most widely cited argument against a potential involvement of MAP in CD is that patients with CD usually respond favourably to immunosuppressive therapeutics such as glucocorticosteroids and TNF-α inhibitors, which have been reported to impact negatively on the course of mycobacterial infections.

Due to the lack of validated MAP diagnostic tools and because it is ethically impossible to fulfil Koch's postulates, researchers have turned towards alternative ways to explore the potential role of MAP in CD. One strategy is to investigate the role of CD-associated genes in the course of an experimental MAP infection. The first aim of this type of work is to uncover if and how MAP could exploit the genetically-determined immune defects associated with CD to establish a chronic infection in humans. The second aim is to use small rodents with targeted deletions in CD-associated loci as models for a chronic intestinal infection with MAP leading to significant intestinal pathology, which, if successful, could potentially prove useful in three distinct research settings: 1) in paratuberculosis research, as an improved mouse model of JD; 2) to compare the histopathological and immunogical features of CD and JD; and 3) to test whether drugs used in the treatment of CD have a deleterious effect on the course of an intestinal MAP infection.

Previous work has been carried out in the Behr lab to investigate the role of the first CD-associated gene *NOD2* (and its murine ortholog *Nod2*) in experimental MAP infections. Specifically, this work has shown that: 1) *Nod2*-/- mice display an impaired control of systemic MAP infection due to impaired innate recognition and killing of MAP, leading to defective adaptive immunity; and 2) *Nod2*-/- mice do not constitute a tractable model of MAP-induced ileo-colitis (no productive infection upon oral challenge and no significant

intestinal pathology upon intra-peritoneal injection).

The work undertaken in the context of this Master's degree has thus concentrated on the function of murine *Irgm1* (ortholog of CD-associated *IRGM*) during experimental infections with MAP. Specifically, we hypothesized that *Irgm1*-/- mice would show an increased susceptibility to systemic infection with MAP and set out to investigate whether a defective control of MAP replication inside of macrophages could account for this phenotype (part 1). Second, we hypothesized that *Irgm1*-/- mice could constitute a tractable model of MAP-driven intestinal pathology and set out to: 1) document the pathological outcome of an intra-intestinal infection with MAP; and 2) use this model to test the effect of CD-associated therapeutics in its clinical evolution.

To conduct some experiments pertaining to part 1, we used both MAP and the closely related opportunistic MAH because: 1) due to its much shorter doubling time (< 12 hours), MAH offered a more amenable tool to study the immune response of *Irgm1*-/- mice to members of the MAC; and 2) it also allowed to investigate if these immune mechanisms were specifically at play during infection with a virulent member of the MAC.

Mice

C57Bl/6 wild-type breeding pairs were obtained from Jackson Laboratory in order to establish breeding colonies at the McGill University Health Center. An *Irgm1*-/- breeding pair was graciously provided by Dr. John MacMicking (Associate Professor of Microbial Pathogenesis at the Yale School of Medicine) and used to derive a colony. *Irgm1*-/- mice were engineered by Colazzo et al. by targeted deletion of the entire Irgm1 protein coding region in CJ7 embryonic stem cells and back-crossing on a C57Bl/6 × 129SvJ genetic background[150,151].

Mice were bred and raised in the Facility Animal Care Committees (FACC)-accredited, specific pathogen-free animal facility of the Montreal General Hospital, and housed in conventional cages by groups of up to 5 animals. All mice used in this study were 8-16 weeks old at initiation of experiments; males and females were used interchangeably, but we tried as much as possible to respect gender-matching between groups in all experiments. All murine experiments followed the guidelines of the animal research ethics boards of McGill University.

Bacterial cultures

All bacterial manipulations were carried out using biosafety level 2 precautions in appropriate level 2a biosafety cabinets (BSCs). Bacterial strains were obtained from American Type Cell Culture (ATCC), unless indicated otherwise. *Mycobacterium avium paratuberculosis* K-10 liquid cultures were grown in Middlebrook 7H9 broth (Becton, Dickinson and Co., Sparks MD) containing 0.2% glycerol (Sigma-Aldrich, St Louis, USA), 0.075% Tween 80 (Sigma-Aldrich, St Louis, USA), 10% albumin-dextrose-complex (ADC) (Becton, Dickson and Co., NJ) and 0.5μL/mL mycobactin J (Allied Monitor, Fayette MO). Cultures were maintained in 250 mL, 5000 mL or 1000 mL polystyrene storage bottles (Corning, Corning, NY) at 37°C with rolling at 0.2 rpm. For cultures on solid media, we used Middlebrook 7H10 (Becton, Dickinson and Co., Sparks MD) supplemented with 0.5%

glycerol, 10% oleic-acid-albumin-dextrose-complex (OADC) (Becton, Dickson and Co, NJ) and 1µL/mL mycobactin J. *Mycobacterium avium hominissuis* strain 104 liquid cultures were grown in Middlebrook 7H9 broth containing 0.2% glycerol, 0.05% Tween 80, 10% albumin-dextrose-complex with no mycobactin J.

In vivo mycobacterial infections

Actively growing mycobacterial cultures with an optical density (OD_{600}) of 0.5 to 0.8 (log phase) were used for experimental infections. To prepare bacterial inocula of a given concentration, we used preliminary data showing that in the case of MAP and MAH 104, OD = 1 corresponds roughly to $2 \cdot 10^8$ CFU/mL. Bacterial solutions were centrifugated at 3000 rcf for 12 min. at 4ºC, re-suspended in phosphate buffered saline (PBS) (Wisent, St-Bruno, Quebec) + 0.05% Tween 80 to reach the targeted concentration, after which the OD was measured a second time for confirmation. All inocula were plated in 2 to 3 replicates to confirm the exact infecting dose.

Mice were infected by gavage (using a specific gavage needle) or by intra-peritoneal injection (using a sterile 25 G needle) of ~ 200 µL of bacteria-containing solutions (bacteria resuspended in PBS previously warmed at 37°C). They were then monitored clinically and weighed weekly, and sacrificed when they reached 85% of their initial weights (or 80% in the case of certain survival experiments) or if they appeared moribund. All mice were euthanized by CO_2 inhalation followed by exanguination by cardiac puncture.

Gavage infections

In a set of gavage experiments testing the effects of various pretreatments on MAP colonization after oral challenge, wild-type mice were randomly assigned to 5 groups:

- "food deprivation group" (n = 5): food withdrawal 24 hours before infection; water withdrawal 4 hours before infection; water and food resumed *ad libitum* 2 hours after infection;
- "sodium bicarbonate group" (n = 5): no food or water restriction; 30 min. before infection, mice are inoculated with 100 µL of a sterile solution of 10% (wt/vol) sodium bicarbonate ($NaHCO_3$) (Sigma-Aldrich, St Louis, USA) dissolved in 0.9% NaCl (Baxter, Mississauga,

ON); water and food resumed *ad libitum* 2 hours after infection[152];

- "streptomycin group" (n = 5): food withdrawal 24 hours before infection; at 20 hrs before infection, mice are inoculated with 20 mg of streptomycine (Sigma-Aldrich, St Louis, USA) in 75-100 µL 0.9% NaCl by gavage, and then supplied with water again (no food); water withdrawal 4 hours before infection; water and food resumed ad libitum 2 hours after infection[153];

- "sodium bicarbonate + streptomycin group" (n = 5): food withdrawal 24 hours before infection; at 20 hrs before infection, mice are inoculated with 20 mg of streptomycine in 75-100 µL 0.9% NaCl by gavage; water withdrawal 4 hours before infection; 30 min. before infection, mice are inoculated with 100 µL of a sterile solution of 10% (wt/vol) sodium bicarbonate dissolved in 0.9% NaCl; water and food resumed *ad libitum* 2 hours after infection;

- "control group" (n = 1): no food or water restriction; 30 min. before infection, mice are inoculated with 100 µL of a sterile solution of 0.9% NaCl; water and food resumed *ad libitum* 2 hours after infection.

Quantitative bacteriology

Organs (livers, spleens, mesenteric lymph nodes, small intestines and colons) were harvested upon necropsy with previously autoclaved surgical instruments, and kept in Middlebrook 7H9 broth containing 0.2% glycerol, 0.05% Tween 80, 10% ADC and 0.5µL/mL mycobactin J on ice until processing.

All quantification of MAP and MAH burden in organs or in cell cultures were carried out by serial dilution in PBS + 0.05% Tween 80 in 24-well plates (Becton, Dickinson and Co., Sparks MD) (for MAP) or 2 mL tubes (Eppendorf, USA) (for MAH) and plating of the dilutions on Middlebrook 7H10 plates supplemented with 0.5% glycerol, 10% OADC and (only in the case of MAP) 1µL/mL mycobactin J. Plates were placed in sealed bags and incubated for 2 weeks in the case of MAH, and for 4-8 weeks in the case of MAP, at 37 ºC, after which MAP and MAH colony-forming-units (CFUs) were enumerated.

For *in vivo* mouse experiments, bacteria from liver tissue homogenates were grown on Middlebrook 7H10 agar supplemented as previously described, with the addition of 2 vials

of reconstituted Bactec PANTA (Becton, Dickinson and Co., Sparks MD) per liter, while spleens and mesenteric lymph nodes were grown without Bactec PANTA. Results are presented as bacterial counts per organ (weights not recorded)

In vitro macrophage infections

Peritoneal macrophages were obtained from *Irgm1*-/- and wild-type mice by peritoneal lavage with 10 mL RPMI-1640 (Wisent, St-Bruno, Quebec). The resulting cell suspension was centrifuged at 700 rcf for 12 min. at 4ºC, and macrophages re-suspended in RPMI-1640 supplemented with 10% FBS, 2% Hepes and 1% penicillin/streptomycin solution. Cells (2.5 to $5 \cdot 10^5$ /well) were cultured in 24-well tissue culture plates and macrophages were purified by adherence overnight.

Bone marrow-derived macrophages were generated by culture of bone marrow cell suspensions harvested from femurs and tibias in RPMI-1640 supplemented with 10% fetal bovine serium (FBS) (Wisent, St-Bruno, Quebec), 2% Hepes (Wisent, St-Bruno, Quebec), 1% penicillin/streptomycin (10 000 IU penicillin/10 000 µg/mL streptomycin) (Wisent, St-Bruno, Quebec), 1% L-glutamine (Wisent, St-Bruno, Quebec), 1% non essential amino acids (NEAA) (Wisent, St-Bruno, Quebec), 1% essential amino acids (EAA) (Wisent, St-Bruno, Quebec), 1% Pyruvate (Wisent, St-Bruno, Quebec) and 10% L929 cell culture supernatant (gracefully provided by Dr. Maziar Divangahi (Assistant Professor in the Department of Immunology and Microbiology, McGill University, Montreal, Canada) during 7 days.

In all macrophages experiments, half of the cells of each genotype were stimulated with mouse recombinant IFN-γ (R&D Systems, Minneapolis, MN) at a concentration of 100 UI/mL. In some experiments the stimulation was interrupted after infection, whereas in some it was pursued throughout the course of the whole experiment.

Macrophages were exposed to a solution of bacteria (bacteria resuspended in PBS previously warmed at 37°C) at an MOI of 5:1 or 10:1. Following a 4 to 6-hour incubation period, macrophages were washed 3 times in PBS and then left incubating at 37ºC. During all *in vitro* macrophage experiments, fresh media was added to the wells every 48 to 72 hours. At different time points (including immediately after the incubation period),

macrophages were lysed in 1-2 mL PBS + 1% Triton-X100 (Sigma-Aldrich, St Louis, USA). The resulting lysates were centrifuged at 3000 rcf for 15 min., re-suspended in 7H9 broth, and serial dilutions were plated on 7H10 agar for CFU enumeration.

Intra-jejunal infection

The surgical procedure starts with injection of buprenorphine 0.03 mg/kg (0.1 mL of buprenorphine at 0.03 mg/mL in 0.9 mL of 0.9% NaCl) by subcutaneous injection (s.c.). Deep anaesthesia is induced in a glass box by administration of O_2 3 L/min. + isoflurane 3%, and maintained by keeping the head of anaesthetized animals in a facial mask delivering O2 2.5 L/min. + isoflurane 2% throughout the whole procedure.

Mice are laid on their back and their four limbs are taped delicately to the surface of a type 2a BSC. The abdomen wall is opened by cutting first the skin (median longitudinal incision of ~ 1 cm.) with surgical scissors, and second the underlying muscular layer. The jejunum is located and removed out of the abdominal cavity and exposed on a sterile gauze. 200 µL of a bacterial suspension containing ~ 10^9 MAP CFUs are then inoculated inside of the gut lumen through a 25G needle.

Both layers of the abdominal wall are sewed with Vicryl 4.0 sutures and the mice are left to recover under a heating lamp for 15 min. They are monitored clinically and receive buprenorphine 0.03 mg/kg s.c. twice daily during the 3 days following surgery.

Histopathological analysis

Small intestine, colons, mesenteric tissues, livers and spleens were harvested upon necropsy and fixed immediately in 10% formalin. Processing of the samples was carried out at the Histology Facility of the Rosalind and Morris Goodman Cancer Research Centre of McGill University. Samples were embedded in parafin and stained by Hemalin & Eosin as well as Ziehl-Niessen staining.

Slides were read independently by Dr. M. Behr, Dr. M. Paquet (veterinarian pathologist) and Louis Kreitmann.

Quantitative polymerase chain reaction (qPCR)-based quantification of MAP DNA in *Irgm1*-/- mice IJ-infected with MAP

Small intestine, colons, mesenteric tissues, livers and spleens were harvested upon necropsy and kept at -80°C until processing.

DNA was extracted from ~ 200 mg of organ by applying the most widely used DNA extraction procedure for mycobacterial DNA[154–157], first described by van Soolingen et al.[158]. Briefly, this procedure includes enzymatic lysis with lysosyme and proteinase K (Sigma-Aldrich, St Louis, USA), removal of polysacharide with CTAB/NaCl (Sigma-Aldrich, St Louis, USA), and removal of proteins with phenol-chloroform-isoamyl-alcool (Sigma-Aldrich, St Louis, USA).

For the detection and quantification of MAP in organs, we used a recently described protocol that amplifies MAP amplicon III f57 from the MAP0865 gene[159]. Quantification was performed by TaqMan real-time PCR. Real-time PCR assays were done using a 7300 Real-Time PCR System (Applied Biosystems). The relative quantification of MAP K-10 DNA (genome of 4,829,781 bp corresponding to 5.30 fg per copy), was performed with independent 10-fold serial dilutions of genome equivalents (ge) from 7 $\log_{10}$ copies until 0 copy in triplicate, and cycle thresholds of 0.02 ΔRn. All real-time PCR analyzes included a negative process control (extracted DNA from non-infected mice) as well as a negative amplification control (reaction with water as template). TaqMan real-time PCR assays (qPCR MasterMix 2X Maxima Probe, Fermentas) were performed according to manufacturer recommendations (final concentrations of 1X TaqMan buffer, 0.3 µmol/L of each primers, 0.2 µmol/L of probe, and 4 mmol/L of $MgCl_2$) in a final volume of 25 µL (2 min. at 50°C, 10 min. at 95°C, 40 cycles of 15 sec. at 95°C, 30 sec. at annealing temperature as elongation and detection step, and 30 sec. at 72°C). For MAP quantification, TaqMan probes were synthesized by Invitrogen with FAM as reporter on 5' side, and MGBNFQ as quencher on 3' side.

Except for the harvesting of mouse organs, Dr. Nicolas Radomski carried out this experiment in its entirety.

Response to treatments used in Crohn's disease

To test the effect of a systemic treatment by glucocorticosteroids on survival, a cohort of 12 *Irgm1*-/- mice infected 1 month before with 10^9 MAP CFUs by IJ was randomly separated in 2 groups, receiving:

- "treatment group" (n = 6): IP injection of 4 mg/kg methylprednisolone (re-suspended in 200 µL of 0.9% NaCl), 5 days per week;
- "placebo group" (n = 6): IP injection of 200 µL 0.9% NaCl, 5 days per week.

The mice were monitored clinically and weighed every week to compare their survival (using a cut-off of 85% of initial weight for sacrifice).

To test the effect of a treatment by TNF-α-inhibitors on bacterial replication, a cohort of 15 *Irgm1*-/- mice infected 1 month before with 10^9 MAP CFUs by IJ was randomly separated in 3 groups:

- "baseline group" (n = 5): the mice were sacrificed at 1 month following IJ inoculation of MAP for qPCR-based quantification of MAP DNA in small intestine, colon, mesenteric tissue, liver and spleen;
- "treatment group" (n = 5): IP injection of LEAF™ Purified anti-mouse TNF-α Antibody (clone MP6-XT22, isotype Rat IgG1κ, Biolegend, CA, USA) re-suspended in sterile PBS, 5 mg/kg at 4 and 6 weeks post-infection; the mice were sacrificed at 2 month post-infection for qPCR-based quantification of MAP DNA;
- "isotype control group" (n = 5): IP injection of LEAF™ Purified Rat IgG1κ Isotype control (Biolegend, CA, USA) resuspended in sterile PBS, 5 mg/kg at 4 and 6 weeks post-infection; the mice were sacrificed at 2 month post-infection for qPCR-based quantification of MAP DNA.

Biostatistics

Log-rank product limit estimates were applied to Kaplan-Meier survival data for determining significance by χ^2 statistics between two groups. The unpaired two-tailed t-test was used to compare means. All statistics were carried out with software JMP 10 or LibreOffice Calc version 4.1 (both on Windows 7).

4) Results

4.1) Part 1: role of Irgm1 in innate immunity to MAP and MAH

4.1.1) *Irgm1* mediates survival during MAH and MAP infections

In all sets of published research on the role of Irgm1 in mycobacterial infections (*M. tuberculosis* Complex or MAC), investigators have shown a decreased survival of experimentally infected *Irgm1*-/- mice when compared to wild-type counterparts. We first sought to reproduce these findings in the context of a systemic infection with virulent MAP and opportunistic MAH.

In a first survival experiment, we infected 21 *Irgm1*-/- and 22 wild-type C57Bl/6 mice with ~ 10^8 CFUs of MAH strain 104 by intra-peritonal (IP) injection. Mice were weighed weekly for 19 weeks and sacrificed when they attained < 85% of initial weight. As shown in figure 4.1a, *Irgm1*-/- mice displayed a clearly decreased survival: they reached their median surviving time after 3 weeks (10 mice dead out of 21), a time point at which 22 out of 22 (100%) wild-type mice were still alive; furthermore, all *Irgm1*-/- mice were dead at week 19, when 16 wild-type animal (73%) were still alive (log-rank test: $\chi^2 = 35.591$, $p < 0.0001$).

In a similar experiment, we infected 12 *Irgm1*-/- and 12 wild-type mice with ~ 10^8 MAH CFUs by IP injection and monitored them weekly for up to 19 weeks, but this time animals were sacrificed when their weight reached < 80% of baseline. Here again, we found that *Irgm1*-/- mice had a decreased survival (figure 4.1b): they had a median surviving time of 9 weeks and only 1 mouse out of 12 (8%) survived until week 19, when 12 out of 12 (100%) wild-type counterparts were still alive (log-rank test: $\chi^2 = 21.164$, $p < 0.0001$).

We then went on to study the survival of *Irgm1*-/- mice infected with MAP. Given that MAP is a successful natural pathogen of mammals and that MAH is in most natural cases an opportunistic bacteria, we reasoned that the mortality rate seen with MAH would be attained with a smaller infectious dose of MAP. To test this, we conducted an experiment where we infected 10 *Irgm1*-/- mice with PBS, 10 *Irgm1*-/- mice with ~ 10^6 MAP CFUs, and

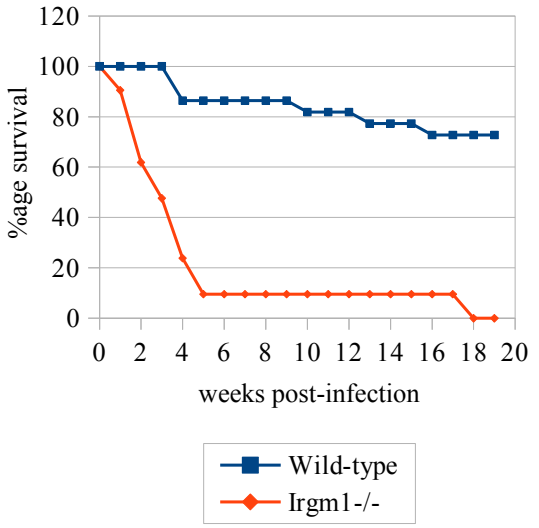

4.1a: survival of *Irgm1-/-* and wild-type mice infected with 10^8 MAH CFUs

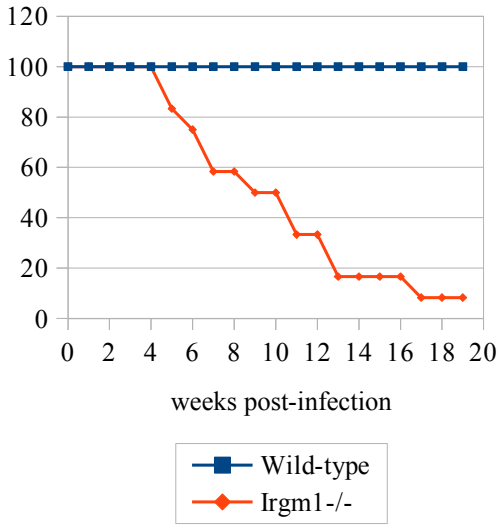

4.1b: survival of *Irgm1-/-* and wild-type mice infected with 10^8 MAH CFUs

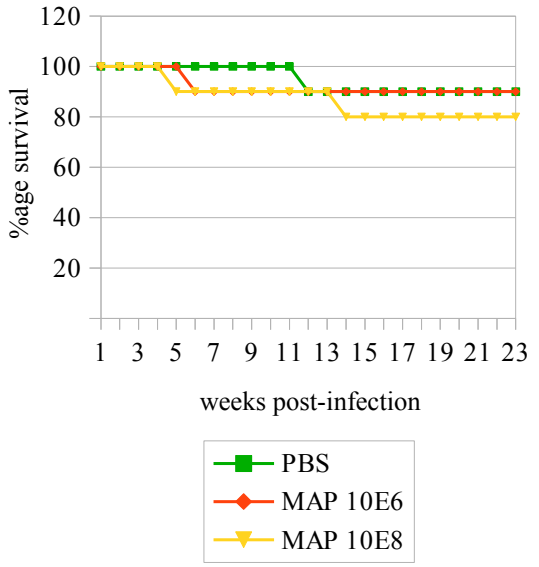

4.1c: survival of *Irgm1-/-* and wild-type mice infected with PBS, 10^6 MAP CFUs, 10^8 MAP CFUs

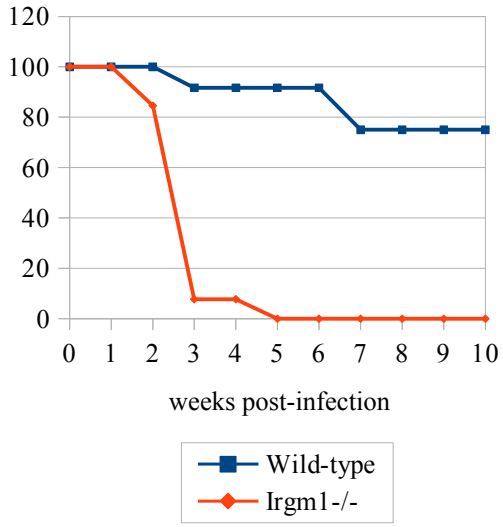

4.1d: survival of *Irgm1-/-* and wild-type mice infected with 10^9 MAP CFU

Figure 4.1: Survival of *Irgm1-/-* and wild-type mice infected with MAH and with MAP. *Irgm1-/-* and *Irgm1+/+* mice were infected by IP injection with ~ 10^8 MAH strain 104 CFUs (fig. 4.1a and 4.1b), with ~10^6 and ~10^8 MAP CFUs (fig. 4.1c), and with ~10^9 MAP CFUs (fig. 4.1d). They were monitored weekly for survival and sacrificed when they attained 85% (fig. 4.1a and 4.1c) or 80% of (fig. 4.1b and 4.1d) of basal weight.

10 *Irgm1*-/- mice with ~ 10^8 MAP CFUs. Mice were monitored weekly for up to 23 weeks, using a weight cut-off of 85% of baseline, under which they were sacrificed. As shown in figure 4.1c, we were not able to show a significant difference of survival between the 3 groups: after 23 weeks of follow-up, 9 out of 10 PBS-injected mice (90%), 9 out of 10 mice infected with ~ 10^6 MAP CFUs (90%), and 8 out of 10 mice infected with ~ 10^8 MAP CFUs (80%) were still alive.

To overcome this apparent reduction of mortality in the context of a MAP infection, we decided to conduct a survival experiment comparing *Irgm1*-/- and wild-type mice infected with a higher dose of MAP. We injected 13 *Irgm1*-/- and 12 wild-type mice with ~ $3 \cdot 10^9$ MAP CFUs intra-peritoneally and monitored survival for 10 weeks (using a weight cut-off of 80% of baseline). In this setting, we were clearly able to demonstrate a role for Irgm1 in mediating survival during MAP infection (see figure 4.1d): *Irgm1*-/- mice had a median survival of less than 3 weeks and were all dead at week 5, while 9 out of 12 wild-type mice (75%) were still alive (log-rank test: $\chi^2 = 19.177$, $p < 0.0001$).

In conclusion, we clearly showed that *Irgm1*-/- mice had a decreased survival during systemic infections with both MAP and MAH.

4.1.2) Irgm1 is necessary to control *in vivo* replication of MAH and MAP

We then set out to investigate more precisely the cause of the accelerated death of the *Irgm1*-/- mouse infected with MAP and MAP. Since Irgm1 has been reported to mediate a wide range of homeostatic mechanisms at play during mycobacterial infections, we divided our investigation in 2 axes, aiming to: 1) assess the role of Irgm1 in controlling the bacterial burden during *in vivo* infections; and 2) explore additional effects of the Irgm1 deficiency during such infections.

In a preliminary experiment, we infected 5 *Irgm1*-/- and 3 wild-type mice with ~ 10^8 MAH CFUs by IP injection, and enumerated CFUs recovered in the mesenteric lymph nodes (MLNs, which collect bacterial antigens from the peritoneal cavity), secondary sites of drainage (liver and spleen) and distant organs (lungs and kidneys) at 4 weeks post-infection. As shown in figure 4.2a, we found that *Irgm1*-/- mice presented a significantly greater bacterial burden than their wild-type counterparts in the MLNs (*Irgm1*-/- 5.0

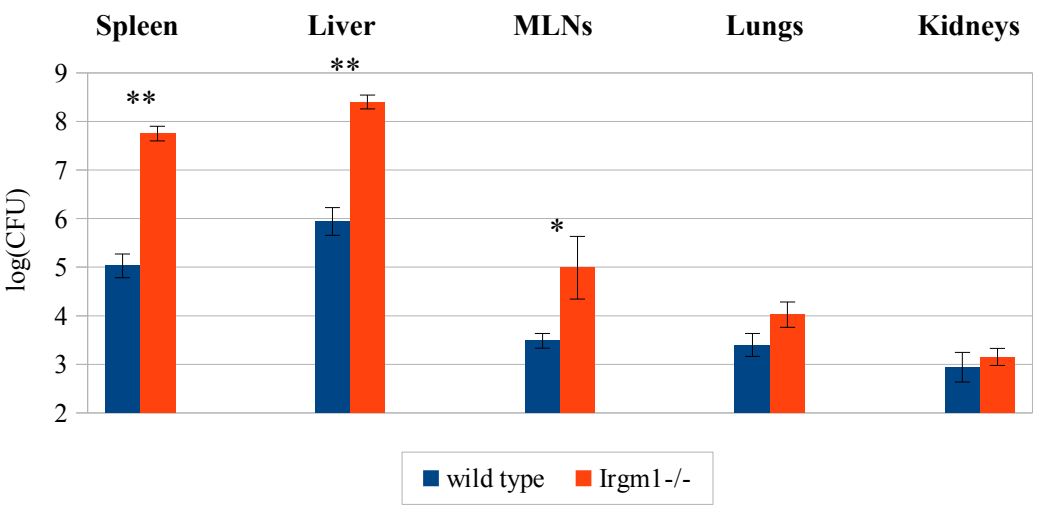

4.2a: CFUs recovered from spleen, liver, MLNs, lungs and kidneys of *Irgm1*-/- and wild-type mice infected IP with ~10^8 MAH CFUs, at 4 weeks post-infection

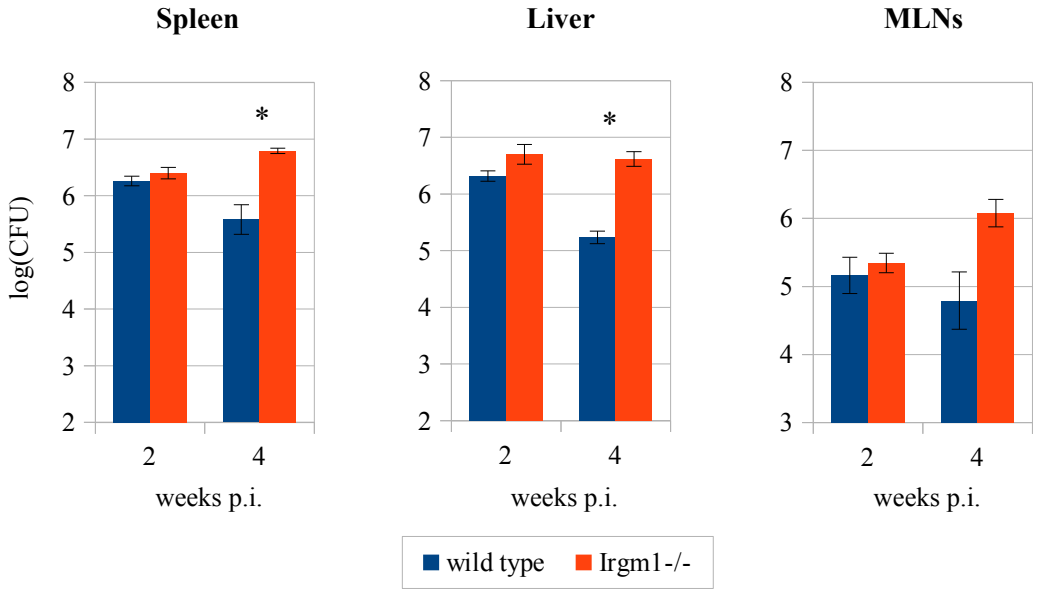

4.2b: CFUs recovered from spleen, liver and MLNs of *Irgm1*-/- and wild-type mice infected IP with ~10^8 MAH CFUs, at 2 and 4 weeks post-infection

Figure 4.2: bacterial quantification in spleens, livers, mesenteric lymph nodes (fig. 4.1a and 4.1b) and kidneys and lungs (figure 4.1a) of Irgm1-/- and wild-type mice infected with 10^8 MAH CFUs.

Irgm1-/- and *Irgm1*+/+ mice were infected by IP injection with ~ 10^8 MAH CFUs. They were sacrificed at different time points and the organs harvested upon necropsy were ground, diluted and plated for subsequent CFU enumeration. Results are indicated in $\log_{10}$(CFU) per organ.

* denotes statistical significance with $p < 0.05$, and ** with $p < 0.01$.

$\log_{10}$(CFU), wild-type 3.5 $\log_{10}$(CFU), p = 0.039), the spleen (*Irgm1*-/- 7.8 $\log_{10}$(CFU), wild-type 5.1 $\log_{10}$(CFU), p < 0.0001) and the liver (*Irgm1*-/- 8.4 $\log_{10}$(CFU), wild-type 5.9 $\log_{10}$(CFU), p < 0.0001). In distant organs, we also found an increased bacterial burden in *Irgm1*-/- mice, but it did not reach statistical significance: in the kidneys, *Irgm1*-/- and wild-type mice had respectively 3.2 and 2.9 $\log_{10}$(CFU) and in the lungs, *Irgm1*-/- and wild-type mice had respectively 4.0 and 3.4 $\log_{10}$(CFU).

We then devised a second experiment to confirm these findings and document their evolution in time more precisely. We infected 12 *Irgm1*-/- and 12 wild-type mice (2 groups of 6 mice each) with ~ 10^8 MAH CFUs by IP injection and enumerated CFUs recovered in the MLNs, spleen and liver at 2 and 4 weeks post-infection. As shown in figure 4.2b, at week 2 *Irgm1*-/- mice presented on average a slightly higher bacterial burden than wild-type mice in all three organs, but this difference was not statistically significant. However at week 4, *Irgm1*-/- mice had a significantly greater bacterial burden in the spleen (*Irgm1*-/- 6.8 $\log_{10}$(CFU), wild-type 5.6 $\log_{10}$(CFU), p = 0.0057) and in the liver (*Irgm1*-/- 6.6 $\log_{10}$(CFU), wild-type 5.2 $\log_{10}$(CFU), p = 0.0035), whereas in the MLNs their bacterial counts were clearly higher (*Irgm1*-/- 6.1 $\log_{10}$(CFU), wild-type 4.8 $\log_{10}$(CFU)) but the difference did not reach statistical significance (p = 0.28) due to greater variability in sampling of the MLNs.

Next, we conducted similar experiments with MAP. First, we infected 2 groups of *Irgm1*-/- and wild-type mice (5 animals per group) with ~ 10^8 MAP CFUs by IP injection and assessed their bacterial burden at 1, 2 and 4 weeks post-infection. As shown in figure 4.3a, we found no difference in bacterial burden between *Irgm1*-/- and wild-type mice at weeks 1 and 2 (at the single exception of the livers at 2 weeks post-infection, where the wild-type mice had surprisingly more bacteria than the *Irgm1*-/- animals). At week 4 however, *Irgm1*-/- mice had significantly more bacteria than wild-type mice in the spleen (5.4 and 4.6 $\log_{10}$(CFU) respectively, p < 0.0001) and in the liver (5.0 and 4.4 $\log_{10}$(CFU) respectively, p = 0.011), whereas in the MLNs there was no statistically significant difference. All these results were in accordance with those observed in the context of an infection with MAH.

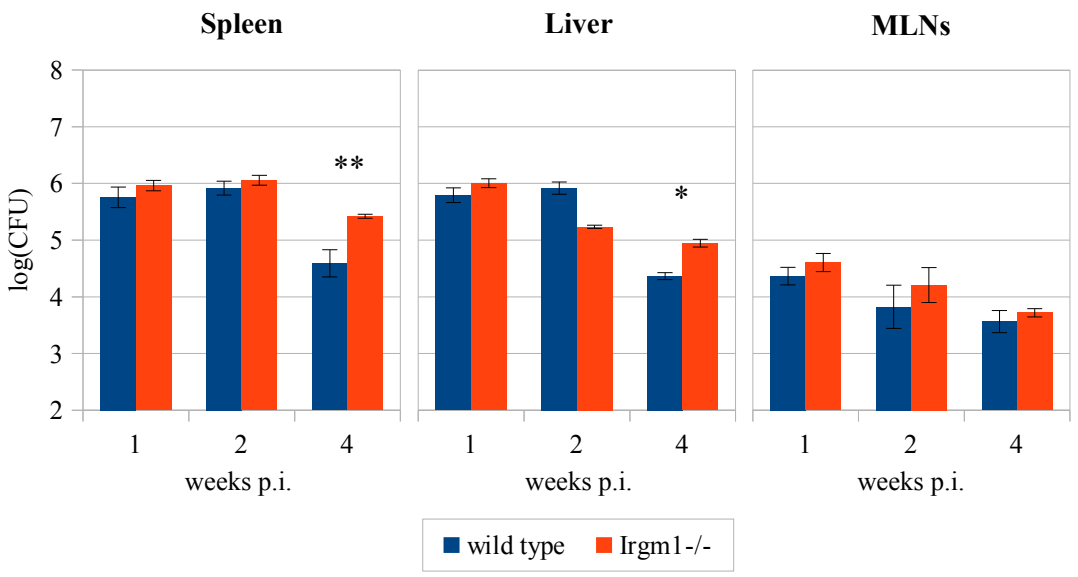

4.3a: MAP CFUs recovered from spleen, liver and MLNs of *Irgm1-/-* and wild-type mice infected IP with ~10^8 MAP CFUs, at 1, 2 and 4 weeks post-infection

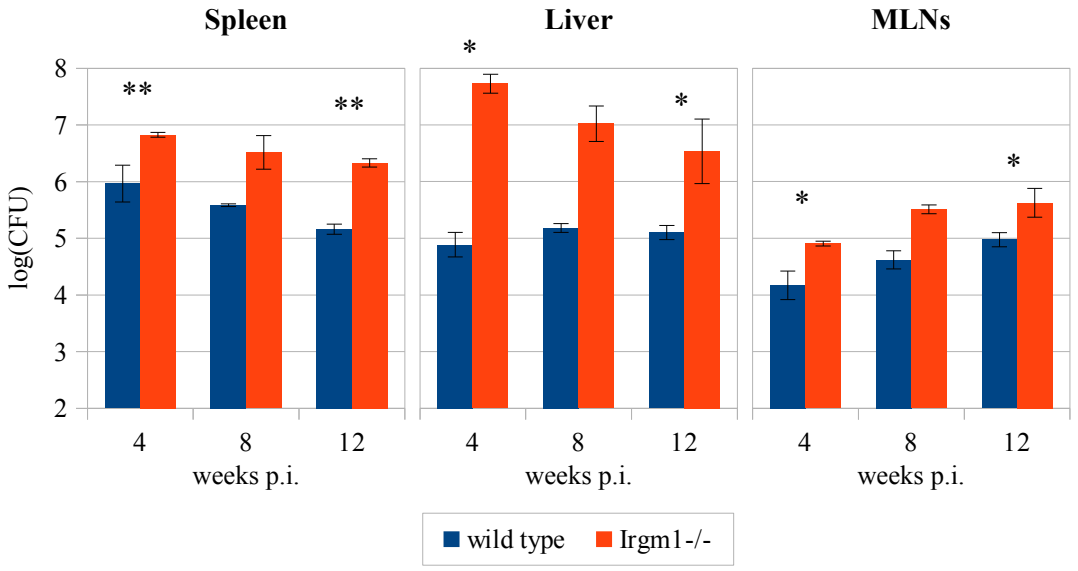

4.3b: MAP CFUs recovered from spleen, liver and MLNs of *Irgm1-/-* and wild-type mice infected IP with ~10^8 MAP CFUs, at 4, 8 and 12 weeks post-infection

Figure 4.3: bacterial quantification in spleens, livers, mesenteric lymph nodes of *Irgm1-/-* and wild-type mice infected with 10^8 MAP CFUs.

Irgm1-/- and *Irgm1+/+* mice were infected by IP injection with ~ 10^8 MAP CFUs. They were sacrificed at different time points and the organs harvested upon necropsy were ground, diluted and plated for subsequent CFU enumeration. Results are indicated in $\log_{10}$(CFU) per organ.

* denotes statistical significance with $p < 0.05$, and ** with $p < 0.01$.

Finally, we carried out a second experiment with MAP, both to confirm our previous findings and to document them further at later time points by comparing CFUs in the MLNs, livers and spleens of 13 *Irgm1*-/- and 17 wild-type mice at weeks 4, 8 and 12 post-infection. In line with our previous observations during MAH and MAP infections, we found that *Irgm1*-/- mice presented an increased bacterial burden in all three organs at 4 weeks post-infection. Furthermore, we found that this difference was maintained throughout the course of the experiment: at week 12 for instance, *Irgm1*-/- mice had 6.3 $\log_{10}$(CFU) in the spleen, versus 5.2 $\log_{10}$(CFU) in wild-type controls (p = 0.0001), 6.5 $\log_{10}$(CFU) in the liver versus 5.1 $\log_{10}$(CFU) in wild-type controls (p = 0.02), and 5.6 $\log_{10}$(CFU) in the MLNs versus 5.0 $\log_{10}$(CFU) in wild-type controls (p = 0.0795) (see figure 3.2d)

In conclusion at this step, we found that *Irgm1*-/- mice infected with MAH and with MAP have impaired control of bacterial replication, as evidenced by increased an bacterial burden in spleen and liver. In both settings, this becomes evident as of the 4th week post-infection, with differences in CFUs attaining a 10-fold factor or more (≥ 1 $\log_{10}$(CFU)) in most organs. And finally, a trend towards more bacteria in the MLNs of *Irgm1*-/- animals is seen, but due to higher variability in sampling, statistical significance is not attained at all time points.

4.1.3) *Irgm1*-/- mice develop pancytopenia upon systemic infection with MAH

We then sought to document other potential abnormalities (not related to immune mechanisms) attributed to the Irgm1 deficiency during a systemic infection with members of the MAC. To this end, we infected 5 *Irgm1*-/- mice and 3 wild-type counterparts with ~ 10^8 MAH CFUs by intra-peritoneal injection and submitted them to a series of analyzes.

First we monitored them clinically. We found that, apart from a progressive loss of weight and the development of an altered nutritional status, *Irgm1*-/- mice did not show major clinical abnormalities when compared to wild-type controls. Specifically, there was no behavioural change, no motor impairment, no focal neurological abnormality, no respiratory distress, no sign of external or internal bleeding, no skin lesion. We conducted a diagnostic necropsy with a professional veterinarian at 4 weeks post-infection, and found that the livers and spleens of *Irgm1*-/- mice were on average paler than those of wild-type controls,

a finding suggestive of anemia. Beside that, there was no significant abnormality in shape, size and composition of all other intra-cranial, intra-thoracic and intra-abdominal organs.

We then set out to assess haematologic abnormalities that could explain (at least in part) the increased death rate of *Irgm1*-/- mice during MAH infections, by examining their complete blood count (CBC) upon necropsy. In accordance with previously published work, we found that *Irgm1*-/- mice underwent a marked pancytopenia upon infection, which was not seen in wild-type controls (see table 4.1). At 4 weeks post-infection (a time point when the difference in CFUs between *Irgm1*-/- and wild-type controls becomes apparent), *Irgm1*-/- mice displayed a profound anemia (hemoglobin content in the blood = 39.6 g/L versus 118.7 g/L in wild-types, $p < 0.0001$), a moderate lymphopenia (total blood lymphocytes $3.5 \cdot 10^9$/L versus $7.13 \cdot 10^9$/L in wild-types, $p = 0.0023$), and a mild thrombocytopenia (platelets $144 \cdot 10^9$/L versus $1282 \cdot 10^9$/L in wild-types, $p < 0.0001$). Interestingly, there was no difference between *Irgm1*-/- and wild-type mice in the blood content of other leucocytes, including granulocytes and monocytes.

	***Irgm1*-/- mice** (n = 5) (mean, sd)	**Wild type mice** (n = 3) (mean, sd)	***p*-value**	**References for C57Bl/6 mice**
Hematocrit (%)	10.1% (4.1%)	33.4% (1.65%)	$9.79 \cdot 10^{-5}$	39% – 49%
Hemoglobin (g/L)	39.6 (13.8)	118.7 (5.1)	$8.65 \cdot 10^{-5}$	102 – 166
WBCs (10^9/L)	6.36 (3.4)	10.7 (2.4)	0.109	6 – 15
Neutrophils (10^9/L)	2.8 (2.4)	3.3 (2.0)	0.780	
Lymphocytes (10^9/L)	3.5 (1.1)	7.13 (0.6)	$2.34 \cdot 10^{-3}$	
Monocytes (10^9/L)	0.1	0.2	0.238	
Platelets (10^9/L)	144 (82)	1282 (204)	$2.59 \cdot 10^{-5}$	160 – 410

Table 4.1: Haematological profile (complete blood count, CBC) of *Irgm1*-/- and wild-type mice infected by IP injection with ~ 10^8 MAH CFUs at 1 month post-infection. References are from reference 160.

To test whether this moderate lymphocytopenia could lead to a state of immunosuppression that could itself be responsible for potentially lethal opportunistic infections, we also undertook a thorough bacteriological assessment of 4-week MAH-infected *Irgm1*-/- animals: we collected brains, lungs, kidneys, spleens and livers and ground and plated them on blood agar plates. We identified 1 isolate of *Candida* sp. in the lung of 1 *Irgm1*-/- mouse, and 1 isolate of *Staphylococcus aureus* in the kidney of another *Irgm1*-/- mouse, but in both cases bacterial enumeration showed ≤ 10^2 CFUs per organ (data not shown). Thus, we concluded that our analysis ruled out the occurrence of an overwhelming opportunistic infection that could explain the accelerated rate of death of MAH-infected *Irgm1*-/- mice.

Finally, we sought to examine if *Irgm1*-/- mice developed other metabolic abnormalities during infection with MAH. We used blood collected on 2 *Irgm1*-/- mice from the same cohort to assess the levels of glucose, albumine, electrolytes, liver enzymes, urea and creatinine (markers of kidney function) and pancreatic enzymes. As shown in table 4.2, all results were normal (at the exception of slightly low albumin and urea contents, a finding attributed to an altered nutritional status), ruling out any renal, hepatic or pancreatic dysfunction.

Thus at this step, we found that *Irgm1*-/- mice infected systemically with MAH showed a progressive weight loss without other significant clinical abnormality, and developed a marked pancytopenia with severe anemia, mild thrombocytopenia and moderate lymphocytopenia. We did not find evidence for a significant immunosuppression attributed to the lymphocytopenia. We reasoned that the most probable cause of death was a conjunction of: 1) increased MAH CFU counts in spleens and livers (and to a lesser extent mesenteric lymph nodes and other organs); and 2) severe anemia (also attributed to the Irgm1 deficiency, see "Discussion" for more information on this) leading progressively to death as a result of cachexia, dehydration and/or cardiac failure.

	MAH-infected *Irgm1*-/- mouse 1	MAH-infected *Irgm1*-/- mouse 2	References for C57Bl/6 mice
Total protein (g/L)	46	45	26 – 66
Albumin (g/L)	17	19	25 – 48
Glucose (mmol/L)	6.7	7.6	5.0 – 10.7
BUN Urea (mmol/L)	13.1	9	6.4 – 10.4
Creatinine (µmol/L)	19	17	18 – 71
Na^+ (mmol/L)	152	150	124 – 174
K^+ (mmol/L)	6.3	6.5	4.6 – 8
Cl^- (mmol/L)	116	112	92 – 120
Bilirubin (µmol/L)	3	3	2 – 15
ASAT (U/L)	45	90	28 – 132
ALAT (U/L)	197	255	59 – 247
AP (U/L)	163	126	62 – 209
GGT (U/L)	< 10	< 10	
Amylase (U/L)	2739	2327	1691 – 3615
Lipase (U/L)	638	705	

Table 4.2: Serum metabolic profile (glucose, proteins, eletrolytes, markers of kidney, liver and pancreas functions) of *Irgm1*-/- and wild-type mice infected by IP injection with ~ 10^8 MAH CFUs, at 1 month post-infection. References are from reference 161.

4.1.4) *In vitro* macrophage infections

Next, we decided to investigate the potential implication of macrophages (which constitute the first innate line of defence during mycobacterial infections) in the defective control of MAH and MAP replication seen in *Irgm1*-/- mice. To this end, we compared the mycobactericidal properties of *Irgm1*-/- and wild-type macrophages pre-stimulated with IFN-γ and infected *in vitro* with MAH and MAP. This seemed even more relevant in this context because of the conflicting literature pertaining to the role of *Irgm1*-/- macrophages in the control of *M. tuberculosis* and members of the MAC, with MacMicking et al. reporting on a macrophage defect (with *M. tuberculosis*) not evidenced by Feng et al. (with *M. avium*).

In a first experiment, we infected peritoneal macrophages harvested from *Irgm1*-/- and wild-type controls *in vitro* with MAH strain 104 (see figure 4.4a). Contrarily to what we

expected, we found that MAH was capable of replicating inside of these cells, most notably when they were not pre-stimulated with IFN-γ: in both genotypes, there was a clear increase in the number of viable intracellular bacteria between day 0 and day 7 (~ 10000%). However, these numbers were not statistically different between non-IFN-γ-stimulated *Irmg1*-/- and wild-type cells, which is logical (because *Irgm1* is expressed selectively upon stimulation with IFN-γ) and in accordance with the results published by all authors in the field. We found that wild-type macrophages showed an enhanced ability to eliminate intracellular bacteria upon stimulation with IFN-γ, as evidenced by the reduction of viable bacteria recovered from stimulated cells (3134% of baseline at day 7 versus 11738% in non-stimulated cells, p = 0.0388), which is in agreement with the results by MacMicking et al (see figure 1.10). In *Irgm1*-/- macrophages, bacterial viability was also reduced upon stimulation with IFN-γ, but to a lesser extent: there was no statistically significant difference between stimulated and non-stimulated *Irgm1*-/- macrophages in terms of bacterial killing. Second, when comparing IFN-γ-stimulated *Irgm1*-/- and *Irgm1*+/+ cells, we found that wild-type cells were more bactericidal (3134% viability at day 7, versus 8276% in Irgm1-/- cells), but due to a high variability around the mean this difference was not statistically significant (p = 0.104). In conclusion, this experiment showed that the Irgm1 deficiency seemed responsible for an intrinsic mycobactericidal defect in peritoneal macrophages, apparent after stimulation with IFN-γ, with substantial variability in the bacterial counts preventing from reaching statistical significance. The trend we observed seemed in accordance with the findings reported by MacMicking et al.

We then went on to conduct a similar *in vitro* infection of peritoneal macrophages with MAP (see figure 4.4b). First, we found that the growth characteristics of MAP inside of non-stimulated peritoneal macrophages were quite different from those of MAH: there was in both genotypes a slight increase in the number of viable bacteria at day 2, followed by second phase of bacterial killing (up to 30.9% viable bacteria in wild-type and 59.0% in *Irgm1*-/- cells). However, we were not able to show the same defect of *Irgm1*-/- macrophages that we found in the case of MAH: stimulation of wild-type macrophages did not result in an enhanced killing of MAP, nor did we observe a difference in bacterial killing between *Irgm1*-/- and wild-type cells upon IFN-γ stimulation.

The same experiment was carried out a second time (figure 4.4c). In this case, we were able to show a significant increase in mycobactericidal properties of wild-type peritoneal macrophages upon stimulation with IFN-γ at day 7 (bacterial viability without prestimulation 128%, versus 67% with prestimulation, p = 0.0391). However, the overall aspect of the curves make it difficult to infer much from this isolated finding. And in accordance with the experiment presented in figure 4.4b, we were not able to show an Irgm1-dependent macrophage killing impairment upon IFN-γ stimulation, with 79% viable bacteria at day 7 in *Irgm1*-/- cells versus 67% in wild-type cells (p = 0.348). In total, these two experiments showed that in the case of MAP, peritoneal macrophages from *Irgm1*-/- and wild-type animals infected *in vitro* had similar mycobactericidal properties.

Next, we infected bone marrow-derived macrophages *in vitro* with MAH (see figure 4.4d). First, we confirmed that MAH was capable of replicating much faster than MAP inside of these cells (attaining at day 7 1661% and 1775% of initial viability in wild-type and *Irgm1*-/- non-stimulated cells, respectively). Here again we were not able to show an effect of the IFN-γ pre-stimulation in wild-type cells at any time point. However, at 5 days post-infection, the percentage of live bacteria harvested from *Irgm1*-/- IFN-γ-stimulated macrophages was 901% (sd = 234%), as opposed to 565% (sd = 247%) in IFN-γ-stimulated wild-type cells (p = 0.0339): this indicated a clear defect of mycobactericidal properties of *Irgm1*-/- macrophages.

Finally, we infected bone marrow-derived macrophages *in vitro* with MAP (see figure 4.4e). Confirming our previous observation on the growth rate of MAP inside of peritoneal macrophages, we found here again a slow decrease in bacterial viability over time in all four experimental conditions, with bacterial viability between ~ 8 and ~ 15% at day 7. However, at day 2 (before the majority of bacteria have been eliminated), we found a statistically significant effect of the IFN-γ pre-stimulation in wild-type macrophages (bacterial viability without pre-stimulation 43% (sd = 9%), versus 17% (sd = 1%) after pre-stimulation, p = 0.0277). Furthermore, we found that both at day 2 and at day 7, the Irgm1 deficiency resulted in impaired bacterial killing upon IFN-γ pre-stimulation; for instance at day 2, *Irgm1*-/- stimulated macrophages had 48% (sd = 6%) viable bacteria, versus 17% (sd = 1%) in wild-type cells (p = 0.0035).

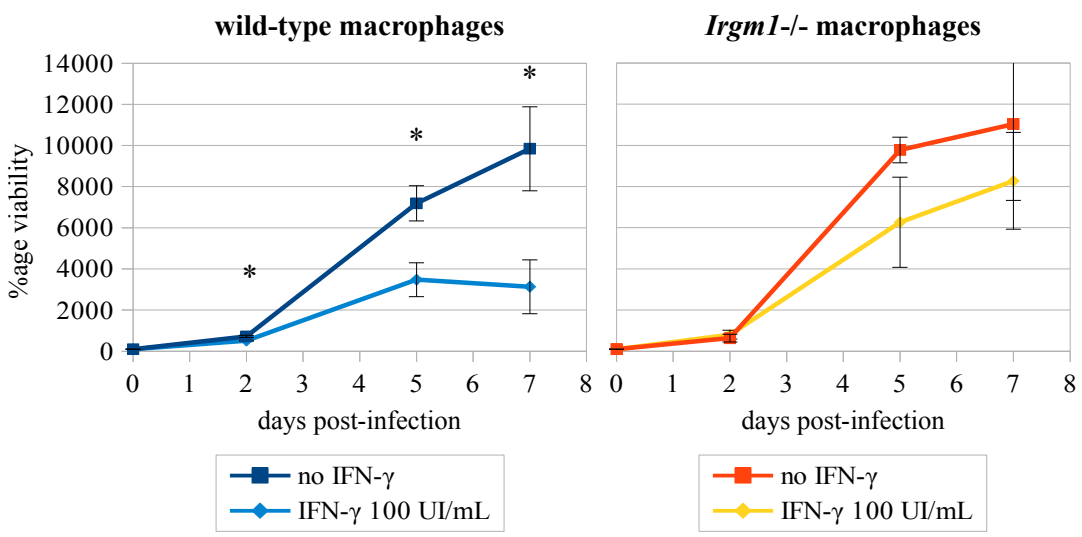

4.4a: *In vitro* infection of peritoneal macrophages from *Irgm1-/-* and wild-type mice with MAH

Figure 4.4: *In vitro* infections of peritoneal and bone marrow-derived macrophages from *Irgm1-/-* and wild-type mice with MAP and MAH.

Peritoneal macrophages (4.4a, 4.4b, 4.4c) and bone marrow-derived macrophages (4.4d, 4.4d) were harvested from *Irgm1-/-* and wild-type mice and infected *in vitro* with MAP (4.4b, 4.4c, 4.4e) and MAH (4.4a, 4.4d), with MOI of 5:1 or 10:1. Cells were left untreated or stimulated with murine recombinant INF-γ at a concentration of 100 UI/mL. At different time points, macrophages were lysed to recover intra-cellular bacteria and the resulting lysates were diluted and plated for subsequent CFU enumeration. Viability is given as a percentage of the starting (4 to 6 hours post-infection) CFU uptake.

The results of these experiments are to be analyzed in light of the results of MacMicking et al. (reference 93) reproduced in figure 1.10.

black * indicates statistically significant difference between IFN-γ-stimulated and non stimulated cells of same genotype with $p < 0.01$.

red * indicates statistically significant difference between IFN-γ-stimulated *Irgm1-/-* and IFN-γ-stimulated wild-type cells with $p < 0.01$.

4.4a: *In vitro* infection of peritoneal macrophages from *Irgm1-/-* and wild-type mice with MAH, MOI of 10:1.

4.4b: *In vitro* infection of peritoneal macrophages from *Irgm1-/-* and wild-type mice with MAP, MOI of 10:1 (1st experiment).

4.4c: *In vitro* infection of peritoneal macrophages from *Irgm1-/-* and wild-type mice with MAP, MOI of 10:1 (2nd experiment).

4.4d: *In vitro* infection of bone marrow-derived macrophages from *Irgm1-/-* and wild-type mice with MAH, MOI of 10:1.

4.4d: *In vitro* infection of bone marrow-derived macrophages from *Irgm1-/-* and wild-type mice with MAP, MOI 5:1.

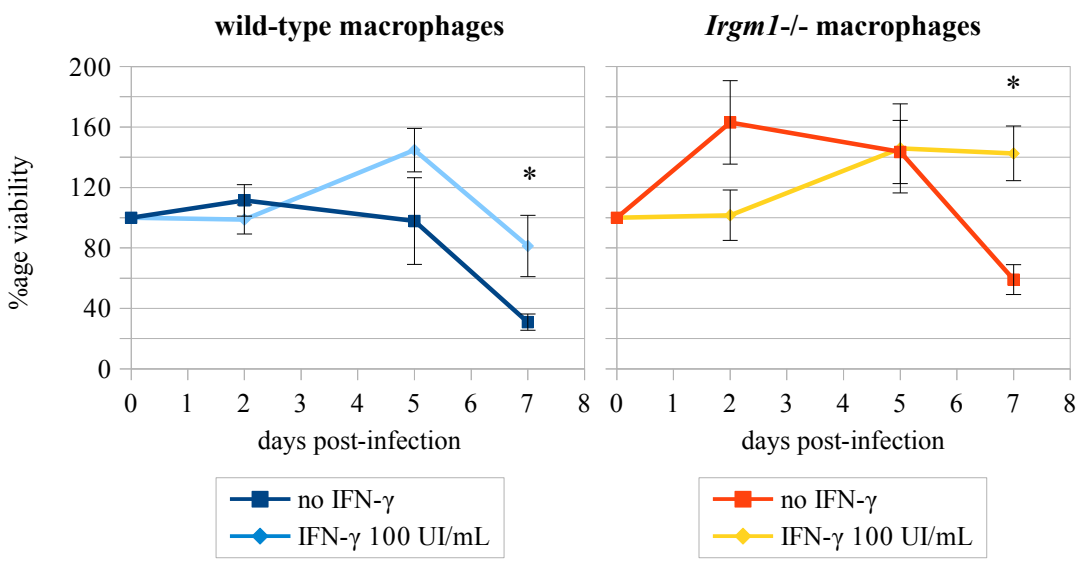

4.4b: *In vitro* infection of peritoneal macrophages from *Irgm1-/-* and wild-type mice with MAP (1st experiment)

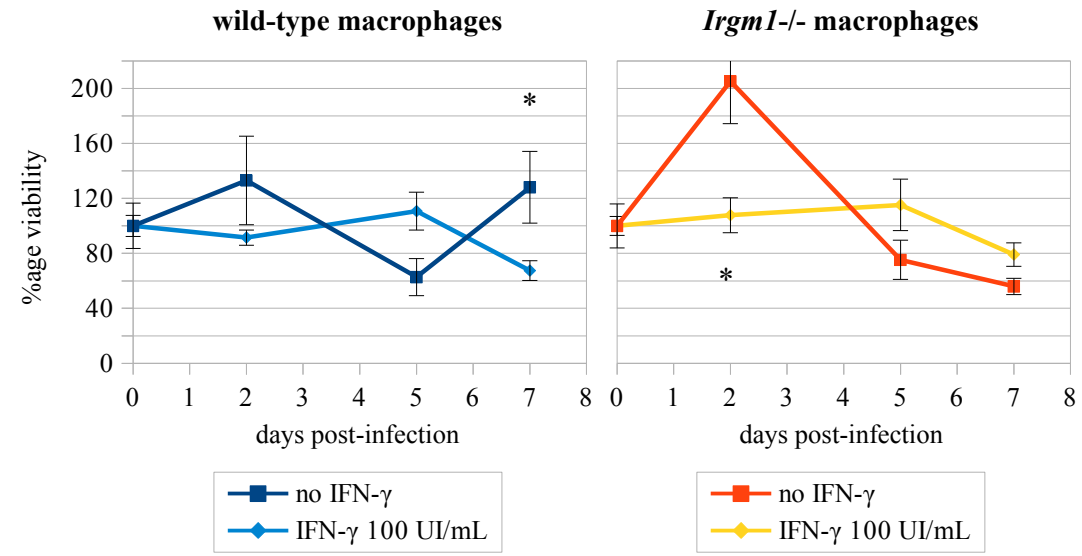

4.4c: *In vitro* infection of peritoneal macrophages from *Irgm1-/-* and wild-type mice with MAP (2nd experiment)

Figure 4.4: *In vitro* infections of peritoneal and bone marrow-derived macrophages from *Irgm1-/-* and wild-type mice with MAP and MAH.

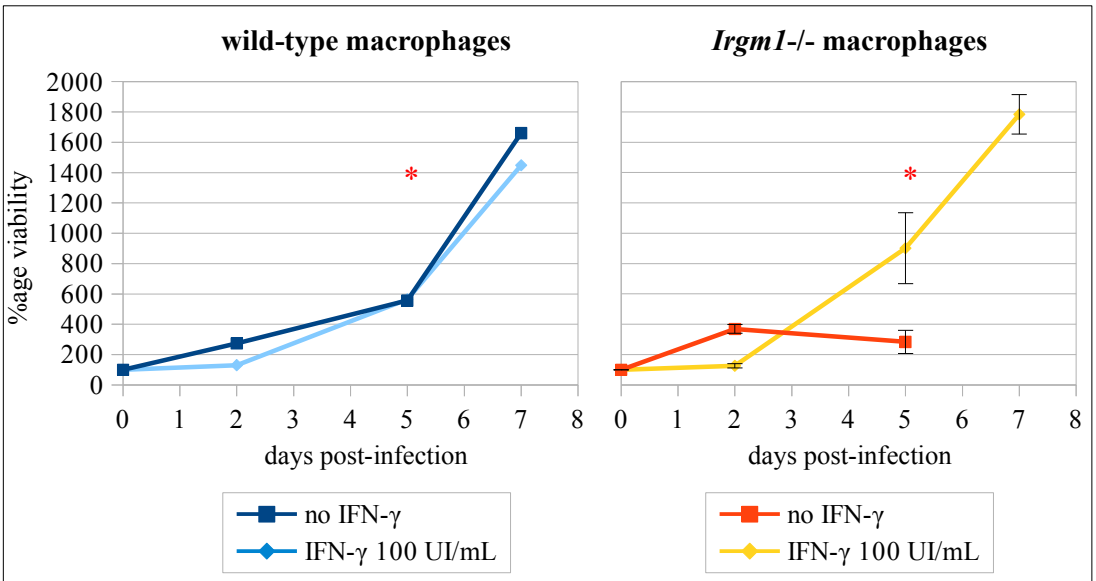

4.4d: *In vitro* infection of bone marrow-derived macrophages from *Irgm1*-/- and wild-type mice with MAH

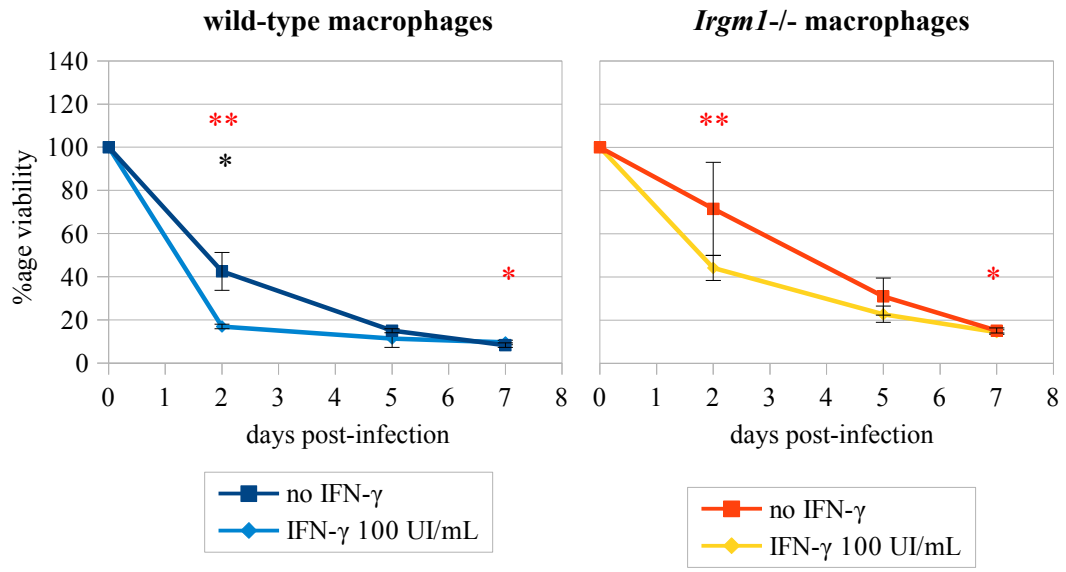

4.43e: *In vitro* infection of bone marrow-derived macrophages from *Irgm1*-/- and wild-type mice with MAP

Figure 4.4: *In vitro* infections of peritoneal and bone marrow-derived macrophages from *Irgm1*-/- and wild-type mice with MAP and MAH.

In conclusion, this set of *in vitro* macrophage infections with MAP and MAH led to the following findings. First, MAH and MAP have strikingly different growth characteristics inside of macrophages: MAH seems to replicate at a faster pace than it is killed, when MAP seems to undergo a slow but constant elimination. Second, it seems that the killing abilities of peritoneal macrophages towards both MAH and MAP are less strong than those of bone marrow-derived macrophages. And finally, in 3 experiments out of 5, we were able to show a difference in mycobacterial killing between IFN-γ-treated *Irgm1*-/- and *Irgm1*+/+ macrophages (which was more evident in bone marrow-derived cells). This seemed to corroborate the findings reported by MacMicking et al. on *Mycobacterium tuberculosis*: in our setting, it seemed that the uncontrolled bacterial replication seen *in vivo* could be explained, at least in part, by an intrinsic mycobactericidal defect of *Irgm1*-/- macrophages.

4.2) Part 2: intestinal infection of the *Irgm1*-/- mouse with MAP

In the first part of this work, we showed that *Irgm1*-/- mice are highly susceptible to systemic infections with MAP and MAH, as a result of a defective control of bacterial replication and the development of a severe anemia. We also observed that in this host, and in spite of its attenuated virulence, MAH was responsible for a more severe disease than MAP. Because we were ultimately interested in studying the course of an intestinal disease characterized by significant pathology but not by an increased acute mortality, MAP appeared a more amenable microorganism to carry out the experiments related to this objective.

Thus, in the second part of our work, we set out to use the *Irgm1*-/- mouse as host suitable for the induction of an intestinal infection with MAP, in order to: 1) attempt to develop a small animal model with intestinal lesions similar to those seen in paratuberculosis (and CD); and 2) document its clinical, bacteriological and pathological evolution.

4.2.1) Gavage infections

As previously indicated, wild-type C57Bl/6 mice are susceptible to MAP, which means that if injected experimentally at sufficient doses (≥ 10^8 CFUs) via the intra-peritoneal route, MAP leads to the establishment of a chronic infection[33,34,37]. More specifically, such a chronic MAP infection is characterized by two types of experimental outcomes: 1) a bacteriological outcome, the maintenance of stable bacterial counts in spleen and liver over the course of several months post-infection; and 2) a pathological outcome, the development and maintenance of granulomatous lesions, mainly in the liver and in the mesenteric lymph nodes. However, C57Bl/6 mice infected by intra-peritoneal injection have never been reported to develop histological lesions located in any of the three layers of the intestinal wall. And furthermore, the intra-intestinal route is not suitable for establishing a chronic infection, as evidenced by the work of Veazey et al., who showed that only 50% of a group of C57Bl/6 mice infected by gavage with 10^{11} MAP CFUs developed histological lesions, all limited to the mesenteric lymph nodes (with no lesion of the intestinal mucosa, nor in the spleen and liver) after 11 months of infection[36].

Previous work undertaken in the Behr lab on *Nod2*+/+ and *Nod2*-/- C57Bl/6 mice infected with MAP by gavage have shown that: 1) only a small fraction of infected animals develop a productive infection, attested by the recovery of MAP (in small numbers) in the mesenteric lymph nodes, with no viable bacteria recovered from spleen and liver; 2) the most salient pathological finding consists in inflammatory lesions of the mesenteric lymph nodes, some of them granulomatous, with no significant pathology in the spleen, liver and intestine (isolated mesenteric adenitis); and 3) the Nod2 deficiency does not result in an increased susceptibility to MAP, neither in terms of bacterial counts nor in terms of pathology.

In our initial attempt to use the *Irgm1*-/- mouse as a potential model to induce experimental MAP-driven intestinal lesions, we decided the study the short-term pathological consequences of a gavage infection with relatively high doses of MAP. We thus infected 2 groups of 4 *Irgm1*-/- mice with ~ 10^9 MAP CFUs by gavage, monitored them clinically for 1 and 2 months (respectively), after which we harvested small intestines, colons, mesentery, spleens and livers and sent them for processing, embedding and

staining (hematoxylin & eosin (H&E) and Ziehl Niessen (ZN)). The slides were not subjected to the assessment of a veterinarian pathologist, but after independent reading by two observers, we were not able to detect any significant histological abnormality in the intestine, the mesentery, the spleen or the liver of infected animals (data not shown). Thus, in our hands, it seemed that the *Irgm1*-/- mouse was not a suitable model for the establishment of intestinal lesions after gavage infection with MAP.

We reasoned that the occurrence of histological lesions in any tissue or organ would necessarily be secondary to its colonization by viable MAP cells (at least in the relatively short time frames of 1 and 2 months in which we had decided to set these experiments), and that subsequently we could expect a roughly positive correlation between histological severity and bacterial counts. For technical purposes, we thus decided to focus on the bacteriological outcome after gavage infections, to devise a protocol for successful intra-intestinal infection with MAP. Our second hypothesis was that *Irgm1*-/- mice would potentially suffer from more severe pathology than wild-type mice when colonized with an identical bacterial burden, but that their intestinal permeability to MAP would not be significantly different from that of wild-type mice, which is the reason why all the experiments described below where conducted on wild-type animals. First, we infected 2 groups of 9 wild-type C57Bl/6 mice with ~ 10^8 MAP CFUs in identical conditions (on the same date and with the same protocol for inocula preparation) by intra-peritoneal injection and by gavage (respectively), and we harvested spleens and mesenteric lymph nodes after 2 weeks for comparative bacteriological assessment. In the group of mice infected by IP, we found viable bacteria colonizing the spleen in 9 out of 9 animals (mean bacterial counts 5.58 $\log_{10}$(CFU) per spleen, sd = 1.01) and the mesenteric lymph nodes in 8 out of 9 animals (mean bacterial counts 3.60 $\log_{10}$(CFU) per lymph node, sd = 1.46); however in the group infected by gavage, we recovered viable bacteria in 0 spleen out of 9 and in 0 mesenteric lymph node out of 9 (while all samples were plated in dilutions ranging from 10^{-7} to 0). This indicated a total failure to colonize wild-type C57Bl6 mice with MAP by gavage, in accordance to previously published work.

Next, we sought to investigate if a pharmacological pre-treatment of the mice could increase the yield of gavage infections. Our first hypothesis was that the MAP inocula

administered orally could be drastically reduced upon transit in the stomach due to the acidic pH of gastric secretions; thus, we decided to test whether an anti-acid treatment before infection would result in better colonization rates, and we chose to use sodium bicarbonate ($NaHCO_3$) for that purpose (as a quick literature search indicated that — at least in the context of gram negative enteric pathogens — it was as efficacious as a proton pomp-inhibitor (omeprazole) in reducing bacterial colonization levels after oral challenge, see reference 152). Second, we reasoned that MAP binding to, and subsequent translocation across the gut epithelium could be impeded by the presence of luminal contents, including food and the resident comensal bacterial flora. Thus, we decided to test the impact of: 1) a short period of fasting; and 2) a brief antibiotic pretreatment before oral infection (for which we followed a protocol detailed in reference 153). The resulting experiment consisted in the gavage infection with ~ 10^9 MAH CFUs of 5 groups of wild-type mice receiving different pre-treatments (as detailed in the "Materials and methods" section): brief food deprivation; sodium bicarbonate; streptomycin; sodium bicarbonate + streptomycin; 0.9% NaCl ("placebo group"). Mice were sacrificed 2 weeks after infection for quantitative bacteriology: here again, were were not able to grow viable MAP from the spleens, livers and mesenteric lymph nodes in any group of mice (data not shown), thus indicating a failure to colonize mice with MAP in all conditions tested.

4.2.2) Intra-jejunal infection of *Irgm1*-/- mice with MAP: pathological assessment

This is why we then turned to the development of a protocol based on the injection of a MAP-containing solution in the lumen of the jejunum of mice submitted to a median laparotomy under general anesthesia (detailed in the "Materials and methods" section, and referred to, as of now, as intra-jejunal (IJ) infections).

We initially infected a group of 5 *Irgm1*-/- mice by IJ-inoculation of a solution containing ~ 10^9 MAP CFUs, and after 1 month, we harvested their small intestine, colon and mesentery, and submitted the resulting H&E-stained slides to the professional assessment of a veterinarian pathologist (not blinded to the experimental design and end-points).

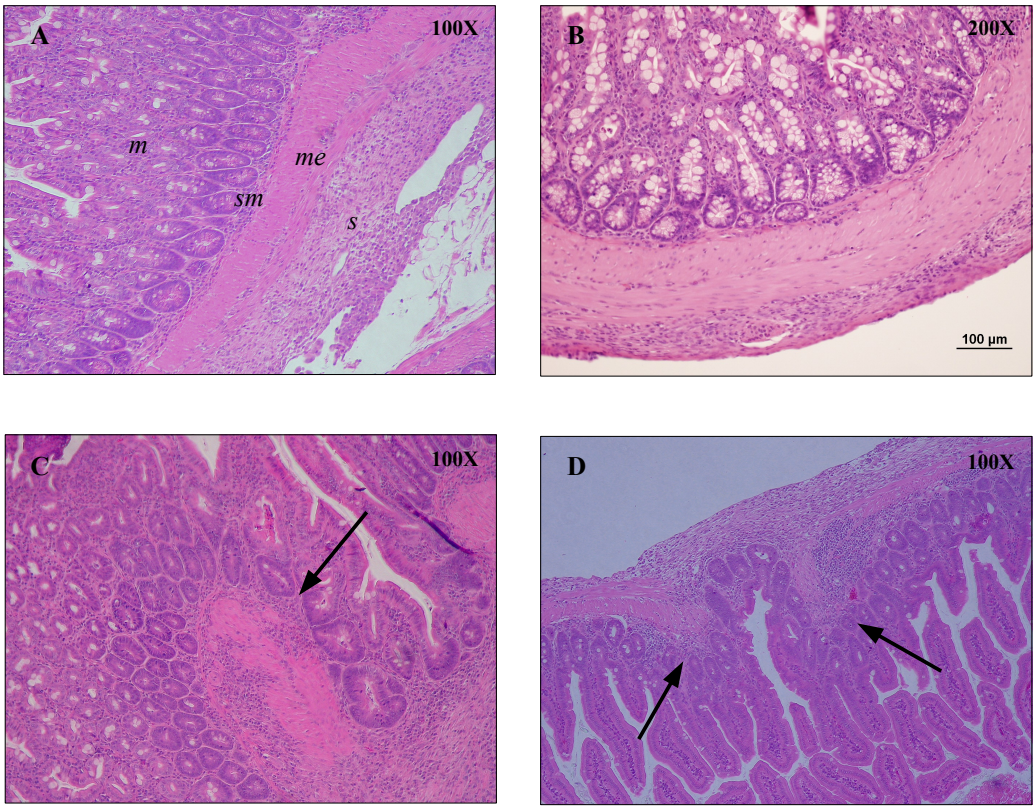

Figure 4.5: Histopathological analysis of small intestine and mesentery of *Irgm1-/-* mice infected by intra-jejunal inoculation of 10^9 MAP CFUs, at 1 month post-infection.
Organs were fixed in Formalin, and embedded in paraffin for hematoxilin & eosin (H&E) (4.5a to 4.5h) and Ziehl Neelsen (ZN) stainings. Data are representative of 5 mice, and gave similar results in another cohort of *Irgm1-/-* examined after 2 months of infection.
100X, 200X, 1000X indicates magnification.
4.5a: *m* designate the mucosa (intestinal epithelium, lamina propria, muscularis mucosa), *sm* designates the submucosa, *me* designates the muscularis externa, *s* designates the serosa. A lympho-histiocytic infiltrate is seen in the serosa.
4.5b: Discrete infiltration of the serosa, oedema and cellular infiltrates in the lamina propria, epithelial lesions (epithelial cell vacuolization), defining a transmural inflammatory lesion.
4.5c: Arrow designates an area where immune-competent cells coming from the serosa are penetrating through the muscularis externa to reach the mucosa.
4.5d: Arrows designate areas of transmural inflammation.
4.5e: Arrow shows the path of immune cells across the muscularis externa (*me*), bridging inflammed areas in the submucosa (*sm*) and in the serosa (*s*).
4.5f: Cellular infiltrates prominent in the lamina propria, signs of epithelial cell damage.

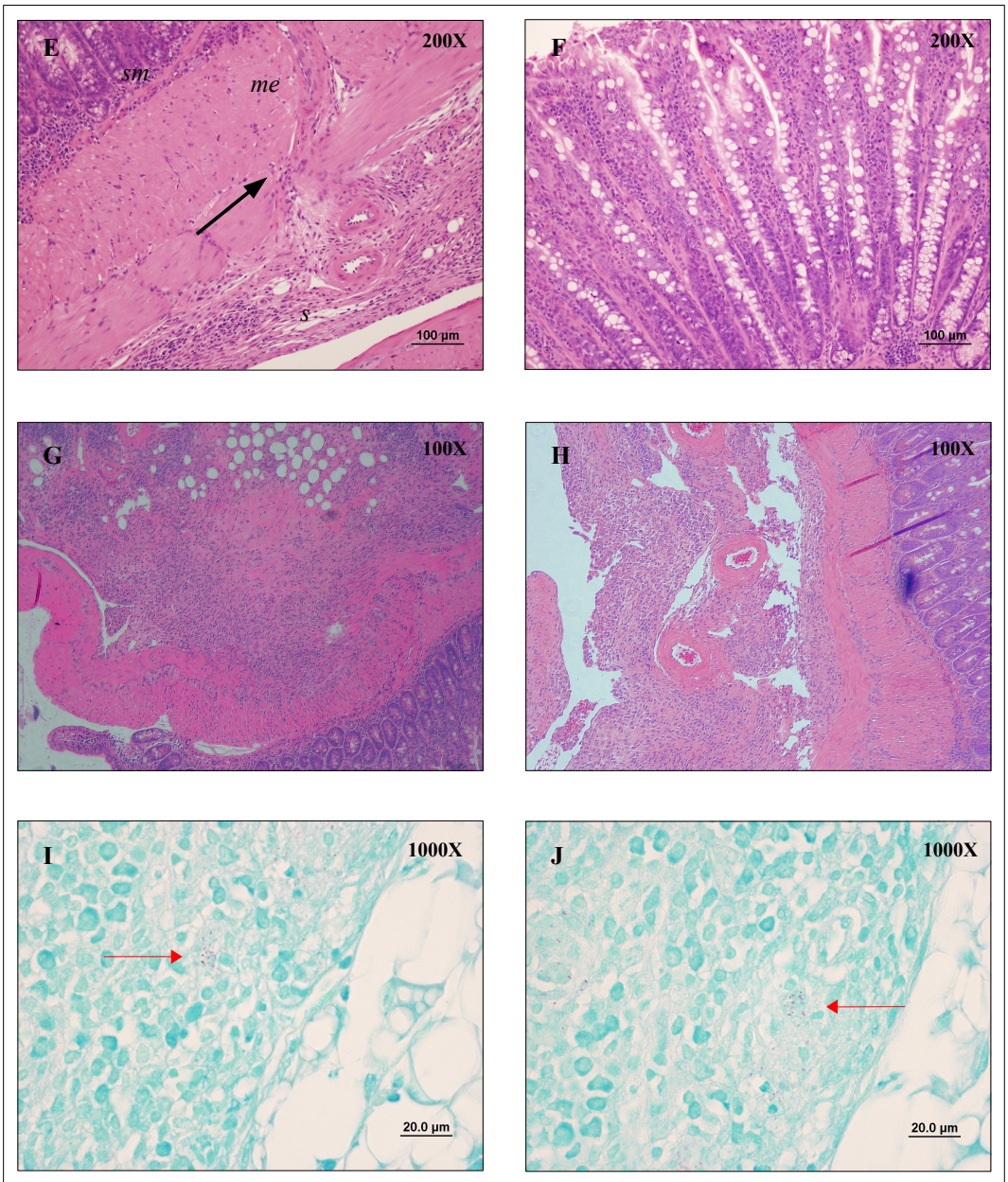

Figure 4.5: Histopathological analysis of small intestine and mesentery of *Irgm1*-/- mice infected by intra-jejunal inoculation of 10^9 MAP CFUs, at 1 month post-infection.
4.5g: Massive inflammation in the serosa and adjacent mesentery.
4.5h: Inflammatory lesions of the mesentery. Note the peri-vascular infiltrates.
4.5i and 4.5j: At higher magnification, foci of red-staining cocoo-bacilli corresponding of MAP, opposite to areas of active inflammation (main foci marked with red arrows)

First, we observed that, at one month post-infection, all mice presented histological signs of an inflammatory reaction affecting the small bowel wall (see figure 4.5). The inflammatory reaction was characterized by cellular aggregates composed mostly of macrophages and lymphocytes (lympho-histiocytic infiltrates) and less importantly of plasma cells and granulocytes. These infiltrates were transmural (see figures 4.5c, 4.5d, 4.5d): commonly most severe at the mesenteric border of the small intestine wall and in the serosa (serositis), they were seen cutting through the muscularis and reaching the mucosa and the submucosa. Histological lesions were also segmental, with a clear demarcation between inflamed and normal areas of the intestine, and seemingly most severe in the termimal ileum. The inflammatory process was both active and chronic, with fibroblastic hyperplasia and some fibrotic lesions seen across the muscularis externa. We established the presence of a few multinucleated giant cells in the deeper layers of the gut wall, while in the lamina propria there was a predominance of lymphocytes and plasma cells (see figure 4.5f). There was no sign of necrosis, no granuloma, no abscess; there were subtle signs of epithelial damage (cell sloughing, vacuolization), but no clear erosion or ulcer. Of note, there was significant variation in severity across samples (with subjective severity scores ranging from 1/5 to 5/5).

Second, we found that the mesenteric tissues were also infiltrated with immune-competent cells, mostly macrophages, lymphocytes and plasma cells (acute mesenteric lymphadenitis, see figure 4.5g and 4.5h). In all five animals, the severity of mesenteric inflammation correlated roughly with that of the gut wall. There were focal aggregates of inflammatory cells with rare multinucleated giant cells (but no actual granuloma) as well as large hyperplastic mesenteric lymph nodes.

Finally, when assessing the complementary ZN-stained slides, we were able to locate numerous acid-fast cocco-bacilli, gathered in foci containing abundant bacteria corresponding to MAP. These aggregates could be seen under a 40X magnification on most slides. Generally, it seemed that the presence of the bacteria correlated well with the location of the inflammatory infiltrates, and that their number per focus of immune cells correlated well with its severity. Bacteria were almost exclusively present in the deeper layers of the gut wall (serosa and adjacent mesentery), and rarely seen in the mucosa or in

the submucosa. In one mouse only did we find isolated cocco-bacilli in the lamina propria, opposite to a discrete cellular infiltrate. In all biospies examined, all bacteria seemed to remain intra-cellular, located around the nucleus and inside the cytosol of histiocytic cells. Similar foci of acid-fast bacteria were seen in the mesentery, located within hyperplasic mesenteric lymph nodes, and organized in a manner similar to that seen in the gut.

Thus, it seemed that inoculating MAP directly in the lumen of the small intestine was efficacious at inducing histopathological lesions affecting the gut wall itself. To confirm these findings, we proceeded to the same experiment and examined tissues harvested on animals at 2 months post-infection. Similarly, we found in all animals lympho-histiocytic infiltrates affecting the serosa, the muscularis externa and the mucosa (transmural pathology), organized in a discrete fashion (segmental pathology). There were important mesenteric lesions, and here again, we were able to identify acid-fast bacteria corresponding to MAP in areas of active inflammation. Just like at 1 month post-infection, there was a major variability in severity across animals. On average, it seemed that the nature and severity of the inflammatory reaction at 2 months was not different from what we had seen at 1 month post-infection.

4.2.3) Intra-jejunal infection of *Irgm1*-/- mice with MAP: clinical and bacteriological assessment

We then went on to characterize the clinical and bacteriological phenotype of the MAP IJ-infected *Irgm1*-/- mice.

Clinically, we monitored the survival of several cohorts of mice. We observed that, if on average 10 to 20% of them died in the immediate post-operative period (usually due to "mechanical complications" of the surgery leading to intestinal obstruction) the remaining animals could survive for several months following surgery with no weight loss, nor any evident clinical abnormality. Specifically, we did not observe diarrhoea, nor rectal bleeding.

We then undertook to quantify the levels of MAP colonization in small intestine, colon, mesenteric tissue, spleen and liver. To this end, we turned to the use of culture-independent techniques, because: 1) most classic quantitative bacteriology protocols (plating of serial 10-fold dilutions and enumeration of CFUs) for MAP quantification in

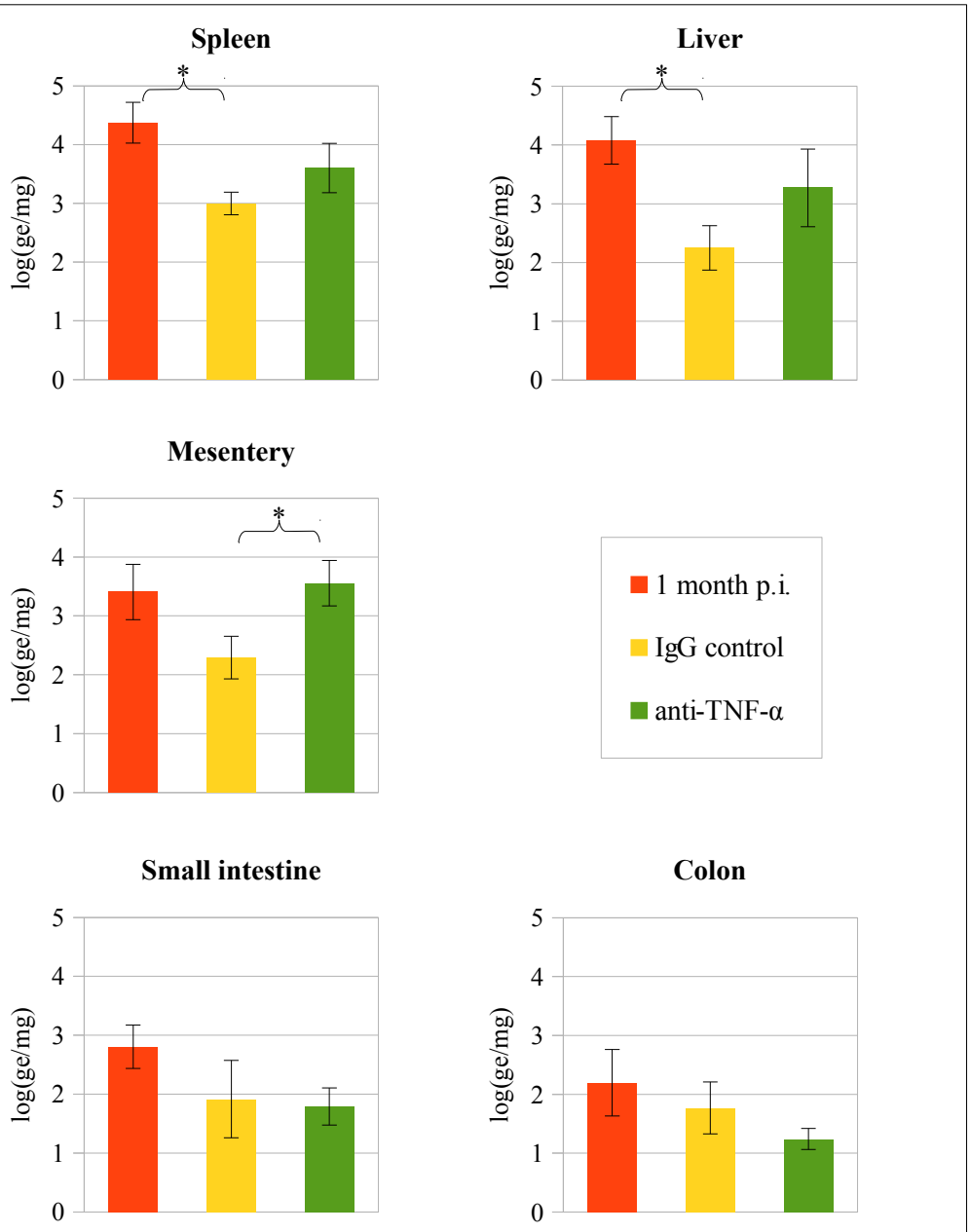

Figure 4.6: MAP quantification by quantitative polymerase chain reaction (qPCR) in spleen, liver, mesenteric lymph nodes, small intestine and colon of *Irgm1*-/- infected by IJ inoculation of 10^9 MAP CFUs.

At 4 weeks post-infection, 5 mice were sacrificed to quantify their bacterial burden.

2 groups of mice (n = 5 each) randomly received a treatment by anti-tumor necrosis factor-alpha (TNF-α) neutralizing antibody or an isotype control (500 mg/kg at 4 and 6 weeks post-infection), and subsequently sacrificed at 8 weeks post-infection to quantify the bacterial burden.

Results are expressed in $\log_{10}$(genome equivalent of MAP per milligram of tissue). * denotes statistical significance with $p < 0.01$.

organs highly contaminated with fast-growing bacteria include "decontamination steps" with hexadecylpyridinium chloride (HPC) which have a significant but quite unpredictable impact on MAP viability; and 2) recent work in the Behr lab has led to the development of a validated protocol for MAP DNA extraction and quantification by quantitative polymerase chain reaction (qPCR) (detailed in the “Materials and methods” section). Of note, the results given by this technique are expressed in MAP genome equivalents per milligram of organ, and for reasons that are still under investigation, in any tissue colonized by MAP qPCR-based quantification consistently yields values that are 1-2 log superior to those obtained by classic CFUs enumeration, which prevents a strict comparison of two experiments carried out independently with the two different techniques. As shown in figure 4.6, intra-jejunal inoculation of MAP in *Irgm1*-/- mice leads to low-level colonization of the small intestine and colon, with slightly more bacteria in the mesenteric tissue and higher bacterial counts in the liver and spleen.

Finally, we infected a cohort of *Irgm1*-/- mice to characterize their haematologic profile at 1 month post-infection. We were specifically interested to see if the mice would develop the haematologic abnormalities associated with a systemic infection with high bacterial counts. As shown in table 4.3, and in line with the attenuated clinical symptomatology seen after IJ infection, we observed a rather normal complete blood count: there was a mild lymphocytopenia, but no anemia and no thrombocytopenia.

4.2.4) Intra-jejunal infection of *Irgm1*-/- mice with MAP: impact of CD therapeutics

The treatment regimens of patients with CD involves (usually as a first line therapy) the systemic or intra-intestinal administration of glucocorticosteroids. However these drugs have been associated in human epidemiology studies with a higher risk of reactivation of latent tuberculosis[162], (see “Discussion” for more information on this), which is an argument used by some authors to refute a possible implication of MAP in CD pathogenesis. To evaluate the effect of a systemic treatment by glucocorticosteroids, we randomly divided a cohort of 12 *Irgm1*-/- mice infected 1 month before with 10^9 MAP CFUs by IJ into two groups: 1) a "treatment group" receiving an IP injection of 4 mg/kg methylprednisolone 5 days per week; and 2) a "placebo group" receiving an IP injection of 200 µL normal saline 5

	MAP IJ-infected *Irgm1*-/- mice (n = 6) (mean, sd)	**References for C57Bl/6 m**
Hematocrit (%)	40.5 (5.0)	39% – 49%
Hemoglobin (g/L)	130 (15)	102 – 166
WBCs (10^9/L)	5.2 (1.3)	6 – 15
Neutrophils (10^9/L)	1.14 (0.84)	
Lymphocytes (10^9/L)	3.95 (1.17)	
Monocytes (10^9/L)	0.05 (0.05)	
Platelets (10^9/L)	599 (70)	160 – 410

Table 4.3: Haematological profile (complete blood count, CBC) of *Irgm1*-/- mice infected by IJ injection of ~ 10^8 MAP CFUs, at 1 month post-infection. References are from reference 160.

days per week). The mice were monitored clinically and weighed every week to compare their survival (using a cut-off of 85% of initial weight for sacrifice). As shown in figure 4.7, the treatment with methylprednisolone did not bring about significant morbidity: actually there was a non significant trend towards longer survival in the treatment group (log-rank test: $\chi^2 = 2.41$, $p = 0.0120$).

Finally, TNF-α inhibitors are prominent in the care of patients with moderately to severely active Crohn's disease that is refractory to conventional therapy[163]. However, they have been reported in numerous epidemiological studies to be associated with an increased risk of TB reactivation[164], and animal studies have also clearly established the role of TNF-α in immune control of *T. tb*[165,166], which seems to argue against a possible involvement of MAP in CD. Thus, we decided to test the effect of treatment with a neutralizing antibody against TNF-α on the outcome of our model of MAP-driven ileo-colitis. We decided to document the evolution of the bacterial burden in IJ-infected mice,

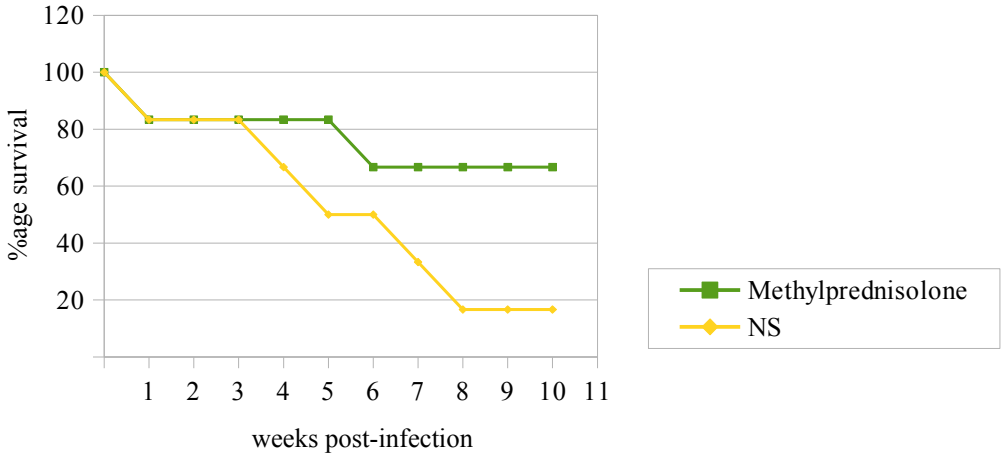

Figure 4.7: Survival *Irgm1*-/- mice infected with MAP by IJ injection treated with methylprednisolone
Irgm1-/- mice (n = 12) were infected by IP injection with ~ 10^9 MAP CFUs and at 1 month post-infection, were randomly assigned to receive methylprednisolone 4 mg/kg by IP injection 5 days per week (treatment group, n = 6), or 0.9% NaCl (NS) (placebo group, n = 6). They were monitored weekly for survival and sacrificed when they attained 85% of basal weight.

because: 1) it has been argued that TNF-α inhibitors lead to an impaired control of mycobacterial replication; and 2) there was too much variability in the pathological severity seen after IJ infections to possibly detect an effect of the treatment on histological lesions (be it positive or negative). A cohort of 15 MAP IJ-infected *Irgm1*-/- was randomly split into 3 groups: the first group was used for qPCR-based quantification of MAP DNA in small intestine, colon, mesenteric tissue, liver and spleen at 1 month post-infection; the treatment group received 2 IP injections of 5 mg/kg of an anti-mouse TNF-α neutralizing antibody (at 4 and 6 weeks post-infection); the placebo group received 2 IP injections of 5 mg/kg of a isotype control (at 4 and 6 weeks post-infection). The treatment dose was chosen because it corresponds to the current recommendations for the maintenance treatment of patients with CD[167]. Mice in the treatment and control groups were monitored weekly and sacrificed at 8 weeks post-infection for quantification of MAP DNA.

The results of this experiment are presented in figure 4.6: we use the bacterial counts in isotype control-treated mice as an indicator of the spontaneous evolution of the infection (between 1 and 2 months post-infection), which allows to comparatively assess the effect

of the anti-TNF-α antibody. In spleen, liver and mesentery, the bacterial burden was reduced by 1 to 2 $\log_{10}$(ge/mg) in the placebo group, but remained unchanged in mice treated with TNF-α neutralizing antibodies, which indicates a deleterious effect of the treatment on bacterial replication in these organs. Interestingly, in the small intestine and the colon, we did not detect a significant decrease in bacterial counts at 2 months (in the placebo group), and there was a non-significant trend towards lower bacteria in the anti-TNF-α-treated group. Taken together, the results of this experiment argue in favour of a moderately deleterious effect of the anti-TNF-α treatment on the bacterial burden of MAP IJ-infected *Irgm1*-/- mice. However, it is important to note that in no case did we observe an increase in the bacterial burden after 1 month of treatment: there was no disseminated disease secondary to treatment (and no increase in the mortality either).

5) Discussion

Rationale

In the first part of this Master's research program, we have attempted to document the function of the IFN-γ-inducible 47-kDa GTPase Irgm1 in the context of a systemic infection with *Mycobacterium avium* ssp. *hominissuis* (MAH) strain 104 and *M. avium* ssp. *paratuberculosis* (MAP).

The first rationale for this is to explore the potential link between MAP and Crohn's disease (CD). As previously explained, MAP has been suggested for diverse reasons to account for a subset of cases of CD[68,83], and human *IRGM* has been specifically associated through genome-wide associations studies (GWAS) to CD[147,148]. As *IRGM* has also been linked experimentally to host defence against mycobacteria[135,95], investigating the molecular defects that render mice deficient in *Irgm1* (murine ortholog of *IRGM*) susceptible to MAP may provide insights into CD pathogenesis. In this regard, this "immunological workup" of the *Irgm1*-/- mouse infected with MAP is a continuation of the work done in the Behr lab on another CD-associated gene, *Nod2* (murine ortholog of human *NOD2*) in experimental MAP infections. However, it is important to note that it does not constitute an attempt to demonstrate the role of MAP in CD, for important conceptual and methodological reasons on which we will come back later.

Second, the results presented in part 1 of this thesis have to be analyzed in the context of what has already been published on the role of Irgm1 during mycobacterial infections (notably by the groups of Dr. MacMicking[93,94] and Dr. Feng[130,132]), which proves a stimulating exercise because the scientific literature on this topic is abundant in studies that, despite their high scientific value, deliver contradictory messages.

MAP and MAH

One asset of the work presented here is that all experiments were conducted using independently MAP and its close relative MAH. As briefly mentioned in the introduction (and as is reviewed in detail in references [3–5]), MAH designates a group of non-pathogenic

organisms prevalent in environmental settings. The reference strain (strain 104, used in this study) was first isolated from an individual with AIDS, and as such, does not possess the set of virulence factors that make pathogenic mycobacteria capable of thwarting the innate and adaptive immune responses in order to establish chronic infections. Rather, MAH infections occur mostly as accidental infections in severely immune-compromised hosts (e.g. AIDS patients with profound CD4 depletion) and do not lead to completion of the life cycle of the organism (because they do not result in transmission to another host). MAP, on the other hand, is a professional pathogen: even if it can survive for prolonged periods of time in the environment, the phagolysosomal compartments of macrophages constitute its natural living niche, and its whole life cycle rests on its capacity to chronically infect a cow (or another ruminant) until pathological events (gut inflammation) in the infected tissues enable its transmission (through diarrhoea) to a new host. In light of this, it is tempting to compare the behaviour of MAP in the gut (and adjacent mesenteric lymph nodes) of cows to that of *M. tuberculosis* in the lungs (and adjacent thoracic lymph nodes) of humans: acquisition via another actively shedding individual (through diarrhoea or coughing), translocation across epithelium with minimal pathology at onset, survival in professional phagocytes via blockage of phagolysosomal maturation and delayed induction of adaptive immunity, migration to the draining lymph nodes where is established a chronic yet mostly silent infection, and finally — as the result of still partly known factors — backwards migration to the site of entry, where the recruitment of immune cells results in pathological changes that are necessary for the excretion of new organisms. Recent work (undertaken partly in the Behr lab) has led to the understanding that MAP had evolved from this heterogeneous group of MAH organisms as the result of the acquisition of several genomic segments (LSPs), which are hypothesized to encode for putative virulence factors. Understanding the molecular details underpinning the emergence of MAP as a professional pathogen is both a fascinating and daunting task, and the object of intensive research effort. In our opinion, it also raises the question of what current microbiology research defines as virulence: if all the genetic elements present in the MAP genome and not shared by MAH underpin its ability to cause Johne's disease in a cow, then what we refer to as “virulence factors” actually designs a vast and heterogeneous group of effectors

with functions as diverse as epithelial translocation, down-regulation of pro-inflammatory signals in the host, switch to a state of dormancy, etc., and it is clear that the common experiments in which mice are infected with a MAP mutant to assess for its "virulence" have no potential to lead to the correct identification of this extremely complex set of mechanisms by which MAP is capable to manipulate the host immune system at its own advantage. However, it is in the context of this simplified (or simplistic) vision of virulence that we sought to compare our immunological findings with MAP and MAH: it was our intent to use potential differences in the way the immune system of the *Irgm1*-/- mouse interacts with these two organisms to shed light on these properties of MAP that single it as a pathogen. In other words, if MAP (and not MAH) causes CD, and if the *Irgm1*-/- mouse can be used as an animal recapitulating the genetic background of CD, then it would be interesting to see if and how *Irgm1*-/- mice are susceptible to MAP, and not to MAH.

Survival

When one looks at the numerous studies on the role of IFN-γ-inducible 47-kDa GTPases (IRGs) in infection, it is evident that *Irgm1*-/- mice display a broad and severe immune defect: several independent groups have demonstrated a markedly decreased survival upon experimental infection with a long list of (apparently unrelated) pathogens, including several strains of virulent mycobacteria (reviewed in reference 21). Thus, the first step of our immunological workup was to try to reproduce these findings in the context of an infection with MAP (which has never been reported before). The second reason that led us to focus initially on *in vivo* infections is that, in our reasoning, there was much less interest in documenting a potential Irgm1-dependent phenotype at the level of the cell if we were not able to show that Irmg1 mattered at the level of the whole organism. To this end, we started by comparing the survival of *Irgm1*-/- and wild-type mice during IP infections with both MAP and MAH. Our first survival experiment was carried out with MAH strain 104, and clearly demonstrated the impact of the Irgm1 deficiency on survival upon infection. However, we were quite surprised by the relatively high death rate of *Irgm1*+/+ mice (with 27% of mice deceased at 19 weeks post-infection) given the non-pathogenicity of MAH. The first thing that comes in mind in this context is the possibility of a contamination of the

mice with another microorganism upon infection, but all bacteria-containing solutions injected to the mice are serial-diluted and plated to quantify inocula, and since one has to wait for ~ 10 days before MAH plates can be counted, we were able to rule out the presence of any other bacterium with shorter doubling time and less demanding conditions of growth. Second, a more detailed analysis of the weight curves revealed that: 1) there was no evident correlation between recorded weights and other clinical signs showing that the mice were suffering from a MAH-driven systemic disease; and 2) some mice that were removed from the analysis but not sacrificed immediately as they went below 85% of their initial weight would eventually resume growth after a few days or weeks. This is why we carried out the same experiment with a less strict weight cut-off of 80%, which showed no death in the wild-type control group (as expected) and a longer median survival despite identical length of survival at the cohort level in the *Irgm1*-/- group; this translated graphically as a right and upward shift of both curves, which is logical and attests to the validity of our findings. The first survival curve we obtained with MAP indicated that at similar doses and routes of inoculation (10^8 by IP injection) there was reduced morbidity compared to MAH, which was not expected given our understanding of the virulence properties of the two organisms. However, this finding seemed corroborated indirectly by the results of a subsequent experiment where we documented the bacterial burden of *Irgm1-/-* mice infected with 10^8 MAP CFUs by IP injection at late time-points (see figure 4.3b), where once again this infective dose was not sufficient to bring about significant mortality (because only a few MAP-infected *Irgm1-/-* mice died during the experiment). The second one, however, was clearly confirmatory, showing that if inoculated at a higher infective dose (10^9 CFUs), MAP could lead to the death of half the cohort of *Irgm1*-/- mice in less than 3 weeks.

Quantitative bacteriology

So at this step, we had reproduced the *in vivo* susceptibility phenotypes reported by others in the field, and we set out to document the function of Irgm1 in host control of bacterial replication. Of note, as is the case for survival experiments, there is agreement in all papers published by Dr. Feng and Dr. MacMicking that *Irgm1*-/- mice have markedly higher

bacterial counts in spleens and livers than wild-type mice upon systemic infection with *M. tuberculosis* and *M. avium*.

Accordingly, in all sets of IP infections with 10^8 CFUs of MAP and MAH, we found a clearly increased bacterial burden in *Irgm1*-/- mice, which could attain more than 2 $\log_{10}$(CFU) in certain instances (see figures 4.2 and 4.3). Interestingly, we found that with both bacteria, the divergence between *Irgm1*-/- and *Irgm1*+/+ mice appeared roughly after 4 weeks of infection, and it is interesting to reflect on this finding in light of what is known about the chronology of innate and adaptive responses during mycobacterial infections. It is estimated that the induction of the adaptive arm of the immune response usually takes ~ 7 days after first encounter with the pathogen[16], and as explained before, virulent mycobacteria have evolved strategies to hinder antigen presentation to CD4+ and CD8+ T lymphocytes, which subsequently delays the triggering of their effector mechanisms, as evidenced by a study on experimental murine infection with *M. tuberculosis* where *M. tb*-specific CD4+ lymphocytes appear only 10 to 12 days following infection[168]. Furthermore, Irgm1 has been repeatedly demonstrated to be induced selectively upon IFN-γ stimulation, and CD4+ and CD8+ T lymphocytes account for the major part of secreted IFN-γ upon mycobacterial infection (even if NK cells are γδ T lymphocytes are known to produce small amounts of the cytokine at a time when the adaptive response has not been triggered yet). So in conclusion, it appears logical not to observe a strong Irgm1-dependent phenotype before ~ 2 weeks post-infection, which explains why the difference in bacterial burden becomes evident (and statistically significant) at 4 weeks post-infection.

Cause of death

Having demonstrated that *Irgm1*-/- mice die faster, and with a higher bacterial burden than their wild-type counterparts, we sought to examine further the exact cause of their death. This question was brought about by the puzzling observation that: 1) in our hands, there seemed to be a counter-intuitive difference of morbidity brought about by MAH and MAP (because MAH, injected at a dose of 10^8 by IP caused the death of *Irgm1*-/- mice, while MAP, a professional pathogen, did not); and 2) there also seemed to be an intrinsic defect about the *Irgm1*-/- mouse that rendered it more susceptible to death upon infectious

challenge (because in some instances *Irgm1*-/- animals died with bacterial levels at which wild-type mice survived). This was also stimulated by our knowledge of the work of several groups that have documented functions for Irgm1 in the brain[169,170], in the liver[171] and in the hematopoietic compartment[141,142] that are not obviously related to the immune response to mycobacteria.

Our "clinical work-up" revealed mainly haematologic abnormalities (anemia, thrombocytopenia, lymphocytopenia) while there was no evidence for pathological processes involved in the brain, the lungs, the intestine, the liver, the pancreas, the kidneys. The thrombocytopenia was not severe enough to result in major bleeding, and we never observed any clinical or pathological sign of external or internal bleeding in our mice. It has been reported by several authors that *Irgm1*-/- mice undergo lymphocytopenia upon infection (including in the context of mycobacterial infections, see the work of Dr. Feng[130,132]), but we reasoned that it did not attain levels which usually predispose lymphopenic patients to opportunistic infections, and we were unsuccessful at isolating a fast-growing bacteria from the blood and tissues of moribund *Irmg1*-/- mice. Finally, the anemia was both profound and fast to appear (< 4 weeks post-infection), and in such it could explain the progressive death of animals confronted with high metabolic demands secondary to a disseminated infection.

Recent studies have documented the role of Irgm1 in hematopoietic stem cells (HSCs), which reside in a dormant state in the bone marrow and can be stimulated to divide and differentiate into all of the blood cell types upon toxic or infectious stress. Specifically, it was shown that: 1) IFN-γ is a powerful activator of HSC proliferation, which serves during the first phase of an infection in maintaining the pool of immune cells, but is accompanied by a secondary functional impairment of these cells; and 2) Irgm1 provides a critical negative regulatory mechanism on IFN-γ signalling in HSC, which is necessary to prevent their depletion over time[141,142]. In light of these findings, we propose the following sequence of events to explain the death of MAP-infected *Irgm1*-/- mice: 1) experimental MAH and MAP infections are not controlled in the *Irgm1*-/- mouse, which results in high levels of colonization for prolonged periods of time; 2) the high bacterial burden leads to the synthesis of large amounts of IFN-γ; 3) IFN-γ signaling in *Irgm1*-/- HSCs is deleterious

and leads to the progressive exhaustion of bone-marrow stem cells, resulting in pancytopenia; 4) *Irgm1*-/- mice develop a profound anemia which, in light of the high metabolic demand imposed by the high bacterial burden, leads to their death as a direct result of dehydration, cachexia and/or heart failure.

Finally, it is interesting to think of this model in light of the difference observed in the morbidity brought by MAH and MAP. First, in a host with an immune defect so severe that it cannot control the growth of mycobacteria, the shorter double time of MAH (12 hours, as opposed to 24 to 36 hours for MAP) may explains why it can reach "lethal levels" sooner than MAP. Second, it is tempting to postulate that MAP, as a professional pathogen, might have evolved strategies to avoid immune recognition, with smaller amounts of IFN-γ secreted by T cells at identical levels of colonization; since death is IFN-γ-dependent in the *Irgm1*-/- mouse, this would explain why MAP seems less lethal than MAH in our survival experiments. One simple way to test this hypothesis could be to compare the levels of IFN-γ in spleen and mesenteric lymph nodes (where the interaction between APCs and T cells takes place), or in the intestine (where the granulomas are formed: interaction macrophage-T cell), 2 and 4 weeks after IP inoculation of identical doses of MAH and MAP.

Macrophage experiments

As previously explained, the requirement of a functional Irgm1 to fight experimental infections has been clearly documented for a broad range of organisms, but the exact nature of the mechanisms by which Irgm1 confers protection are still debated. Specific to the context of a mycobacterial infection, different groups have reported that the Irgm1 deficiency was responsible for either a bactericidal defect of macrophages due to impairment of the phagolysosomal maturation[93], or for a defective adaptive response due to increase cell death rates of CD4+ T cells[132]. Having demonstrated the uncontrolled growth of both MAP and MAH in *Irgm1*-/- mice, we next sought to document the functionality of the cell types involved in host defence to mycobacteria in this model.

We started by *in vitro* macrophage infections because: 1) *Irgm1*-/- macrophages have been studied extensively and these experiments offered a simple way to compare our data

with published findings; and 2) it also offered an attractive comparison to studies carried out in the Behr lab on the killing properties of macrophages harvested from mice deleted in another CD-associated gene, *Nod2*. Beside general information on the difference of growth behaviour of MAH and MAP inside of macrophages (which could reflect the difference in their doubling time, factors related to their virulence, or a combination of both), the results of these experiments are difficult to interpret with confidence. In peritoneal macrophages, where MAH seemed to replicate actively (even inside of wild-type cells), we were able to demonstrate an effect of IFN-γ pre-stimulation, and there was a clear trend towards better killing abilities of wild-type cells compared to *Irgm1*-/- cells (even if the variability was too high to reach statistical significance), a finding that reproduces those of Dr. MacMicking. In contrast, the results of MAP infections of peritoneal macrophages, if anything, showed that MAP maintained a balance between replication and killing, because at all time-points the number of live MAP cells recovered in our assays seemed to roughly fluctuate around its initial value, with little difference between IFN-γ-treated and non-treated cells, or wild-type and *Irgm1*-/- cells. The last experiment we carried out with MAP in bone marrow-derived macrophages is perhaps the most informative, showing both an effect of the IFN-γ pre-stimulation and a subtle but statistically significant defect of killing in *Irgm1*-/- macrophages. In conclusion, it seemed that in our model, the uncontrolled bacterial replication seen in *Irgm1*-/- mice could be explained, at least in part, by an intrinsic impairment of the killing mechanisms of macrophages, which is in line of the results published by MacMicking et al[94,123]. In any case, these findings still warrant further confirmation.

It is rather disappointing to see that apparently simple *in vitro* macrophage infections can give discordant results when working with peritoneal and bone marrow-derived macrophages, or with MAH and MAP, but a thorough look at the existing literature is humbling: 1) in the context of virulent mycobacteria, two groups of recognized scientists have shown opposite findings while using seemingly identical protocols[93,130]; 2) in different models, the role of Irgm1 in cell-autonomous immunity is not always evident (see for instance an article on *Salmonella* where the authors conclude in a macrophage defect that is far from evident when looking in detail at the experimental results[172]); and 3) even more

complexity has arisen when researchers have attempted to document the behaviour of Irgm1 inside of phagocytes at a smaller scale (see references [93,94,138,139,173], all pertaining to the intracellular localization of Irgm1 during macrophage infection with different pathogens). Several reasons for this can be proposed, including: the inherent sensitivity of these *in vitro* assays and the variability associated with eukaryotic cell cultures; subtle variations in the protocol used across labs (for instance Dr. MacMicking sees an Irgm1-dependent phenotype at day 7 post-infection[93], and Dr. Feng reports no difference between *Irgm1*-/- and wild-type cells but only reports the result of a 3-day infection[130]); the persistent difficulties inherent to the quantification of mycobacteria by classic quantitative bacteriology (partly due to clumping of mycobacterial cells in liquid cultures[174,175]); the different properties of peritoneal and bone marrow-derived macrophages, etc. It has been proposed that macrophage development and differentiation might be disturbed in Irgm1-deficient mice; their motility as well as the intracytoplasmic organization of certain organelles seems to be disturbed, even in the absence of IFN-γ pre-stimulation[140,172,176]. The differences in viability, morphology, activation profile of *Irgm1*+/+ and *Irgm1*-/- macrophages have not been studied in this work, and this could have been carried out simply by the use of rather simple techniques, using first optical microscopy and if needed FACS analysis of key activation markers. This is a clear limitation of our work, and it constitutes an obstacle to conducting a more precise analysis of the *in vitro* bacterial killing ability of these cells.

Further dissection of the immune response of the *Irgm1*-/- mouse to MAP and MAH could start by a study of the function of their dendritic cells (DCs). This could be justified first by the description of rare forms of genetically-determined immunodeficiency combining a selective absence of circulating DCs and a high susceptibility to mycobacterial infections[177], and second by the reported role of DCs in the pathogenesis of CD[113,178]. To this end, we would start by *in vitro* assays where DCs harvested from *Irgm1*-/- and *Irgm1*+/+ mice are infected with a strain of MAP carrying a plasmid encoding the protein ovalbumin (MAP-ova), and subsequently co-incubated with CFSE-loaded CD4+ or CD8+ T cells harvested from OT-2 or OT-1 mice (respectively), which express a T-cell receptor (TCR) specific for an ovalbumin-derived epitope. These types of experiments allow to measure the expression of MHC class I and II molecules, as well as co-stimulatory

molecules at the surface of DCs, and evaluate their ability to stimulate the antigen-specific activation and expansion of T cells (by quantifying the dilution of CFSE in their progeny). Similar experiments can be carried out *in vivo* by injecting MAP-ova into the foot pad of *Irgm1*-/- and *Irgm1*+/+ mice previously transfused with OT-1 or OT-2 T cells, and measure the recruitment and degree of activation of T cells in the popliteal lymph nodes at 3 and 5 days post-infection by fluorescence-activated cell sorting (FACS). It is interesting to note that the work of Dr. Feng with *M. avium* brings about indirect evidence for a normal function of *Irgm1*-/- DCs, most importantly because: 1) *Irgm1*-/- mice display a normal T cell priming upon infection with *M. avium* (no difference between KO and wild-type animals in the percentage of activated $CD44^{hi}CD62L^{lo}CD4+$ T cells in spleen upon infection (before induction of lymphopenia), nor in the amounts of IFN-γ released by T cells exposed to mycobacterial antigens *in vitro*); and 2) adoptive transfer experiments where T cells from *Irgm1*-/- and *Irgm1*+/+ mice infected for 2 weeks with *M. avium* (and thus primed respectively by *Irgm1*-/- and *Irgm1*+/+ DCs) are transferred to *Rag2*-/- mice infected secondarily with *M. avium* show no difference in bacterial burden[130].

Finally, examining the function of T cells in the course of a MAP infection would have been a logical next step, and for this we would have probably concentrated on CD4+ T cells, because: 1) conserved CD4+ T cell function is know to be critical for host defence against mycobacteria (see for instance the increased rate of non-tuberculous mycobacterial infections in patients infected with HIV-associated CD4+ depletion); 2) reports have been published showing that CD8+ T cells do not impact significantly in the course of a MAP infection[179]; and 3) CD4+ T cells have also been implicated in the pathogenesis of CD. Once again, Dr. Feng has provided much information on the function of the *Irgm1*-/- CD4+ T cell in the context of an infection with virulent *M. avium*. It is interesting to note that if abnormal cell death rate upon exposure to IFN-γ have been reported *in vitro*, the results of *in vivo* infections do not appear to point towards defective effector mechanisms of these cells, and nothing indicates that the moderate lymphopenia observed in the mice is actually responsible for their inability to control bacterial replication.

Intestinal infection of *Irgm1*-/- mice with MAP: a mouse model of Johne's disease?

In the second part of this work, we asked whether the *Irgm1*-/- mouse could be a suitable host for testing whether chronic MAP infection of the intestine would lead to demonstrable pathology. This is justified first by the absence of satisfactory mouse model in paratuberculosis research, and second in the context of the MAP-CD link, because it provides a way to: 1) compare the clinical, pathological and immunological features of chronic MAP infection of the intestine (JD) and CD; and 2) document the response of this model to current therapeutics used to treat patients with CD.

In line with numerous previous attempts at inducing gut pathology with MAP in a mouse[33,34], our attempt with *Irgm1*-/- animals infected by gavage were unsuccessful. This could be explained by several factors, including: 1) the action of the acidic pH of the stomach on MAP survival; the action of biliary and pancreatic secretions on MAP survival; a too rapid transit time in the intestine; the presence of luminal contents preventing MAP from gaining access to the intestinal epithelium, including food and comensal bacterial colonies; a possible species-specificity of MAP attachment proteins used to bind epithelial cells (as is the case for Listeria[180]), etc. Several experimental procedures could be used to test these hypotheses, and we tried: 1) to overcome the acidic pH by feeding our mice with sodium bicarbonate; 2) to decrease the amounts of luminal contents by submitting them to a short period of fasting before infection; 3) to eliminate the resident flora through the use of antibiotics. However, all our attempts were unsuccessful, and this is why we turned to the intra-jejunal injection of a MAP-containing solution under general anaesthesia to generate gut pathology.

Irgm1-/- mice, 1 month after infection with 10^9 MAP under this protocol, develop histological signs of terminal ileitis similar to those seen in JD: there are focal infiltrates of macrophages, T cells and plasma cells that affect all three layers of the gut (transmural pathology); some histiocytes form multinucleated giant cells surrounded by lymphocytes (granulomatous structures); the infection seems persistent because fibrotic lesions can be observed; MAP is seen after ZN staining in inflammed areas; and finally there is also inflammation in the adjacent mesenteric lymph nodes and channels (chronic mesenteric lymphadenitis). Another cohort of mice sacrificed after two months of infection showed that

these histological signs were stable in time. Clinically, our mice proved rather stable too: they neither presented clinical signs seen in JD (notably weight loss and diarrhoea), nor displayed the features of morbidity associated with systemic infections with MAP in this host (weight loss, pancytopenia) and were able to survive for several months following infection. In this respect, it would be interesting to assess if these mice ever shed MAP in their feces; this could be achieved by attempting to grow and quantify MAP in fecal pellets, a technique that seems easier to achieve than it actually is, mainly due to the requirement for a thorough decontamination of the feces to kill all fast-growing members of the intestinal flora that would hinder MAP growth *in vitro*.

If validated, our pathological findings are exciting because they would provide one of the rare examples of intestinal pathology secondary to a MAP infection in a mouse[33,34,39–41]. As such, they could potentially be used in paratuberculosis research, mostly in studies of host-pathogen interaction, for instance to study the function of bacterial genetic elements in the colonization of the gut and the induction of pathology, or to assess the role of distinct immune cell types in the development of intestinal lesions.

However, several key points need to be addressed before this model can be disseminated more broadly. First and foremost, we still need at this stage a more precise evaluation of the pathological lesions brought about by an IJ-inoculation of MAP in *Irgm1*-/- mice, at different doses (for instance 10^6, 10^8, 10^{10} MAP CFUs) and at later time points (for instance 4, 6 and 12 months), in comparison to sham-infected *Irgm1*-/- mice. Second, we need to evaluate the extent to which our results are dependent: 1) on the Irgm1 deficiency in the host; and 2) on MAP, as opposed to other mycobacteria, or even to other microorganisms. To this end, we have already proceeded to similar IJ infections of wild-type mice with 10^9 MAP CFUs, and of *Irgm1*-/- mice with 10^9 MAH CFUs and *E. coli* LF82 (a strain of adherent and invasive *E. coli*), the results of which are still pending. Third, we need to precisely document the time-course of bacterial burden in small intestine, colon, mesentery and secondary organs (spleen and liver) during the course of the injection, which would probably be more easily attained by the use of PCR-based techniques, but could also be attempted by classical quantitative bacteriology. Fourth, it would be interesting to provide a more detailed analysis of the migration path of MAP across the

mouse intestine and adjacent tissues after surgery: indeed, if it seems logical to observe only pathology in the mesentery after IP infection and intestinal lesions when the bacteria are directly deposited at close contact with the intestinal epithelium, one can still wonder why in our model cellular infiltrates and visible MAP cells are predominant in the deeper layers of the gut, seemingly reaching the mucosa from the serosa (and not the opposite). This could be explained by the natural ability of MAP to replicate only transiently at the site of entry, and usually with minimal pathology, before reaching the mesenteric lymph nodes where it establishes its niche preferentially. Such investigation could be done: 1) by the use of simple experimental procedures, for instance by instilling methylene blue in the jejunum to make sure there is no leak in the peritoneum immediately after surgery; 2) by the use of MAP cells expressing fluorescent dyes (for instance MAP transfected with a plasmid encoding the green fluorescent protein (GFP)) coupled with fluorescence microscopy.

Finally, it is necessary to consider the different limitations of such a potential model of JD. First, there is of course the technical challenge that is the surgical procedure itself, because it requires technical skills, well equipped facilities (allowing to operate on a mouse anaesthetized with isoflurane in a level 2 BSC), and time, making this model difficult to export. Second, one major limitation of our surgical protocol is the important variability in the pathological outcome; this is why, when testing whether anti-TNF would have deleterious effect on the course of the infection, we had to focus on the bacterial burden and not on the pathological score, because even before treatment some mice had almost no pathology and some had severe lesions. Finally, it is important to note that, if the words we use to describe the pathology in our *Irgm1*-/- mice echo those used in paratuberculosis, our model is still far from recapitulating the disease in its natural host, as it lacks some of its key pathological features (severe epithelial lesions, granulomas, transverse ridges, etc.); it is possible that these features necessitate months to years of evolution to appear, which would make them extremely difficult to reproduce in the mouse.

A good model of Crohn's disease?

One of the main reasons why we were interested in developing an animal model of a chronic granulomatous enteritis secondary to a MAP infection is to provide some insight

into the similarities and differences between Johne's disease and Crohn's disease.

Specifically, it is possible to document a set of clinical, immunological, bacteriological features in the MAP-infected *Irgm1*-/- mice and compare them with what is know about Crohn's disease. A first step would be to document more precisely the relative abundance and spatial distribution of the different immune cell types seen in intestinal lesions by immunohistochemistry or immunohistofluoresence (immunostaining of macrophages, DCs, granulocytes, CD4+ and CD8+ T cells, B cells and plasma cells). To document a certain Th1/Th2/Th17 cytokine profile, one can extract inflammed intestinal tissue and measure the amounts of selected cytokines by ELISA or qPCR-based techniques. Another interesting type of study would consist in extracting and purifying cells from different layers of the gut wall by FACS, which allows to study various phenotypic characteristics *ex vivo*; this could be coupled to intracellular staining of T cells, here again to document the Th1/Th2/Th17 balance at play in the lesions (see reference 73 for an example of that type of work).

Interestingly, a very recent study published in Nature used a similar methodological approach to document the ability of adherent and invasive *E. coli* (AIEC) to induce CD-like intestinal lesions[181]. Its authors showed that one strain of AIEC, namely NRG857c, induces persistent intestinal lesions predominant in the terminal ileum and the caecum after gavage infection of streptomycine-pre-treated C57Bl/6 and CD1 mice; they also document a cytokine response skewed towards Th1 and Th17 profiles, as well as fibrotic lesions, findings that link their model to CD. Is it enough to say that Koch's postulates have been fulfilled with AIEC? More work is probably needed to assess if one can actually compare the course of CD to that of a 21-day experimental gavage infection with 10^9 *E. coli*.

In the case of MAP, the question of the fulfilment of Koch's postulates is different, because MAP has already been proven to induce a disease very similar to CD in a wide range of hosts. Thus, the doubt that persists in the scientific community on the implication of MAP in CD probably stems from the apparent difficulty in isolating it reproducibly from CD biopsies. This could be due to a combination of factors, including: the fastidious nature of MAP *in vitro* growth (even more so for type I strains) associated with high levels of fast-growing contaminants; the enrichment of MAP in deeper layers of the gut and in the

mesentery, tissues that are not usually targeted for biopsy during endoscopic procedures; the existence of forms of mycobacterial diseases characterized by low numbers of living organisms in active inflammatory lesions (pauci-bacillary leprosy[15], pauci-bacillary forms of paratuberculosis in goats[6]); high limits of quantification of MAP DNA and the use of inappropriate DNA extraction protocols in qPCR-based studies; or maybe the possibility that MAP be responsible only for a subset (if any) of CD cases. In any case, it should be possible to use our model of a MAP-induced ileo-colitis in the mouse to assess if, at similar levels of pathology, one can quantify similar levels of MAP DNA in murine samples and human CD biopsies.

The results of our immunological workup in the *Irgm1*-/- mouse provide interesting information on the ability of MAP (and other non-virulent mycobacteria) to use genetically-determined immune defects to establish a productive infection. In terms of logic, it is far from providing a demonstration of the role of MAP in CD pathogenesis. In this respect, several conceptual hurdles remain: the specificity of our findings to a MAP infection (as opposed to mycobacteria in general) has not been validated; and once again, it seems difficult to link the uncontrolled bacterial growth seen in the mouse with the constant difficulty in isolating MAP from CD patients.

Finally, much more work is needed to understand the effects of therapeutics used in CD in the course of an infection with MAP. A brief review of the literature shows that: 1) there is an increased risk of TB reactivation amongst patients treated with glucocorticosteroids[162,182] and with TNF-α blocking agents[164]; 2) glucocorticosteroids do not appear to predispose to infections with MAC (certainly because due to their lesser virulence, these species usually cause disease in more severely immunocompromised patients); 3) reports on the effect of glucocorticosteroids in experimental murine TB are conflincting[183,184], but they have been shown to exacerbate the severity of intestinal lesions in one of the rare models of murine paratuberculosis with significant intestinal pathology[185], and to result in increased bacterial counts during MAP infection of laboratory hamsters[186]; 4) TNF-α blocking agents are responsible for a deleterious outcome in murine[165,187,188] and simian[166] models of TB. In light of this, it remains difficult to conceive how a chronic MAP infection could respond favourably to these agents (at least without the concomitant use of

antibiotics). Our studies on the effect of methylprednisolone and anti-TNF-α neutralizing antibodies have failed to demonstrate an accelerated death or a clear increased in the bacterial burden secondary to treatment (but there was a trend towards more bacteria in spleen, liver and mesentery in the anti-TNF-α-treated mice). If confirmed, they would provide interesting experimental data that might be best analyzed in light of recent epidemiological and experimental reports depicting an unexpectedly complex balance of regulatory effects for TNF-α in mycobacterial infections[189–191].

6. Conclusion and summary

In the first part of this Master's research program, we have studied the function of 47 kDa IFN-γ-inducible GTPase Irgm1 in the immune response to *Mycobacterium avium* ssp. *paratuberculosis* (MAP) and ssp. *hominissuis* (MAH). We have shown that *Irgm1*-/- mice present a high susceptibility to systemic infection with MAP and MAH, with accelerated mortality and uncontrolled bacterial replication in spleen, liver and mesenteric lymph nodes after intra-peritoneal inoculation. However this route of infection was not suitable to induce significant intestinal pathology. We have conducted a series of *in vitro* infections of peritoneal and bone marrow-derived macrophages from *Irgm1*-/- and wild-type mice to document their mycobactericidal activity, and found evidence for a defective control of intracellular bacterial growth in macrophages deficient in Irgm1. We have also documented significant haematological abnormalities leading to the death of the Irgm1-/- animals, notably a severe anemia.

In the second part of this work, we have attempted to develop a protocol for the surgical inoculation of a MAP-containing solution in the jejunum of *Irgm1*-/- mice. We have observed the development of histological lesions of the small intestine and adjacent mesentery that resemble those seen in Johne's disease: focal lympho-histiocytic infiltrates attaining the three layers of the intestine (transmural pathology), fibrotic lesions, mesenteric lymphadenitis, and foci of acid-fast cocco-bacilli corresponding to MAP in inflammed areas. Animals infected according to this protocol did not develop signs of systemic disease, and no haematological abnormality. One cohort of mice was submitted to a treatment by glucocorticosteroids that did not result in increased mortality; another cohort was treated with an anti-tumor necrosis factor-alpha (TNF-α) neutralizing antibody, which did not lead to an increase in bacterial tissue colonization. These results, if confirmed, could prove useful first as a murine model of paratuberculosis with intestinal pathology, and second in the research on the potential role of MAP in the pathogenesis of Crohn's disease.

References

1. Cosma, C. L., Sherman, D. R. & Ramakrishnan, L. The secret lives of the pathogenic mycobacteria. *Annu. Rev. Microbiol.* **57,** 641–676 (2003).
2. Veyrier, F., Pletzer, D., Turenne, C. & Behr, M. A. Phylogenetic detection of horizontal gene transfer during the step-wise genesis of Mycobacterium tuberculosis. *BMC Evolutionary Biology* **9,** 196 (2009).
3. Turenne, C. Y., Wallace, R., Jr & Behr, M. A. Mycobacterium avium in the postgenomic era. *Clin. Microbiol. Rev.* **20,** 205–229 (2007).
4. Turenne, C. Y., Collins, D. M., Alexander, D. C. & Behr, M. A. Mycobacterium avium subsp. paratuberculosis and M. avium subsp. avium are independently evolved pathogenic clones of a much broader group of M. avium organisms. *J. Bacteriol.* **190,** 2479–2487 (2008).
5. Alexander, D. C., Turenne, C. Y. & Behr, M. A. Insertion and deletion events that define the pathogen Mycobacterium avium subsp. paratuberculosis. *J. Bacteriol.* **191,** 1018–1025 (2009).
6. Behr, M. A. & Collins, D. M. *Paratuberculosis: Organism, Disease, Control*. (CABI, 2010).
7. Thorel, M.-F., Krichevsky, M. & Lévy-Frébault, V. V. Numerical Taxonomy of Mycobactin-Dependent Mycobacteria, Emended Description of Mycobacterium avium, and Description of Mycobacterium avium subsp. avium subsp. nov., Mycobacterium avium subsp. paratuberculosis subsp. nov., and Mycobacterium avium subsp. silvaticum subsp. nov. *Int J Syst Bacteriol* **40,** 254–260 (1990).
8. Chacon, O., Bermudez, L. E. & Barletta, R. G. Johne's Disease, Inflammatory Bowel Disease, and Mycobacterium Paratuberculosis. *Annual Review of Microbiology* **58,** 329–363 (2004).
9. Harris, N. B. & Barletta, R. G. Mycobacterium avium subsp. paratuberculosis in Veterinary Medicine. *Clin. Microbiol. Rev.* **14,** 489–512 (2001).
10. Twort, F. W. & Ingram, G. L. Y. A Method for Isolating and Cultivating the Mycobacterium enteritidis chronicae pseudotuberculosae bovis, Johne, and some Experiments on the Preparation of a Diagnostic Vaccine for Pseudo-tuberculous Enteritis of Bovines. *Proc. R. Soc. Lond. B* **84,** 517–542 (1912).
11. Twort, C. The experimental production of Johne's disease in some laboratory animals. *Vet. News* **11:79–81,** (1914).
12. NAHMS. Johne's Disease on U.S. Dairy Operations. (1997). at <http://www.aphis.usda.gov/animal_health/nahms/dairy/downloads/dairy96/Dairy96_dr_Johnes.pdf>
13. Nielsen, S. S. & Toft, N. A review of prevalences of paratuberculosis in farmed animals in Europe. *Prev. Vet. Med.* **88,** 1–14 (2009).
14. Stabel, J. R. Johne's disease: a hidden threat. *J. Dairy Sci.* **81,** 283–288 (1998).
15. Britton, W. J. & Lockwood, D. N. J. Leprosy. *Lancet* **363,** 1209–1219 (2004).
16. Murphy, K. *Janeway's immunobiology.* (Garland Science, 2008).
17. Casanova, J.-L. & Abel, L. The human model: a genetic dissection of immunity to infection in natural conditions. *Nat Rev Immunol* **4,** 55–66 (2004).
18. Van de Vosse, E., Hoeve, M. A. & Ottenhoff, T. H. M. Human genetics of intracellular infectious diseases: molecular and cellular immunity against mycobacteria and salmonellae. *Lancet Infect Dis* **4,** 739–749 (2004).
19. Van de Vosse, E., van Dissel, J. T. & Ottenhoff, T. H. M. Genetic deficiencies of innate

immune signalling in human infectious disease. *Lancet Infect Dis* **9,** 688–698 (2009).
20. MacMicking, J. D. Interferon-inducible effector mechanisms in cell-autonomous immunity. *Nat. Rev. Immunol.* **12,** 367–382 (2012).
21. Kim, B.-H., Shenoy, A. R., Kumar, P., Bradfield, C. J. & MacMicking, J. D. IFN-inducible GTPases in host cell defense. *Cell Host Microbe* **12,** 432–444 (2012).
22. Ramakrishnan, L. Revisiting the role of the granuloma in tuberculosis. *Nat Rev Immunol* **12,** 352–366 (2012).
23. Russell, D. G. Who puts the tubercle in tuberculosis? *Nat. Rev. Microbiol.* **5,** 39–47 (2007).
24. Miller, H., Zhang, J., Kuolee, R., Patel, G. B. & Chen, W. Intestinal M cells: the fallible sentinels? *World J. Gastroenterol.* **13,** 1477–1486 (2007).
25. Bermudez, L. E., Petrofsky, M., Sommer, S. & Barletta, R. G. Peyer's Patch-Deficient Mice Demonstrate That Mycobacterium avium subsp. paratuberculosis Translocates across the Mucosal Barrier via both M Cells and Enterocytes but Has Inefficient Dissemination. *Infect Immun* **78,** 3570–3577 (2010).
26. Stewart, G. R., Robertson, B. D. & Young, D. B. Tuberculosis: a problem with persistence. *Nat. Rev. Microbiol.* **1,** 97–105 (2003).
27. Rowe, M. t. & Grant, I. r. Mycobacterium avium ssp. paratuberculosis and its potential survival tactics. *Letters in Applied Microbiology* **42,** 305–311 (2006).
28. Koul, A., Herget, T., Klebl, B. & Ullrich, A. Interplay between mycobacteria and host signalling pathways. *Nat. Rev. Microbiol.* **2,** 189–202 (2004).
29. Kuehnel, M. P. *et al.* Characterization of the intracellular survival of Mycobacterium avium ssp. paratuberculosis: phagosomal pH and fusogenicity in J774 macrophages compared with other mycobacteria. *Cell. Microbiol.* **3,** 551–566 (2001).
30. Weiss, D. J. & Souza, C. D. Review paper: modulation of mononuclear phagocyte function by Mycobacterium avium subsp. paratuberculosis. *Vet. Pathol.* **45,** 829–841 (2008).
31. Coussens, P. M. Mycobacterium paratuberculosis and the bovine immune system. *Anim Health Res Rev* **2,** 141–161 (2001).
32. Coussens, P. M. Model for Immune Responses to Mycobacterium avium Subspecies paratuberculosis in Cattle. *Infect. Immun.* **72,** 3089–3096 (2004).
33. Hines, M. E., 2nd *et al.* Experimental challenge models for Johne's disease: a review and proposed international guidelines. *Vet. Microbiol.* **122,** 197–222 (2007).
34. Begg, D. J. & Whittington, R. J. Experimental animal infection models for Johne's disease, an infectious enteropathy caused by Mycobacterium avium subsp. paratuberculosis. *Vet. J.* **176,** 129–145 (2008).
35. Tanaka, S., Sato, M., Taniguchi, T. & Yokomizo, Y. Histopathological and Morphometrical Comparison of Granulomatous Lesions in BALB/c and C3H/HeJ Mice Inoculated with Mycobacterium paratuberculosis. *Journal of Comparative Pathology* **110,** 381–388 (1994).
36. Veazey, R. S. *et al.* Histopathology of C57BL/6 mice inoculated orally with Mycobacterium paratuberculosis. *Journal of Comparative Pathology* **113,** 75–80 (1995).
37. Veazey, R. S. *et al.* Comparison of the resistance of C57BL/6 and C3H/He mice to infection with Mycobacterium paratuberculosis. *Vet. Microbiol.* **47,** 79–87 (1995).
38. Tanaka, S., Itohara, S., Sato, M., Taniguchi, T. & Yokomizo, Y. Reduced formation of granulomata in gamma(delta) T cell knockout BALB/c mice inoculated with Mycobacterium avium subsp. paratuberculosis. *Vet. Pathol.* **37,** 415–421 (2000).
39. Mutwiri, G. K. *et al.* Mycobacterium avium subspecies paratuberculosis triggers intestinal pathophysiologic changes in beige/scid mice. *Comp. Med.* **51,** 538–544 (2001).
40. Hamilton, H. L., Follett, D. M., Siegfried, L. M. & Czuprynski, C. J. Intestinal multiplication of Mycobacterium paratuberculosis in athymic nude gnotobiotic mice. *Infect. Immun.* **57,** 225–230 (1989).

41. Hamilton, H. L., Cooley, A. J., Adams, J. L. & Czuprynski, C. J. Mycobacterium paratuberculosis monoassociated nude mice as a paratuberculosis model. *Vet. Pathol.* **28,** 146–155 (1991).
42. Baumgart, D. C. & Carding, S. R. Inflammatory bowel disease: cause and immunobiology. *Lancet* **369,** 1627–1640 (2007).
43. Abraham, C. & Cho, J. H. Inflammatory Bowel Disease. *New England Journal of Medicine* **361,** 2066–2078 (2009).
44. Baumgart, D. C. & Sandborn, W. J. Crohn's disease. *The Lancet* **380,** 1590–1605 (2012).
45. Peppercorn, M. A. in *UpToDate* (UpToDate in Waltham, MA, 2013).
46. Geboes, K. in *Inflammatory Bowel Diseases* (Churchill Livingstone, 2003).
47. Von Roon, A. C. *et al.* The risk of cancer in patients with Crohn's disease. *Dis. Colon Rectum* **50,** 839–855 (2007).
48. Selby, W. S., Janossy, G., Bofill, M. & Jewell, D. P. Intestinal lymphocyte subpopulations in inflammatory bowel disease: an analysis by immunohistological and cell isolation techniques. *Gut* **25,** 32–40 (1984).
49. Cho, J. H. & Abraham, C. Inflammatory bowel disease genetics: Nod2. *Annu. Rev. Med.* **58,** 401–416 (2007).
50. Manichanh, C., Borruel, N., Casellas, F. & Guarner, F. The gut microbiota in IBD. *Nat Rev Gastroenterol Hepatol* **9,** 599–608 (2012).
51. Man, S. M., Kaakoush, N. O. & Mitchell, H. M. The role of bacteria and pattern-recognition receptors in Crohn's disease. *Nat Rev Gastroenterol Hepatol* **8,** 152–168 (2011).
52. Nell, S., Suerbaum, S. & Josenhans, C. The impact of the microbiota on the pathogenesis of IBD: lessons from mouse infection models. *Nat. Rev. Microbiol.* **8,** 564–577 (2010).
53. Cho, J. H. The genetics and immunopathogenesis of inflammatory bowel disease. *Nat. Rev. Immunol.* **8,** 458–466 (2008).
54. Bouma, G. & Strober, W. The immunological and genetic basis of inflammatory bowel disease. *Nat. Rev. Immunol.* **3,** 521–533 (2003).
55. Xavier, R. J. & Podolsky, D. K. Unravelling the pathogenesis of inflammatory bowel disease. *Nature* **448,** 427–434 (2007).
56. Khor, B., Gardet, A. & Xavier, R. J. Genetics and pathogenesis of inflammatory bowel disease. *Nature* **474,** 307–317 (2011).
57. Maloy, K. J. & Powrie, F. Intestinal homeostasis and its breakdown in inflammatory bowel disease. *Nature* **474,** 298–306 (2011).
58. Hedin, C. R., Stagg, A. J., Whelan, K. & Lindsay, J. O. Family studies in Crohn's disease: new horizons in understanding disease pathogenesis, risk and prevention. *Gut* **61,** 311–318 (2011).
59. Lees, C. W., Barrett, J. C., Parkes, M. & Satsangi, J. New IBD genetics: common pathways with other diseases. *Gut* **60,** 1739–1753 (2011).
60. Fritz, T., Niederreiter, L., Adolph, T., Blumberg, R. S. & Kaser, A. Crohn's disease: NOD2, autophagy and ER stress converge. *Gut* **60,** 1580–1588 (2011).
61. Brand, S. Crohn's disease: Th1, Th17 or both? The change of a paradigm: new immunological and genetic insights implicate Th17 cells in the pathogenesis of Crohn's disease. *Gut* **58,** 1152–1167 (2009).
62. Gaya, D. R., Russell, R. K., Nimmo, E. R. & Satsangi, J. New genes in inflammatory bowel disease: lessons for complex diseases? *Lancet* **367,** 1271–1284 (2006).
63. Van Limbergen, J., Wilson, D. C. & Satsangi, J. The genetics of Crohn's disease. *Annu Rev Genomics Hum Genet* **10,** 89–116 (2009).
64. Abraham, C. & Cho, J. H. IL-23 and autoimmunity: new insights into the pathogenesis of inflammatory bowel disease. *Annu. Rev. Med.* **60,** 97–110 (2009).

65. Pizarro, T. T. & Cominelli, F. Cytokine therapy for Crohn's disease: advances in translational research. *Annu. Rev. Med.* **58,** 433–444 (2007).
66. Farrell, R. J. & Peppercorn, M. A. in *UpToDate* (UpToDate in Waltham, MA, 2013).
67. Casanova, J.-L. & Abel, L. Revisiting Crohn's disease as a primary immunodeficiency of macrophages. *J. Exp. Med.* **206,** 1839–1843 (2009).
68. Lalande, J.-D. & Behr, M. A. Mycobacteria in Crohn's disease: how innate immune deficiency may result in chronic inflammation. *Expert Rev Clin Immunol* **6,** 633–641 (2010).
69. Fiocchi, C. Inflammatory bowel disease: Etiology and pathogenesis. *Gastroenterology* **115,** 182–205 (1998).
70. Fuss, I. J. *et al.* Both IL-12p70 and IL-23 are synthesized during active Crohn's disease and are down-regulated by treatment with anti-IL-12 p40 monoclonal antibody. *Inflamm. Bowel Dis.* **12,** 9–15 (2006).
71. Verspaget, H. W., Pena, A. S., Weterman, I. T. & Lamers, C. B. Disordered regulation of the in vitro immunoglobulin synthesis by intestinal mononuclear cells in Crohn's disease. *Gut* **29,** 503–510 (1988).
72. Strober, W., Zhang, F., Kitani, A., Fuss, I. & Fichtner-Feigl, S. Pro-Inflammatory Cytokines Underlying the Inflammation of Crohn's Disease. *Curr Opin Gastroenterol* **26,** 310–317 (2010).
73. Fuss, I. J. *et al.* Disparate CD4+ lamina propria (LP) lymphokine secretion profiles in inflammatory bowel disease. Crohn's disease LP cells manifest increased secretion of IFN-gamma, whereas ulcerative colitis LP cells manifest increased secretion of IL-5. *J. Immunol.* **157,** 1261–1270 (1996).
74. Deban, L., Correale, C., Vetrano, S., Malesci, A. & Danese, S. Multiple Pathogenic Roles of Microvasculature in Inflammatory Bowel Disease: A Jack of All Trades. *Am J Pathol* **172,** 1457–1466 (2008).
75. Hayee, B., Rahman, F. Z., Sewell, G., Smith, A. M. & Segal, A. W. Crohn's disease as an immunodeficiency. *Expert Rev Clin Immunol* **6,** 585–596 (2010).
76. Rahman, F. Z. *et al.* Phagocyte dysfunction and inflammatory bowel disease. *Inflamm. Bowel Dis.* **14,** 1443–1452 (2008).
77. Segal, A. W. & Loewi, G. Neutrophil dysfunction in Crohn's disease. *Lancet* **2,** 219–221 (1976).
78. Marks, D. J. B. *et al.* Defective acute inflammation in Crohn's disease: a clinical investigation. *Lancet* **367,** 668–678 (2006).
79. Smith, A. M. *et al.* Disordered macrophage cytokine secretion underlies impaired acute inflammation and bacterial clearance in Crohn's disease. *J. Exp. Med.* **206,** 1883–1897 (2009).
80. Vinh, D. C. & Behr, M. A. Crohn's as an immune deficiency: from apparent paradox to evolving paradigm. *Expert Rev Clin Immunol* **9,** 17–30 (2013).
81. Somerville, K. W., Logan, R. F., Edmond, M. & Langman, M. J. Smoking and Crohn's disease. *BMJ* **289,** 954–956 (1984).
82. Koutroubakis, I., Manousos, O. N., Meuwissen, S. G. & Pena, A. S. Environmental risk factors in inflammatory bowel disease. *Hepatogastroenterology* **43,** 381–393 (1996).
83. Behr, M. A. & Schurr, E. Mycobacteria in Crohn's disease: a persistent hypothesis. *Inflamm. Bowel Dis.* **12,** 1000–1004 (2006).
84. Lowe, A.-M., Yansouni, C. P. & Behr, M. A. Causality and gastrointestinal infections: Koch, Hill, and Crohn's. *Lancet Infect Dis* **8,** 720–726 (2008).
85. Austin, C. M., Ma, X. & Graviss, E. A. Common nonsynonymous polymorphisms in the NOD2 gene are associated with resistance or susceptibility to tuberculosis disease in African Americans. *J. Infect. Dis.* **197,** 1713–1716 (2008).

86. Pan, H., Dai, Y., Tang, S. & Wang, J. Polymorphisms of NOD2 and the risk of tuberculosis: a validation study in the Chinese population. *Int. J. Immunogenet.* **39,** 233–240 (2012).
87. Grant, A. V. *et al.* Crohn's disease susceptibility genes are associated with leprosy in the Vietnamese population. *J. Infect. Dis.* **206,** 1763–1767 (2012).
88. Zhang, F.-R. *et al.* Genomewide association study of leprosy. *N. Engl. J. Med.* **361,** 2609–2618 (2009).
89. Bahari, G. *et al.* Association of IRGM polymorphisms and susceptibility to pulmonary tuberculosis in Zahedan, Southeast Iran. *ScientificWorldJournal* **2012,** 950801 (2012).
90. King, K. Y. *et al.* Polymorphic allele of human IRGM1 is associated with susceptibility to tuberculosis in African Americans. *PLoS ONE* **6,** e16317 (2011).
91. Ferwerda, G. *et al.* NOD2 and toll-like receptors are nonredundant recognition systems of Mycobacterium tuberculosis. *PLoS Pathog.* **1,** 279–285 (2005).
92. Divangahi, M. *et al.* NOD2-deficient mice have impaired resistance to Mycobacterium tuberculosis infection through defective innate and adaptive immunity. *J. Immunol.* **181,** 7157–7165 (2008).
93. MacMicking, J. D., Taylor, G. A. & McKinney, J. D. Immune control of tuberculosis by IFN-gamma-inducible LRG-47. *Science* **302,** 654–659 (2003).
94. Tiwari, S., Choi, H.-P., Matsuzawa, T., Pypaert, M. & MacMicking, J. D. Targeting of the GTPase Irgm1 to the phagosomal membrane via PtdIns(3,4)P(2) and PtdIns(3,4,5)P(3) promotes immunity to mycobacteria. *Nat. Immunol.* **10,** 907–917 (2009).
95. Singh, S. B., Davis, A. S., Taylor, G. A. & Deretic, V. Human IRGM induces autophagy to eliminate intracellular mycobacteria. *Science* **313,** 1438–1441 (2006).
96. Chiodini, R. J., Van Kruiningen, H. J., Merkal, R. S., Thayer, W. R., Jr & Coutu, J. A. Characteristics of an unclassified Mycobacterium species isolated from patients with Crohn's disease. *J. Clin. Microbiol.* **20,** 966–971 (1984).
97. Van Kruiningen, H. J. *et al.* Experimental disease in infant goats induced by a Mycobacterium isolated from a patient with Crohn's disease. A preliminary report. *Dig. Dis. Sci.* **31,** 1351–1360 (1986).
98. Abubakar, I., Myhill, D., Aliyu, S. H. & Hunter, P. R. Detection of Mycobacterium avium subspecies paratuberculosis from patients with Crohn's disease using nucleic acid-based techniques: a systematic review and meta-analysis. *Inflamm. Bowel Dis.* **14,** 401–410 (2008).
99. Feller, M. *et al.* Mycobacterium avium subspecies paratuberculosis and Crohn's disease: a systematic review and meta-analysis. *Lancet Infect Dis* **7,** 607–613 (2007).
100. Darfeuille-Michaud, A. *et al.* Presence of adherent Escherichia coli strains in ileal mucosa of patients with Crohn's disease. *Gastroenterology* **115,** 1405–1413 (1998).
101. Darfeuille-Michaud, A. *et al.* High prevalence of adherent-invasive Escherichia coli associated with ileal mucosa in Crohn's disease. *Gastroenterology* **127,** 412–421 (2004).
102. Martinez-Medina, M. *et al.* Molecular diversity of Escherichia coli in the human gut: new ecological evidence supporting the role of adherent-invasive E. coli (AIEC) in Crohn's disease. *Inflamm. Bowel Dis.* **15,** 872–882 (2009).
103. Krause, D. O., Little, A. C., Dowd, S. E. & Bernstein, C. N. Complete genome sequence of adherent invasive Escherichia coli UM146 isolated from Ileal Crohn's disease biopsy tissue. *J. Bacteriol.* **193,** 583 (2011).
104. Clarke, D. J. *et al.* Complete Genome Sequence of the Crohn's Disease-Associated Adherent-Invasive Escherichia coliStrain HM605. *J. Bacteriol.* **193,** 4540–4540 (2011).
105. Bringer, M.-A., Rolhion, N., Glasser, A.-L. & Darfeuille-Michaud, A. The oxidoreductase DsbA plays a key role in the ability of the Crohn's disease-associated adherent-invasive Escherichia coli strain LF82 to resist macrophage killing. *J. Bacteriol.* **189,** 4860–4871

(2007).
106. Rolhion, N., Carvalho, F. A. & Darfeuille-Michaud, A. OmpC and the sigma(E) regulatory pathway are involved in adhesion and invasion of the Crohn's disease-associated Escherichia coli strain LF82. *Mol. Microbiol.* **63,** 1684–1700 (2007).
107. Barnich, N. *et al.* CEACAM6 acts as a receptor for adherent-invasive E. coli, supporting ileal mucosa colonization in Crohn disease. *J. Clin. Invest.* **117,** 1566–1574 (2007).
108. Spehlmann, M. E. *et al.* Epidemiology of inflammatory bowel disease in a German twin cohort: results of a nationwide study. *Inflamm. Bowel Dis.* **14,** 968–976 (2008).
109. Ogura, Y. *et al.* A frameshift mutation in NOD2 associated with susceptibility to Crohn's disease. *Nature* **411,** 603–606 (2001).
110. Hugot, J. P. *et al.* Association of NOD2 leucine-rich repeat variants with susceptibility to Crohn's disease. *Nature* **411,** 599–603 (2001).
111. Strober, W. & Watanabe, T. NOD2, an intracellular innate immune sensor involved in host defense and Crohn's disease. *Mucosal Immunol* **4,** 484–495 (2011).
112. Travassos, L. H. *et al.* Nod1 and Nod2 direct autophagy by recruiting ATG16L1 to the plasma membrane at the site of bacterial entry. *Nat. Immunol.* **11,** 55–62 (2010).
113. Cooney, R. *et al.* NOD2 stimulation induces autophagy in dendritic cells influencing bacterial handling and antigen presentation. *Nat. Med.* **16,** 90–97 (2010).
114. Jostins, L. *et al.* Host-microbe interactions have shaped the genetic architecture of inflammatory bowel disease. *Nature* **491,** 119–124 (2012).
115. Saleh, M. & Trinchieri, G. Innate immune mechanisms of colitis and colitis-associated colorectal cancer. *Nat Rev Immunol* **11,** 9–20 (2011).
116. Strober, W., Murray, P. J., Kitani, A. & Watanabe, T. Signalling pathways and molecular interactions of NOD1 and NOD2. *Nat Rev Immunol* **6,** 9–20 (2006).
117. Coulombe, F. *et al.* Increased NOD2-mediated recognition of N-glycolyl muramyl dipeptide. *J. Exp. Med.* **206,** 1709–1716 (2009).
118. Watanabe, T., Kitani, A., Murray, P. J. & Strober, W. NOD2 is a negative regulator of Toll-like receptor 2–mediated T helper type 1 responses. *Nat Immunol* **5,** 800–808 (2004).
119. Noguchi, E., Homma, Y., Kang, X., Netea, M. G. & Ma, X. A Crohn's disease–associated NOD2 mutation suppresses transcription of human IL10 by inhibiting activity of the nuclear ribonucleoprotein hnRNP-A1. *Nat Immunol* **10,** 471–479 (2009).
120. Biswas, A. *et al.* Induction and rescue of Nod2-dependent Th1-driven granulomatous inflammation of the ileum. *PNAS* **107,** 14739–14744 (2010).
121. Magalhaes, J. G. *et al.* Nod2-dependent Th2 polarization of antigen-specific immunity. *J. Immunol.* **181,** 7925–7935 (2008).
122. MacMicking, J. D. IFN-inducible GTPases and immunity to intracellular pathogens. *Trends Immunol.* **25,** 601–609 (2004).
123. MacMicking, J. D. Immune control of phagosomal bacteria by p47 GTPases. *Curr. Opin. Microbiol.* **8,** 74–82 (2005).
124. Taylor, G. A., Feng, C. G. & Sher, A. p47 GTPases: regulators of immunity to intracellular pathogens. *Nat. Rev. Immunol.* **4,** 100–109 (2004).
125. Hunn, J. P., Feng, C. G., Sher, A. & Howard, J. C. The immunity-related GTPases in mammals: a fast-evolving cell-autonomous resistance system against intracellular pathogens. *Mamm. Genome* **22,** 43–54 (2011).
126. Howard, J. C., Hunn, J. P. & Steinfeldt, T. The IRG protein-based resistance mechanism in mice and its relation to virulence in Toxoplasma gondii. *Curr. Opin. Microbiol.* **14,** 414–421 (2011).
127. Bekpen, C. *et al.* The interferon-inducible p47 (IRG) GTPases in vertebrates: loss of the cell autonomous resistance mechanism in the human lineage. *Genome Biol.* **6,** R92 (2005).

128. Ghosh, A., Uthaiah, R., Howard, J., Herrmann, C. & Wolf, E. Crystal Structure of IIGP1: A Paradigm for Interferon-Inducible p47 Resistance GTPases. *Molecular Cell* **15,** 727–739 (2004).
129. Howard, J. The IRG proteins: a function in search of a mechanism. *Immunobiology* **213,** 367–375 (2008).
130. Feng, C. G. *et al.* Mice deficient in LRG-47 display increased susceptibility to mycobacterial infection associated with the induction of lymphopenia. *J. Immunol.* **172,** 1163–1168 (2004).
131. Blumenthal, A. *et al.* Common and Unique Gene Expression Signatures of Human Macrophages in Response to Four Strains of Mycobacterium avium That Differ in Their Growth and Persistence Characteristics. *Infect. Immun.* **73,** 3330–3341 (2005).
132. Feng, C. G. *et al.* The immunity-related GTPase Irgm1 promotes the expansion of activated CD4+ T cell populations by preventing interferon-gamma-induced cell death. *Nat. Immunol.* **9,** 1279–1287 (2008).
133. Deretic, V. Autophagy as an innate immunity paradigm: expanding the scope and repertoire of pattern recognition receptors. *Curr. Opin. Immunol.* **24,** 21–31 (2012).
134. Levine, B., Mizushima, N. & Virgin, H. W. Autophagy in immunity and inflammation. *Nature* **469,** 323–335 (2011).
135. Gutierrez, M. G. *et al.* Autophagy is a defense mechanism inhibiting BCG and Mycobacterium tuberculosis survival in infected macrophages. *Cell* **119,** 753–766 (2004).
136. Martens, S. *et al.* Disruption of Toxoplasma gondii parasitophorous vacuoles by the mouse p47-resistance GTPases. *PLoS Pathog.* **1,** e24 (2005).
137. Khaminets, A. *et al.* Coordinated loading of IRG resistance GTPases on to the Toxoplasma gondii parasitophorous vacuole. *Cell. Microbiol.* **12,** 939–961 (2010).
138. Butcher, B. A. *et al.* p47 GTPases regulate Toxoplasma gondii survival in activated macrophages. *Infect. Immun.* **73,** 3278–3286 (2005).
139. Hunn, J. P. *et al.* Regulatory interactions between IRG resistance GTPases in the cellular response to Toxoplasma gondii. *EMBO J* **27,** 2495–2509 (2008).
140. Hunn, J. P. & Howard, J. C. The Mouse Resistance Protein Irgm1 (LRG-47): A Regulator or an Effector of Pathogen Defense? *PLoS Pathog* **6,** (2010).
141. King, K. Y. *et al.* Irgm1 protects hematopoietic stem cells by negative regulation of IFN signaling. *Blood* **118,** 1525–1533 (2011).
142. Feng, C. G., Weksberg, D. C., Taylor, G. A., Sher, A. & Goodell, M. A. The p47 GTPase Lrg-47 (Irgm1) links host defense and hematopoietic stem cell proliferation. *Cell Stem Cell* **2,** 83–89 (2008).
143. Bekpen, C. *et al.* Death and resurrection of the human IRGM gene. *PLoS Genet.* **5,** e1000403 (2009).
144. Bekpen, C., Xavier, R. J. & Eichler, E. E. Human IRGM gene 'to be or not to be'. *Semin Immunopathol* **32,** 437–444 (2010).
145. Singh, S. B. *et al.* Human IRGM regulates autophagy and cell-autonomous immunity functions through mitochondria. *Nat. Cell Biol.* **12,** 1154–1165 (2010).
146. Palomino-Morales, R. J. *et al.* Association of ATG16L1 and IRGM genes polymorphisms with inflammatory bowel disease: a meta-analysis approach. *Genes Immun.* **10,** 356–364 (2009).
147. Parkes, M. *et al.* Sequence variants in the autophagy gene IRGM and multiple other replicating loci contribute to Crohn's disease susceptibility. *Nat. Genet.* **39,** 830–832 (2007).
148. McCarroll, S. A. *et al.* Deletion polymorphism upstream of IRGM associated with altered IRGM expression and Crohn's disease. *Nat Genet* **40,** 1107–1112 (2008).
149. Brest, P. *et al.* A synonymous variant in IRGM alters a binding site for miR-196 and causes deregulation of IRGM-dependent xenophagy in Crohn's disease. *Nat. Genet.* **43,** 242–245 (2011).

150. Taylor, G. A. *et al.* Pathogen-specific loss of host resistance in mice lacking the IFN-γ-inducible gene IGTP. *PNAS* **97,** 751–755 (2000).
151. Collazo, C. M. *et al.* Inactivation of Lrg-47 and Irg-47 Reveals a Family of Interferon γ–Inducible Genes with Essential, Pathogen-Specific Roles in Resistance to Infection. *J Exp Med* **194,** 181–188 (2001).
152. Tennant, S. M. *et al.* Influence of gastric acid on susceptibility to infection with ingested bacterial pathogens. *Infect. Immun.* **76,** 639–645 (2008).
153. Barthel, M. *et al.* Pretreatment of Mice with Streptomycin Provides a Salmonella enterica Serovar Typhimurium Colitis Model That Allows Analysis of Both Pathogen and Host. *Infect. Immun.* **71,** 2839–2858 (2003).
154. Bull, T. J. *et al.* Detection and verification of Mycobacterium avium subsp. paratuberculosis in fresh ileocolonic mucosal biopsy specimens from individuals with and without Crohn's disease. *J. Clin. Microbiol.* **41,** 2915–2923 (2003).
155. Cheng, J. *et al.* Mycobacterium avium Subspecies Paratuberculosis in the Inflamed Gut Tissues of Patients with Crohn's Disease in China and its Potential Relationship to the Consumption of Cow's Milk: A Preliminary Study. *World Journal of Microbiology and Biotechnology* **21,** 1175–1179 (2005).
156. Singh, S. & Gopinath, K. Mycobacterium avium subspecies Paratuberculosis and Crohn's Regional Ileitis: How Strong is Association? *J Lab Physicians* **3,** 69–74 (2011).
157. Miller, J. M., Jenny, A. L. & Ellingson, J. L. Polymerase Chain Reaction Identification of Mycobacterium Avium in Formalin-Fixed, Paraffin-Embedded Animal Tissues. *J VET Diagn Invest* **11,** 436–440 (1999).
158. Soolingen, D. van, Hermans, P. W., Haas, P. E. de, Soll, D. R. & Embden, J. D. van. Occurrence and stability of insertion sequences in Mycobacterium tuberculosis complex strains: evaluation of an insertion sequence-dependent DNA polymorphism as a tool in the epidemiology of tuberculosis. *J. Clin. Microbiol.* **29,** 2578–2586 (1991).
159. Imirzalioglu, C. *et al.* Highly Specific and Quick Detection of Mycobacterium avium subsp. paratuberculosis in Feces and Gut Tissue of Cattle and Humans by Multiple Real-Time PCR Assays. *J. Clin. Microbiol.* **49,** 1843–1852 (2011).
160. C57BL/6 Mouse Hematology. (2012). at <http://www.criver.com/files/pdfs/rms/c57bl6/rm_rm_r_c57bl6_mouse_clinical_pathology_data.aspx>
161. C57BL/6 Mouse Biochemistry. (2012). at <http://www.criver.com/files/pdfs/rms/c57bl6/rm_rm_r_c57bl6_mouse_clinical_pathology_data.aspx>
162. Targeted tuberculin testing and treatment of latent tuberculosis infection. This official statement of the American Thoracic Society was adopted by the ATS Board of Directors, July 1999. This is a Joint Statement of the American Thoracic Society (ATS) and the Centers for Disease Control and Prevention (CDC). This statement was endorsed by the Council of the Infectious Diseases Society of America. (IDSA), September 1999, and the sections of this statement. *Am. J. Respir. Crit. Care Med.* **161,** S221–247 (2000).
163. MacDermott, R. D. & Lichtenstein, G. R. in *UpToDate* (UpToDate, 2013).
164. Wallis, R. S. in *UpToDate* (UpToDate, 2013).
165. Flynn, J. L. *et al.* Tumor necrosis factor-alpha is required in the protective immune response against Mycobacterium tuberculosis in mice. *Immunity* **2,** 561–572 (1995).
166. Lin, P. L. *et al.* Tumor necrosis factor neutralization results in disseminated disease in acute and latent Mycobacterium tuberculosis infection with normal granuloma structure in a cynomolgus macaque model. *Arthritis Rheum.* **62,** 340–350 (2010).
167. Hanauer, S. B. *et al.* Maintenance infliximab for Crohn's disease: the ACCENT I randomised

trial. *Lancet* **359,** 1541–1549 (2002).
168. Wolf, A. J. *et al.* Initiation of the adaptive immune response to Mycobacterium tuberculosis depends on antigen production in the local lymph node, not the lungs. *J. Exp. Med.* **205,** 105–115 (2008).
169. Wang, C. *et al.* Immune-related GTPase Irgm1 exacerbates experimental auto-immune encephalomyelitis by promoting the disruption of blood-brain barrier and blood-cerebrospinal fluid barrier. *Mol. Immunol.* **53,** 43–51 (2013).
170. He, S. *et al.* Immune-related GTPase M (IRGM1) regulates neuronal autophagy in a mouse model of stroke. *Autophagy* **8,** 1621–1627 (2012).
171. Chang, C.-P., Yang, M.-C. & Lei, H.-Y. Concanavalin A/IFN-gamma triggers autophagy-related necrotic hepatocyte death through IRGM1-mediated lysosomal membrane disruption. *PLoS ONE* **6,** e28323 (2011).
172. Henry, S. C. *et al.* Impaired macrophage function underscores susceptibility to Salmonella in mice lacking Irgm1 (LRG-47). *J. Immunol.* **179,** 6963–6972 (2007).
173. Springer, H. M., Schramm, M., Taylor, G. A. & Howard, J. C. Irgm1 (LRG-47), a Regulator of Cell-Autonomous Immunity, Does Not Localize to Mycobacterial or Listerial Phagosomes in IFN-γ-Induced Mouse Cells. *J. Immunol.* **191,** 1765–1774 (2013).
174. Elguezabal, N. *et al.* Estimation of Mycobacterium avium subsp. paratuberculosis growth parameters: strain characterization and comparison of methods. *Appl. Environ. Microbiol.* **77,** 8615–8624 (2011).
175. Grant, I. R., Kirk, R. B., Hitchings, E. & Rowe, M. T. Comparative evaluation of the MGIT and BACTEC culture systems for the recovery of Mycobacterium avium subsp. paratuberculosis from milk. *J. Appl. Microbiol.* **95,** 196–201 (2003).
176. Henry, S. C. *et al.* Regulation of macrophage motility by Irgm1. *J. Leukoc. Biol.* **87,** 333–343 (2010).
177. Hambleton, S. *et al.* IRF8 mutations and human dendritic-cell immunodeficiency. *N. Engl. J. Med.* **365,** 127–138 (2011).
178. Kramer, M., Netea, M. G., de Jong, D. J., Kullberg, B. J. & Adema, G. J. Impaired dendritic cell function in Crohn's disease patients with NOD2 3020insC mutation. *J. Leukoc. Biol.* **79,** 860–866 (2006).
179. Petrofsky, M. CD4 T cells but Not CD8 or gammadelta lymphocytes are required for host protection against Mycobacterium avium infection and dissemination through the intestinal route. *Infection and immunity* **73,** (2005).
180. Lecuit, M. *et al.* A transgenic model for listeriosis: role of internalin in crossing the intestinal barrier. *Science* **292,** 1722–1725 (2001).
181. Small, C.-L. N., Reid-Yu, S. A., McPhee, J. B. & Coombes, B. K. Persistent infection with Crohn's disease-associated adherent-invasive Escherichia coli leads to chronic inflammation and intestinal fibrosis. *Nat Commun* **4,** (2013).
182. Jick, S. S., Lieberman, E. S., Rahman, M. U. & Choi, H. K. Glucocorticoid use, other associated factors, and the risk of tuberculosis. *Arthritis Rheum.* **55,** 19–26 (2006).
183. McCune, R. M., Feldmann, F. M., Lambert, H. P. & McDermott, W. Microbial Persistence I. the Capacity of Tubercle Bacilli to Survive Sterilization in Mouse Tissues. *J Exp Med* **123,** 445–468 (1966).
184. Scanga, C. A. *et al.* Reactivation of Latent Tuberculosis: Variations on the Cornell Murine Model. *Infect. Immun.* **67,** 4531–4538 (1999).
185. Follett, D. M. & Czuprynski, C. J. Cyclophosphamide and prednisolone exacerbate the severity of intestinal paratuberculosis in Mycobacterium paratuberculosis monoassociated mice. *Microb. Pathog.* **9,** 407–415 (1990).
186. Larsen, A. B. & Miller, J. M. Effect of dexamethasone on Mycobacterium paratuberculosis

infection in hamsters. *Am. J. Vet. Res.* **39,** 1866–1867 (1978).
187. Mohan, V. P. *et al.* Effects of tumor necrosis factor alpha on host immune response in chronic persistent tuberculosis: possible role for limiting pathology. *Infect. Immun.* **69,** 1847–1855 (2001).
188. Plessner, H. L. *et al.* Neutralization of tumor necrosis factor (TNF) by antibody but not TNF receptor fusion molecule exacerbates chronic murine tuberculosis. *J. Infect. Dis.* **195,** 1643–1650 (2007).
189. Tobin, D. M. *et al.* Host Genotype-Specific Therapies Can Optimize the Inflammatory Response to Mycobacterial Infections. *Cell* **148,** 434–446 (2012).
190. Lalvani, A., Behr, M. A. & Sridhar, S. Innate Immunity to TB: A Druggable Balancing Act. *Cell* **148,** 389–391 (2012).
191. Roca, F. J. & Ramakrishnan, L. TNF dually mediates resistance and susceptibility to mycobacteria via mitochondrial reactive oxygen species. *Cell* **153,** 521–534 (2013).